IEEE POWER ENGINEERING SOCIETY
ENERGY DEVELOPMENT AND POWER GENERATION COMMITTEE

PANEL SESSION: INTERNATIONAL PRACTICES IN DISTRIBUTED GENERATION DEVELOPMENT WORLDWIDE[#]

(Tom Hammons, and L. L. Lai)

IEEE 2007 General Meeting, Tampa, USA, 24-28 June 2007
Thursday 9:00 am—4:00 pm, Technical CC Room 22

Sponsored by: International Practices for Energy Development and Power Generation

Chairs: T. J. Hammons, University of Glasgow, Scotland, UK, E-mail: T.Hammons@ieee.org
L L. Lai, City University London, UK, E-mail: L.L.Lai@city.ac.uk

Track 2: Securing New Sources of Energy

PAPERS

Paper 07GM 0434

INTRODUCTION

On behalf of the Energy Development and Power Generation Committee, welcome to this Panel Session on International Practices in Distributed Generation Development Worldwide.

Distributed generation (DG) plants produce power on a customer's site or at the site of a local distribution utility and supply power to the local distribution network directly.

DG is fundamentally distinct from the traditional central plants for power generation and delivery. DG can deliver electrical energy directly to the power distribution network or to where it is consumed, rather than via the transmission system. Also, DG facilities are smaller than traditional central plants.

Usually, DG is more economical in applications where it covers base load electricity and uses utility electricity to cover peak consumption and the load during DG equipment outages. On-site power production avoids transmission and distribution costs which otherwise amount to about of 30% of the cost of delivered electricity.

The relative prices of retail electricity and fuel costs are critical to the competitiveness of any DG option. This ratio varies greatly from country to country. For example, where electricity and natural gas prices are high, DG is attractive only for oil-fired generation. In other countries, where gas is inexpensive compared to electricity, DG can become economically attractive.

A DG plant can operate during periods of high electricity prices (peak periods) and then be switched off during low price periods. The ease of installation of DG allows capacity to be expanded readily to take advantage of anticipated high prices. Some DG assets are portable. They can literally 'follow the market'.

In addition to this technological flexibility, DG may add value to some power systems by delaying the need to upgrade a congested transmission or distribution network, by reducing distribution losses, and by providing support or ancillary services to the local distribution network.

[#] Document prepared and edited by T J Hammons

DG is less capital intensive and can be up and running in a fraction of the time necessary for the construction of large central generating stations. Certain types of DG can dramatically reduce carbon and other pollutant emissions as compared to these plants. DG also reduces the exposure of critical energy infrastructure to the threat of terrorism.

However, DG is not necessarily a benefit for all players in the electricity industry. Utilities may see customers with on-site generation as problematic because they have different consumption patterns than other customers.

The most commonly cited barrier to DG development is interconnecting with utilities' power distribution and transmission systems. Other barriers that are commonly cited in some regions include high capital costs, non-uniform regulatory requirements, lack of experience with DG, and tariff structures.

Under traditional cost-of-service regulation, distribution company profits are directly linked to sales. The more kWhs of electricity that move over their lines, the more money they make. Interconnecting with customer-owned DG is plainly not in line with a utility's profit motive.

Presently, most micro-generation solutions have a very small and possibly negative payback if assessed on commercial terms (using expected lifetime, capital and installed cost and a true discount rate). Micro-generation will only become widespread with either substantial increases in the costs of grid-supplied electricity, or some form of carbon credit for domestic low carbon generation.

DG technologies include electric power generation by fuel cells and photovoltaic systems and other small renewable generation technologies such as small hydro or small wind systems.

Fuel cells are compact, quiet power generators that use hydrogen and oxygen to make electricity. They are seen as a market in which they could be commercialized more quickly. Fuel cells can convert fuels to electricity at very high efficiencies (40%-65%), compared with conventional technologies. Their efficiency limits the emissions of greenhouse gases. As there is no combustion, other noxious emissions are low. Fuel cells can operate with very high reliability and so could supplement or replace grid-based electricity. Capital costs are approximately US$ 4500 per kW.

Regarding wind power, the electricity output of a domestic wind turbine will depend on the location and size of the home and can be as low as 1 kW - but is more commonly between 2 and 6 kW. Domestic wind turbines can be roof-mounted with a nominal output of 1 kW designed to generate energy from low wind speeds and are typically mounted on the gable end of buildings. Recent developments include turbines that can be attached to the building sidewalls or included as part of a building's natural ventilation. Electrical power from small-scale wind generators is generally highly variable. Proprietary systems have been developed to interface between the generator and the domestic supply.

Wind power is sometimes considered to be distributed generation, because the size and location of some wind farms makes it suitable for connection at distribution voltages. Wind power is rapidly growing in importance as a share of worldwide electricity supply.

The status of DG differs in each OECD country. While economics are certainly a fundamental factor, differences in government policy can also affect the role that DG plays.

CHP is economically attractive for DG because of its higher fuel efficiency and low incremental capital costs for heat-recovery equipment. Much of the CHP capacity in the OECD has been developed as a consequence of supportive government policies. Such policies have also encouraged systems to produce power for export to the grid.

DG in the US is limited by relatively low electricity prices and affected by the widely varied pace of retail electricity market liberalization in the states. CHP accounts for over 50 GW or about 6% of total US electrical generating capacity, nearly all of it in large industrial plants. Emergency power generators have been identified as a potential source of emergency grid capacity. A detailed survey of standby generators in California, by the California Energy Commission, found 3.2 GW of such capacity, equivalent to over 6% of peak electricity demand in the state.

There are several challenges to DG in the US beyond the question of economic competitiveness. Permitting processes make it difficult and expensive, on a per kilowatt basis, to get

siting approval. The lack of a national standard for interconnection further increases transaction costs for DG companies, although such a standard is now under development. Incomplete regulatory reform has left distribution utilities competing with DG. Environmental standards have been toughened in some states, with the same standard applying regardless of the size of the generator. This approach effectively rules out fossil-fired DG in these states.

The UK has policies that favor development of CHP and renewable sources of energy and considers the development of DG in general as an important way to increase competition among electricity producers. Nevertheless, the electricity trading rules have proved disadvantageous to small-distributed generators because of higher transaction costs, requirements for balancing output against forecast. In wholesale markets that are designed with large central generation in mind, smaller distributed generators may be at a disadvantage because of the additional costs and complexities of dealing with the market.

Variation of fault level depends on network operation. In the event of an electrical fault on a distribution network, circuit breakers in the network are tripped in order to isolate the fault from the supply. One or more distributed generators could continue to operate supplying power to loads that are connected to the same section of the network. Different DG technologies come with widely varying fault current contribution and provision needs to be made for adequate network protection under all possible system configurations. Problems will be experienced if fault levels become significantly reduced, for example, during islanded operation or significantly increased due to significant penetration levels of DG.

Unplanned islanded operation of distributed generators is generally regarded as unsafe and undesirable. To prevent unplanned islanding, all distributed generators must be fitted with loss of mains protections, which aims to detect when the generator is islanded and to disconnect it from the network. Several generators must not feed into circuits that have been de-energized from the main grid. DG units have to be disconnected before reclosing. The sensitivity of loss-of-mains protection is challenged by the potential for close matching of local load and generation. Nuisance trips may also occur as a result of too sensitive a setting. In some countries, a specific loss-of-mains protection is necessary.

The assumption of unidirectional power flow that was adopted for designing protection in many cases is no longer valid. Other aspects such as the intermittency of certain types of renewable sources and limited control capability already put pressure on various aspects of network operation protection and control. Increased levels of DG affect relay co-ordination within distribution systems. Weak distribution networks with the addition of large amounts of nonlinear loads and inverter connected generators experience power quality deterioration that results in protection mal-operation.

It should be noted that some utilities practice direct inter-tripping, but it has not been widely accepted due to high cost.

DG offers grid benefits like reduced line loss and increased reliability. From a grid security standpoint, many small generators are collectively more reliable than a few large ones. Small generators can be repaired more quickly and the consequences of a small unit’s failure are less catastrophic. The provision of reliable power represents the most important market niche for DG. Growing consumer demand for higher quality electricity (e.g., 'six nines' or 99.9999% reliability) requires on-site power production. DG is also well suited to provide the ancillary services necessary for the stability of the electrical system. New power electronics systems offer ways to control the routing of electricity and also provide flexible DG interfaces to the network.

This panel presents various issues with examples, case studies and practices as discussed above.

The Panelists and Titles of their Presentations are:

1. T J Hammons (International Practices for Energy Development and Power Generation IEEE, University of Glasgow, Scotland, UK) and L L Lai (City University London, UK). International Practices in Distributed Generation Development Worldwide (Paper 07GM0434).

2. Kwang Y. Lee (Pennsylvania State University, USA) and Se-Ho Kim (Cheju National University, Korea). Progress in Distributed Generation in Korea (Paper 07GM0963).
3. Norman Tse (City University of Hong Kong, Hong Kong). Wavelet Based Algorithm for Power Quality Analysis (Paper 07GM0496).
4. V. S. Pappala and I. Erlich (University of Duisburg, -Essen, Germany). Management of Distributed Generation Units under Stochastic Load Demands using Particle Swarm Optimization (Paper 07GM0751).
5. Nikos Hatziargyriou, Zoe Vrontisi, and Antonis G. Tsikalakis {National Technical University of Athens, Greece), and Vasilis Kilias (Center of Renewable Energy (CRES), Athens, Greece). The Effect of Island Interconnections on the Increase of Wind Power Penetration in the Greek System (Paper 07GM1075).
6. Tze-Fun Chan (Hong Kong Polytechnic University, Hong Kong) and Loi Lei Lai (City University London, UK). Permanent-Magnet Machines for Distributed Power Generation: A Review. (Paper 07GM0593).
7. Khaled A. Nigim (University of Waterloo, Canada), and Wei-Jen Lee (University of Texas at Arlington, TX, USA). Micro Grid Integration Opportunities and Challenges. (Paper 07GM0284).
8. Yuping Lu, Lidan Hua, Ji'an Wu, Gang Wu, *and* Guangting Xu (Southeast University, Nanjing, China). A Study on Effect of Dispersed Generator Capacity on Power System Protection. (Paper 07GM0503).
9. Umakant Dhar Dwrivedi, S. N Singh and S. C. Srivastava (IIT, India). Analysis of Transient Disturbances in Distribution Systems: A Hybrid Approach (Paper 07GM1015).
10. Ringo Lee, Director, "Your Network System Integrator", Powerpeg NSI Limited, Hong Kong and L. L. Lai (City University London, UK). A Practical Approach to Wireless GPRS On-line Power Quality Monitoring System (Paper 07GM1010).
11. Invited Discussers.

Each Panelist will speak for approximately 20 minutes. Each presentation will be discussed immediately following the respective presentation. There will be a further opportunity for discussion of the presentations following the final presentation.

The Panel Session has been organized by L. L. Lai (City University London, UK) and T. J. Hammons (Chair of International Practices for Energy Development and Power Generation IEEE PES, University of Glasgow, UK). Tom Hammons and Loi Lei Lai will moderate the Panel Session.

BIOGRAPHIES

Thomas James Hammons (F'96) received the degree of ACGI from City and Guilds College, London, U.K. and the B.Sc. degree in Engineering (1st Class Honors), and the DIC, and Ph.D. degrees from Imperial College, London University.

He is a member of the teaching faculty of the Faculty of Engineering, University of Glasgow, Scotland, U.K. Prior to this he was employed as an Engineer in the Systems Engineering Department of Associated Electrical Industries, Manchester, U. K. He was Professor of Electrical and Computer Engineering at McMaster University,Hamilton, Ontario, Canada in 1978-1979. He was a Visiting Professor at the Silesian Polytechnic University, Poland in 1978, a Visiting Professor at the Czechoslovakian Academy of Sciences, Prague in 1982, 1985 and 1988, and a Visiting Professor at the Polytechnic University of Grenoble, France in 1984. He is the author/co-author of over 350 scientific articles and papers on electrical power engineering. He has lectured extensively in North America, Africa, Asia, and both in Eastern and Western Europe.

Dr Hammons is Chair of International Practices for Energy Development and Power Generation of IEEE, and Past Chair of United Kingdom and Republic of Ireland (UKRI) Section

IEEE. He received the IEEE Power Engineering Society 2003 Outstanding Large Chapter Award as Chair of the United Kingdom and Republic of Ireland Section Power Engineering Chapter (1994~2003) in 2004; and the IEEE Power Engineering Society Energy Development and Power Generation Award in Recognition of Distinguished Service to the Committee in 1996. He also received two higher honorary Doctorates in Engineering. He is a Founder Member of the International Universities Power Engineering Conference (UPEC) (Convener 1967). He is currently Permanent Secretary of UPEC. He is a registered European Engineer in the Federation of National Engineering Associations in Europe.

Loi Lei Lai (SM'92, F'2007) received the B.Sc. (First Class Honors) and the Ph.D. degrees from the University of Aston in Birmingham, UK. He also gained his D.Sc. from City University London. Currently he is Head of Energy Systems Group at City University, London, UK. He is a Visiting Professor at Southeast University, Nanjing, China and also a Guest Professor at Fudan University, Shanghai, China. He has authored/co-authored over 200 technical papers. In 1998, he also wrote a book entitled Intelligent System Applications in Power Engineering Evolutionary Programming and Neural Networks. Recently, he edited a book entitled Power System Restructuring and Deregulation Trading, Performance and Information Technology. In 1995, he received a high-quality paper prize from the International Association of Desalination, USA. Among his professional activities are his contributions to the organization of several international conferences in power engineering and evolutionary computing, and he was the Conference Chairman of the IEEE/IEE International Conference on Power Utility Deregulation, Restructuring and Power Technologies 2000. Dr. Lai is a Corporate Member of the IEE. He was awarded the IEEE Third Millennium Medal, 2000 IEEE Power Engineering Society UKRI Chapter Outstanding Engineer Award, and 2003 IEEE Power Engineering Society Outstanding Large Chapter Award.

Received January 29 2007

2. PROGRESS IN DISTRIBUTED GENERATION IN KOREA (PAPER 07GM0963).

Kwang Y. Lee , Pennsylvania State University, USA
Se-Ho Kim, Cheju National University, Korea

Abstract--This paper presents the progress in distributed generation in Korea. The government policy has emphasized mainly on three different renewable energy sources, namely, hydrogen and fuel cell, photovoltaic, and wind power. Concerning renewable energy, the government plans to replace 5% of the primary energy source by the year 2011. The road map for the three major renewable energy sources is presented.

Index Terms—Distributed generation, renewable energy, hydrogen, fuel cell, photovolataic, wind power.

I. INTRODUCTION

For the protection of environment and to meet the ever-increasing energy consumption, interest in renewable energy and distributed generation has been increasing worldwide. Wind is the fastest growing energy source today, and there are widespread plans to significantly increase their penetration in power systems. Various planning and operating problems arise as wind power penetration increases in a power system [1]. Fuel cells are static energy conversion devices that convert the chemical energy of fuel directly into electrical energy. Compared with conventional power plants, they have many advantages, such as high efficiency, zero or no emission and flexible modular structure [2]. Photovoltaic (PV) device converts solar radiation incidence directly to electrical energy. Since the output of each PV cell is quite small, a large number of cells have to be connected together in a series-parallel configuration in order to get the desired voltage and power output. A power electronic converter is required to convert its dc output to ac output.[3-6]

In Korea, air pollution of thermal power plants is likely to be a major impediment to generating electricity. Driven by air pollution and global climate change, the government has become interested in renewable energy and distributed sources. Concerning renewable energy, the government plans to replace 5% of the primary energy source by the year 2011.

This panel paper is organized as follows:

II. DISTRIBUTED GENERATION IN KOREA

The Korea Electric Power Co. (KEPCO) has constructed generating plants with a capacity of about 65GW, 28,867km of transmission lines and 389,551km of distribution lines to supply the power demand. Power demand has increased at an average annual rate of over 10% until the year 2000 and 6% after the year 2000 (Table I) [7]. Korea imports about 98% of primary energy from other countries. The generating plants have been diversified such as nuclear, coal, LNG, oil and hydro, etc. However, air pollution results from oil- and coal-fired thermal plants.

TABLE I. STATISTICS OF THE ELECTRICITY INDUSTRY IN KOREA

UNIT: MW

year	Capacity		Peak power		Average power	
		Increase rate		Increase rate		Increase rate
1999	44,427	2.7	37,293	13.0	27,320	11.2
2000	47,876	7.8	41,007	10.0	30,328	11.0
2001	49,632	3.7	43,125	5.2	32,560	7.4
2002	52,799	6.4	45,773	6.1	34,986	7.5
2003	56,081	6.2	47,385	3.5	36,810	5.2
2004	59,129	5.4	51,264	8.2	39,058	6.1
2005	61,737	4.4	54,631	6.6	41,625	6.6
2006.1-8	64,778	4.9	58,994	8.0	43,665	4.9

As concerns over environmental problem and global climate change increase, this might be an important constraint in supplying power demand in the future. Therefore, air pollution of thermal power plants is likely to be a major impediment to generating electricity. Driven by these circumstances, the government has become interested in renewable energy and distributed sources. Concerning renewable energy, the government plans to replace 5% of the primary energy source by the year 2011.

The capacity of wind power is 90MW in the year 2005 and photovoltaic capacity is 9.3MW in the year 2004. In November 21, 2005, 1,000kWp PV generation station was constructed, which is the largest commercial station in Korea.

In Korea, the category of renewable energy is as follows:
fuel cell, hydrogen, photovoltaic, bio, wind, hydro, ocean, waste matter, and geothermal. The government policy has emphasized mainly on the development of three major sources of renewable energy (hydrogen and fuel cell, photovoltaic, and wind power).

The road map of these renewable energy sources is as follows:

1). Hydrogen & Fuel Cell:

- Generation efficiency 45 % and life time above 40,000 hours for the Morton Carbonate Fuel Cell (MCFC).
- Construction system development: 250kW for building and 3kW for house
- Transportation system development: 80kW for car and 200kW for bus

2). Photovoltaic:

- Efficiency improvement: 12% -> 15% -> 18%
- Development: 3kW for house
- Market penetration and cost-cut
- 100,000 homes of photovoltaic house: 30,000 homes by 2010, 60,000 homes by 2011, 100,000 homes by 2012

3). Wind Power

Large scale wind generator: 1MW -> 1.5MW -> 3MW

- 750kW - 3MW wind generation system development
- Domestic production and construction of offshore platform for wind power
- Reliability establishment of domestic generator and development of offshore wind power generator
- Evaluation of domestic generator and commercial production

TABLE II. GENERATION OF RENEWABLE ENERGY
UNIT: KTOE [KILO TONNAGE OF OIL EQUIVALENT]

year	Solar heat	PV	Bio	Waste matter	Hydro	Wind power	Geo-thermal	Fuel cell	Sum
1988	7.3	0.1	51.5	90.8	16.9	0.0	-	-	166.6
1989	8.5	0.2	53.5	133.4	18.3	0	-	-	213.9
1990	9.9	0.2	59.6	246.9	18.5	0	-	-	335.1
1991	11.4	0.3	62.6	318.7	18.6	0	-	-	411.6
1992	12.6	0.4	57.3	461.2	19.5	0.1	-	-	551.1
1993	14.1	0.5	58.8	545.6	28.8	0.3	-	-	648.1
1994	16.8	0.5	57.2	678.8	22.5	0.3	-	-	776.1
1995	22.1	0.5	59.2	804.5	20.4	0.1	-	-	906.8
1996	32.0	0.6	50.4	1,056.4	20.3	0.1	-	-	1,159.8
1997	45.5	0.7	67.6	1,282.5	22.5	0.2	-	-	1,419
1998	44.0	0.9	63.2	1,577.2	27.2	0.4	-	-	1,712.9
1999	42.1	1.1	64.9	1,760.5	27.1	1.5	-	-	1,897.2
2000	41.7	1.3	82.0	1,977.7	20.5	4.2	-	-	2,127.4
2001	37.2	1.5	82.5	2,308.0	20.9	3.1	-	-	2,453.2
2002	34.8	1.8	116.8	2,732.5	27.6	3.7	0.1	-	2,917.3
2003	32.9	1.9	131.1	3,039.3	1,225.6	5.2	0.4	-	4,436.4
2004	36.1	2.5	135.0	3,313.3	1,082.3	11.8	1.4	-	4,582.4
2005	34.7	3.6	181.3	3,705.5	918.5	32.5	2.6	0.5	4,879.2

TABLE III. HYDROGEN & FUEL CELL DEVELOPMENT STAGE

Section	Stage 1 (2003-2005) Technology development and reliability establishment	Stage 2 (2006-2008) evidence application	Stage 3 (2009-2012) market entrance and expansion
hydrogen station	1	10	50
distributed source	cumulative units: 300 (250-1,000kW)		
building	cumulative units: 2000 (10-50kW)		
house	cumulative units: 10,000 (below 3kW)		
transportation	car 10	car 150 bus 10	car 3,200 bus 200
portable	core commercial technology development	promotion of enterprise	

TABLE IV. PV DEVELOPMENT STAGE

Stage 1 (2003-2006) development and promotion	Stage 2 (2006-2009) development for wide application	Stage 3 (2009-2012) development of low cost products
• 3kW system development for homes • 10kW system development for commercial building • cost cut of PV • increased reliability and mass production	• development of crystalloid ultra-thin PV • development of next generation thin PV • unit development for spread of PV generation system	• product development of crystalloid ultra-thin PV • product development of next generation thin PV • package development for spread of PV generation system

TABLE V. WIND POWER DEVELOPMENT STAGE

Stage 1 (2003-2005)	Stage 2 (2006-2008)	Stage 3 (2009-2012)
• development and commercial use of medium scale 750kW wind generator • commercial use of 30kW small wind generator • light weight and cost reduction • interconnection technology establishment and distribution of small wind generator • data base construction for wind resource and development of forecasting technologies	• development and commercial use of large-scale 1,500kW wind generator • development and commercial use of off-shore wind generator • data base construction for off-shore wind resource	• development and commercial use of ultra large scale 3MW wind generator • distribution and integration of off-shore wind farm • export of wind generation technology

To increase the renewable energy and distributed generation as energy resources, the government provides the subsidies for generation margin (The average SMP (System Marginal Price) was 61.59 won/kWh in 2005 year).(1$ = 1,000 won)

The generation margin is paid as follows:

- photovoltaic 714.40 won
- wind power 107.77 won
- small hydro power 73.69 won
- tidal power 62.81 won
- LFG(LandFill Gas) 65.20 won (below 20,000kW), 61.80 won (20,000 - 50,000kW)
-

The support period is given as follows:

- 15 years from operation time (photovoltaic, wind power)
- 5 years from operation time (small hydro power, tidal power, LFG (LandFill Gas), waste matter)

III. POWER SYSTEM IN JEJU ISLAND

Jeju is the largest tourist island in Korea, located approximately 100km south of the mainland, and had a peak load of about 490MW in 2006, with an average growth rate 8.6% over the last 5 years.

The power system network in Jeju consists of 3 power plants and 360km of 154KV lines. Power plants are smaller and generation cost is higher in comparison with the mainland. To meet the increasing demand and preserve the environment of Jeju, HVDC transmission system links with a 100km submarine cable from Haenam on the mainland to Jeju. The HVDC system provides Jeju with the high quality power of the mainland and avoids the difficulty of securing generation sites.[8]

The general rating of HVDC link is:

- Voltage and capacity: DC 180kV, 150MW x 2 Pole, Bipole
- HVDC cable: 800 mm^2 Solid Cable 101km 2 line (sea bottom 96km, land 5km)
- Electrode line: ACSR/AW 410 mm^2 2 line (Jeju 12km, Haenam 16km)
- Normal operation: below 150MW, below 50 % of Jeju demand, frequency mode operation
- Basic control mode: constant current mode, constant frequency mode, constant power mode

The frequency mode operation of HVDC absorbs the load variation and maintains 60Hz frequency in Jeju.

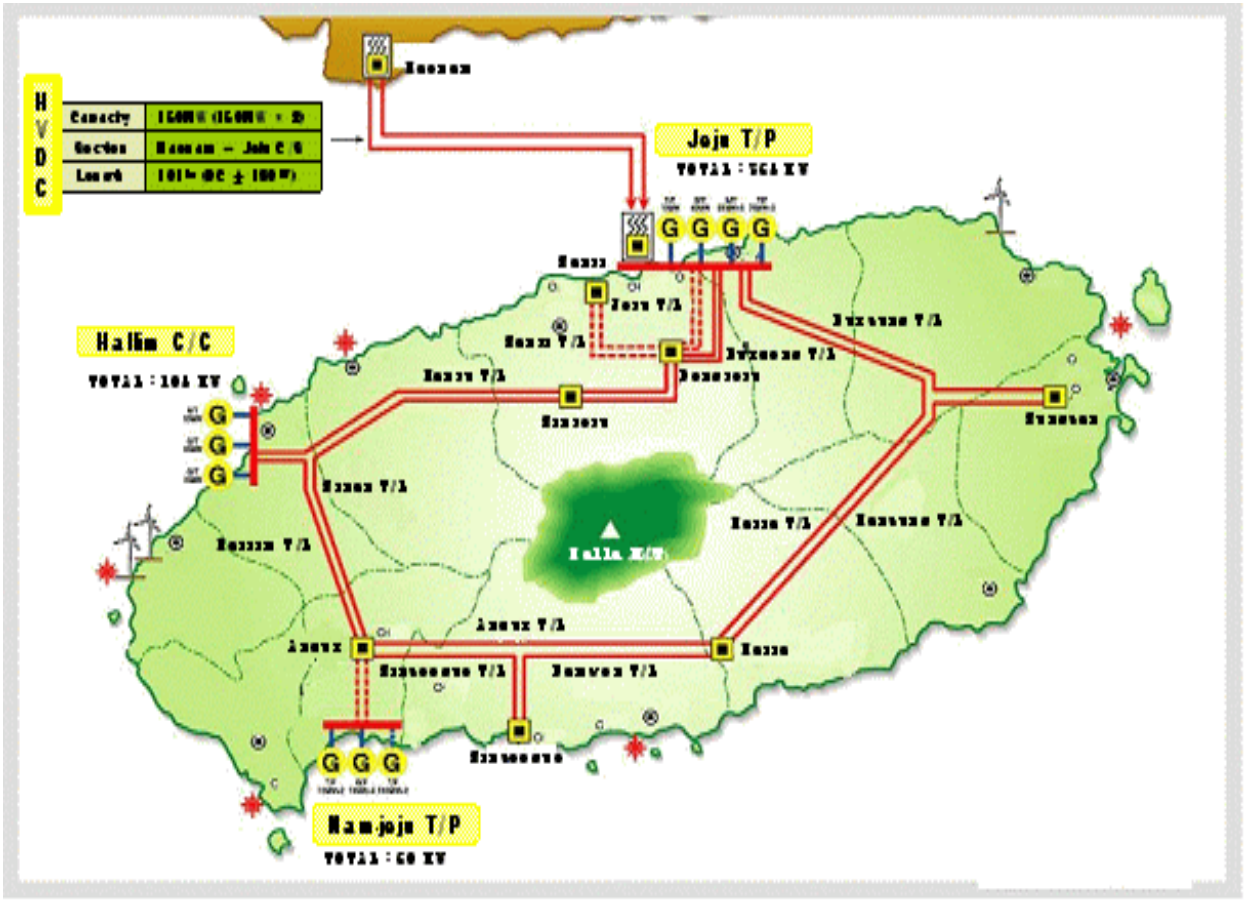

Fig. 1. Jeju power system.

IV. WIND POWER IN JEJU ISLAND

The east and west side of Jeju Island have good wind conditions and the average wind velocity is 6-

7 m/s. Good wind conditions have led to an increased number of wind turbines. By 2006, the total wind power capacity in Jeju is 19MW, and it is expected to increase to 230MW by 2009 (Table VII) [9].

Hangwon wind farm has the 9.8MW capacity and is the first commercial wind farm in Korea. In 2004, Hankyung wind farm with 6MW capacity was constructed by KOSPO generation company.

TABLE VI. THE PRESENT COMPOSITION OF GENERATION COMPANIES IN JEJU

Utility / Power Plant		Capa-city [MW]	Supply Capacity[MW]		Operation
			Sum-mer	Othe rs	
KOMIPO	Jeju T/P#1 Jeju T/P#2 Jeju T/P#3	10.0 75.0 75.0	10.0 79.0 79.0	10.0 79.0 79.0	Weekly start & stop, Always in operation Always in operation
	Jeju D/P#1	40.0	40.0	40.0	Always in operation
	Jeju G/T#3	55.0	43.0	50.0	In charge of daily peak
KOSPO	Namjeju T/P#1 Namjeju T/P#2 Namjeju T/P#3 Namjeju T/P#4 (2007.3 scheduled)	10.0 10.0 100,0 (100.0)	10.0 10.0 100.0 (100.0)	10.0 10.0 100.0 (100.0)	In charge of peak season
	Namjeju D/P#1 Namjeju D/P#2 Namjeju D/P#3 Namjeju D/P#4	10.0 10.0 10.0 10.0	9.0 9.0 9.0 9.0	9.0 9.0 9.0 9.0	Always in operation Always in operation Always in operation Always in operation
	Hallim G/T#1 Hallim G/T#2 Hallim S/T	35.0 35.0 35.0	32.0 32.0 31.0	35.0 35.0 35.0	In charge of daily peak & peak season
KEPCO	HVDC	(150.0)	150.0	150.0	Within 150MW & 50% of demand
	Jeju G/T#1 Jeju G/T#2	55.0 55.0	-	-	Control reactive power or emergency generator
Total		630.0 (880)			

TABLE VII. WIND POWER GENERATION STATUS IN JEJU

section		generator	capacity	cumulative capacity	completion date	enterprise or province
present	hangwon	600kW×2(Vestas) 660kW×7(Vestas) 225kW×1(Vestas) 700kW×5(NEG-Micon)	9,795	9,795	2002. 4	Jeju province
	hankhung(I)	1,500kW×4(NEG-Micon)	6,000	15,795	2004. 3	KOSPO
	sinchang	850kW×2(Vestas)	1,700	17,495	2006. 3	Jeju province
	wolgeong	1,500kW×1	1,500	18,995	2006. 7	KIER
present capacity			18,995	18,995	-	-
schedule	nansan	2,100kW×7	14,700	33,695	2006. 9	Jeju wind power
	pyosun	1,500kW×2	3,000	36,695	2006. 7	Unison
	dukchon	2,100kW×10	21,000	57,695	2007. 9	Jeju wind power
	hankyung(II)	3,000kW×5	15,000	72,695	2007.10	KOSPO
	sungsan	2,000kW×10	20,000	92,695	2007.11	KOSPO
	sangdo	undecided	31,500	124,695	2008. 2	Jeju wind power
	sangmyung	undecided	16,000	140,195	2008. 6	Unison
	chungsu	undecided	3,000	143,195	2008. 6	Unison
	sammu	3,000kW×10	30,000	173,195	2008. 9	Sammu
	daehuel	undecided	18,000	191,195	2009. 7	Unison
	dukchon	undecided	40,000	231,195	2009. 7	KOMIPO
scheduled capacity			212,200	231,195	-	-

1). Power Production iby Jeju Wind Farms.

Wind power production of Hangwon and Hankyung wind farms is total 36GWh, which is 1.3% of the total demand and 2.2% of the production in Jeju during the last two years.

The contribution of wind power to Jeju power demand is high in winter and low in summer.

TABLE VIII. AVERAGE POWER PRODUCTION IN JEJU WIND FARM (2004. 3 2006.2)

wind farm	Month (GWh)												Total
	3	4	5	6	7	8	9	10	11	12	1	2	
Hangwon	2.41	1.41	1.17	0.60	0.73	0.93	1.38	1.65	1.42	2.27	2.70	2.52	19.19
Hankyung	2.11	1.34	0.93	0.71	0.86	0.86	1.12	1.51	1.27	1.88	1.88	2.33	16.80
Total	4.52	2.75	2.10	1.31	1.59	1.79	2.50	3.16	2.69	4.15	4.58	4.85	35.99
	9.37 (spring)			4.69 (summer)			8.35 (fall)			13.58 (winter)			

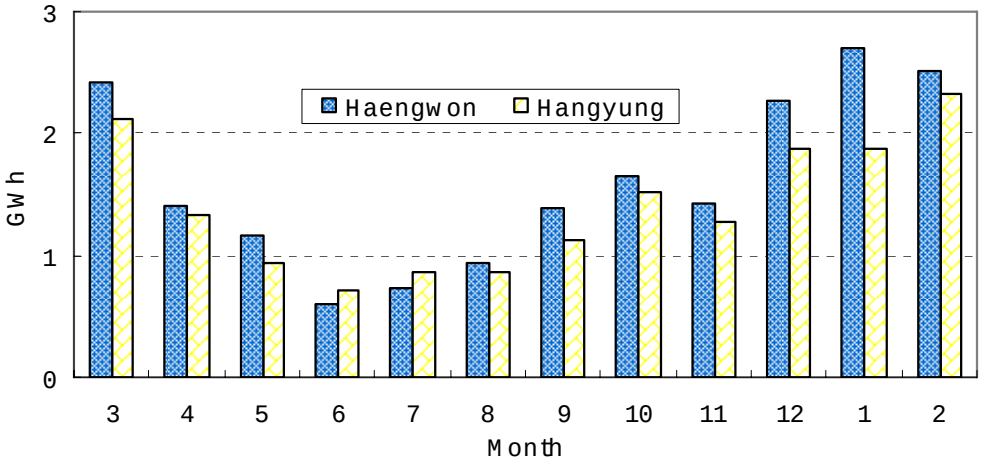

Fig. 2. Average power production in Jeju wind farm (2004. 3 2006. 2).

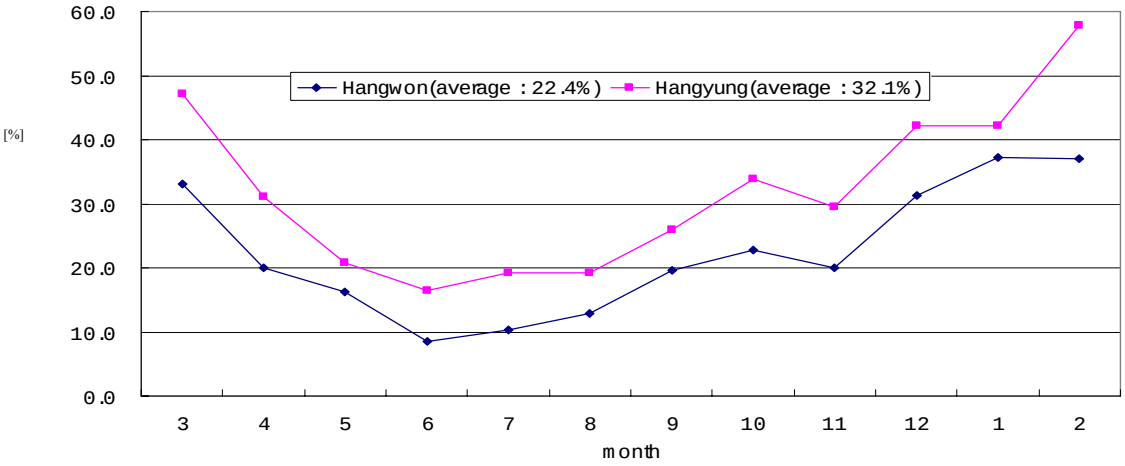

Fig. 3. Monthly capacity factor in Jeju wind farm.

2). Capacity Factor of Jeju Wind Farms.

The average power as the percentage of the nominal capacity (capacity factor, CF) of wind farm in Jeju is 22.4 % for Hangwon and 32.1 % for Hankyung. These monthly capacity factors are high compared to other countries (England 27%, Denmark 20%, Germany 15%).

3). Occupation Rate of Power Production.

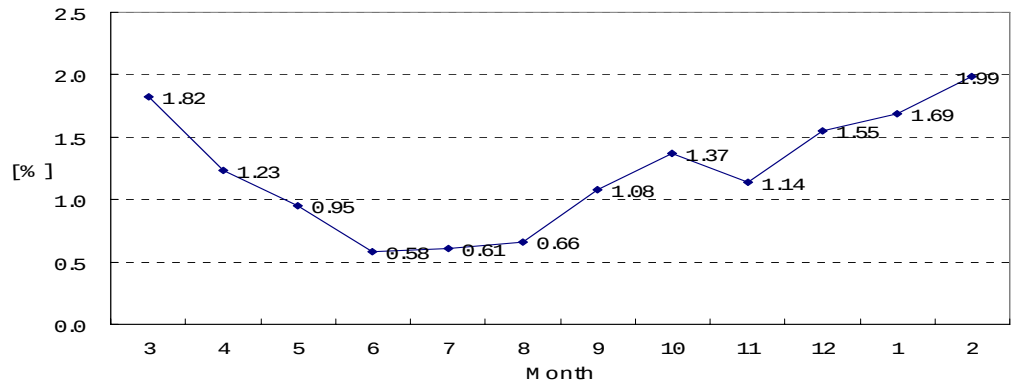

Fig. 4. Occupation rate of power production (2004.3 2006.2).

The occupation rate of wind power production to Jeju power generation is 1.22% in average and 1.99% for maximum. Until now, wind power has not affected Jeju power system operation owing to its small capacity compared to conventional generation capacity.

4). Wind Power Production Variation.

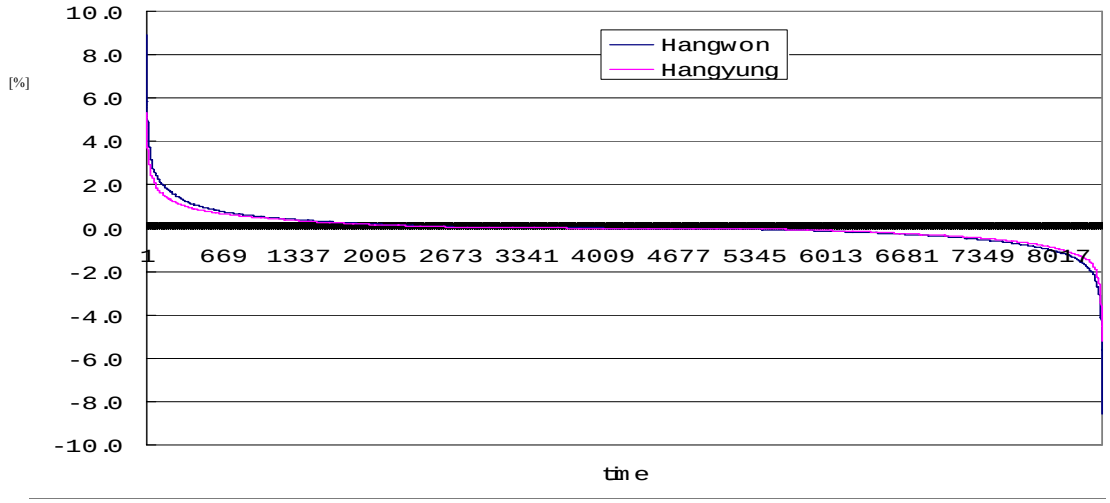

Fig. 5. Wind power fluctuation (one hour).

For the two wind farms, variation of the wind power production is as follows:

- For 32.4% (2,717hour) of the time (for 8,395hour), the wind power production does not vary at all
- For 89.4% (7,507hour) of the time (for 8,395hour), the wind power production varies below 1%
- For 0.6% (53hour) of the time (for 8,395hour), the wind power production varies above 3%
- For 0.008% (7hour) of the time (for 8,395hour), the wind power production varies above 5%

5). Frequency Distribution of Wind Power Production Variation.

For the two wind farm, frequency distribution of wind power production variation is as follows:

- For 41% of the time (for one month), the wind power production does not vary all or varies below 2%
- For 91.1% of the time (for one month), the wind power production varies below 10%
- For 98.7% of the time (for one month), the wind power production varies below 20%
- For 1.3% of the time (for one month), the wind power production varies above 20%

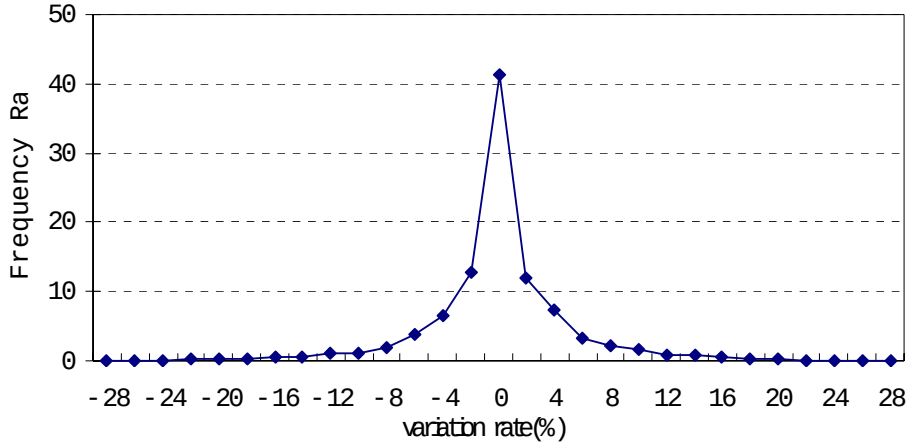

Fig. 6. Frequency rate versus wind power production variation rate in capacity 16MW (10 minutes average production)

6). Consideration of Wind Power Generation in Jeju.

There are a number of issues to be resolved when implementing wind power generation. These include the followings:

- HVDC system response characteristics according to wind variation and wind power generation
- Wind power operation limit considering HVDC and conventional generator capacity
- Technical countermeasure with wind power generation above operation limit
- Network operation characteristic analysis according to occupation of wind power generation
- Forecasting of wind generation power using weather data

V. FUEL CELL PLANTS

The power transfer through the HVDC link is about 50% of the total demand in the Jeju island, and more than 40% in the average annually. Recently, relatively larger units are being planned and thus, the impact of failure of a unit is expected to be greater than before.

A. LARGE FUEL CELL PLANTS.

To reduce the dependency on the HVDC cable, large fuel cell plants are proposed in various locations. Fuel cell plants require the basic fuel in the form of LNG or bunker-C oil. In principle, all current oil-based thermal plants can be replaced or augmented by fuel cell plants in order to increase the fuel efficiency. Assuming the scenario that an LNG port will be available in South Jeju, the following plants are possible sites in the southern Jeju Island [10]:

- Two 40 MW Fuel Cell Plants in South Jeju near the LNG port.
- One 40 MW Fuel Cell Plants in Joongmoon/Seoquipo

- One 40 MW Fuel Cell Plants in Hanra S/S
- One 40 MW Fuel Cell Plants in Hanrim S/S

In addition to the sites in the southern Jeju Island, fuel cell plants can be located in the following sites in the northern Jeju Island:

- Two 40 MW Fuel Cell Plants in Jeju T/S
- One 40 MW Fuel Cell Plants in Shinjeju S/S
- One 40 MW Fuel Cell Plants in Dongjeju S/S

Some units can be in the hybrid with gas turbine in order to increase the fuel efficiency to over 80%.

B. SMALL FUEL CELL PLANTS

In addition to the large fuel cell plants for maintaining capacity for the Jeju Power System, there are number of applications for localized use of fuel cell plants:

- Industrial
- Government facilities
- Universities
- Hospitals
- Apartment complex

Some units can be in the hybrid with combined heat and power production (CHP), such as ones used for industrial and apartment complex. As long as there are fuel lines available, either for LNG or buncker-C oil, a unit of 250 kW can be installed on site next to the buildings.

VI. CONCLUSIONS

Presently, widespread integration of distributed generation and wind power in Korea is still in infancy. However, by the governmental and provincial policies, distributed generation will play an important role. Korean government emphasizes in the three kinds of renewable energy (hydrogen & fuel cell, photovoltaic, and wind power). Also, to increase the renewable energy and distributed generation as energy resources, the government provides subsidies for generation margin. Jeju island, located approximately 100km south of the mainland, is an area with good wind conditions and it is expected to install a number of wind turbines in a few years.

VII. REFERENCES

[1] R. Karki, "Wind Power in Power System Planning," *Electrical and Computer Engineering, 2004 Canadian Conference,* Vol. 3, pp. 1511- 1514, May 2004.

[2] M. H. Nehrir, C. Wang, and S. R. Shaw, "Fuel Cell: Promising Devices for Distributed Generation," *IEEE Power & Energy Magezine,* pp. 47-53, January/Feb. 2006.

[3] M. D. Lukas, K. Y. Lee, and H. Ghezel-Ayagh, "Development of a Stack Simulation Model for Control Study on Direct Reforming Molten Carbonate Fuel Cell Power Plant," *IEEE Trans. on Energy Conversion,* Vol. 14, No. 4, pp. 1651-1657, November 1999.

[4] M. D. Lukas, K. Y. Lee, and H. Ghezel-Ayagh, "An Explicit Dynamic Model for Direct Reforming Carbonate Fuel Cell Stack," *IEEE Trans. on Energy Conversion,* Vol. 16, No. 3, pp. 289-295, September 2001.

[5] M. D. Lukas, K.Y. Lee, and H. Ghezel-Ayagh, "Modeling and Cycling Control of Carbonate Fuel Cell Power Plants," *Control Engineering Practice,* Vol. 10, pp. 197-206, 2002.
[6] K. Y. Lee, "The Effect of DG Using Fuel Cell under Deregulated Electricity Energy Markets," a Panel at the *IEEE Power Engineering Society General Meeting,* Montreal, June 2006.
[7] www.kpx.or.kr
[8] D. W. Park, "Impact of New Technology on the Korean Electricity Industry," *IEEE Power Engineering Review, pp.* 15-18, July 2001.
[9] K. B. Song and S. H. Kim," The Analysis of the Effects of the Renewable Energy on Power Systems and Operation Plans for Integrating Renewable Energy into Power Systems," *KPX Report,* Korea, October 2006.
[10] K. Y. Lee, S. H. Kim, E. W. Kim, and H. C. Kim, "Fuel Cell as an Alternative Distributed Generation Source under Deregulated Power System," *Proceeding of the 37th the KIEE Summer Annual Conference 2006*, pp. 331-332, July 2006.

VIII. BIOGRAPHIES

Kwang Y. Lee received his B.S. degree in Electrical Engineering from Seoul National University, Korea, in 1964, M.S. degree in Electrical Engineering from North Dakota State University, Fargo, in 1968, and Ph.D. degree in System Science from Michigan State University, East Lansing, in 1971. He has been with Michigan State, Oregon State, Univ. of Houston, and the Pennsylvania State University, where he is now a Professor of Electrical Engineering and Director of Power Systems Control Laboratory. His interests include power system control, operation, planning, and intelligent system applications to power systems. Dr. Lee is a Fellow of IEEE, Associate Editor of IEEE Transactions on Neural Networks, and Editor of IEEE Transactions on Energy Conversion. He is also a registered Professional Engineer.

Se Ho Kim was born in Seoul, Korea in 1961. He received his B.S., M.S. and Ph.D. degrees in electrical engineering from Yonsei University, in 1983, 1985 and 1992, respectively. Currently, he is a Full Professor in the Department of Electrical and Electronics Engineering, Cheju National University, Jeju, Korea. He is a Visiting Scholar at the Pennsylvania State University for February 2007 – February 2008. His current research interests include power system operation, renewable energy resources, wind power system, distributed system automation, and grounding systems. Dr. Kim is a member of IEEE and KIEE.

Received January18 2007

3. WAVELET-BASED ALGORITHM FOR POWER QUALITY ANALYSIS (PAPER 07GM0496).

Norman Tse , City University of Hong Kong, Hong Kong, China.

***Abstract*--**This paper presents a computational algorithm for identifying power frequency harmonics and oscillatory transients by using wavelet-based transform. The Continuous Wavelet Transform (CWT) using the Complex Morlet Wavelet (CMW) is adopted. A frequency detection algorithm is developed from the wavelet scalogram and ridges. A necessary condition is established to discriminate adjacent frequencies. By using adaptive wavelet filters, the instantaneous frequency identification approach is applied to determine the frequencies components and the oscillatory transient. Simulated data was used to demonstrate the accuracy of this approach.

Index Terms—Complex Morlet Wavelet (CMW), Continuous Wavelet Transform (CWT), frequency estimation, system harmonics, scalogram, wavelet ridges, oscillatory transients.

I. INTRODUCTION

POWER quality has become a major concern in recent years. International standards have been formulated to address the power quality issues [1]. The sources and causes of such disturbance must be known on demand sides before appropriate corrective or mitigating actions can be taken [2-3]. A traditional approach is to use Discrete Fourier Transform (DFT) to analyse harmonics contents of a power signal. The DFT is implemented by FFT which has the greatest feature of fast computational speed. Discrete Fourier Transform is basically a steady state analysis approach; it will interpret transient signal variations as a global phenomenon.

Nowadays power quality issues such as sub-harmonics, integer harmonics, inter-harmonics, transients, voltage sag and swell, waveform distortion, power frequency variations, etc. are experienced by electricity users. This paper attempts to develop an algorithm based on continuous wavelet transform to identify harmonics and oscillatory transients in a power signal [4].

II. WAVELET TRANSFORM AND ANALYSING WAVELET

Wavelet Transform can be continuous or discrete. Recent researches have been focused on Discrete Wavelet Transform (DWT) due to its fast computational speed, the orthogonal nature of wavelets and multi-resolution characteristics. However DWT is limited by its poor frequency resolution at high frequencies and poor time resolution at low frequencies.

Continuous Wavelet Transform (CWT) can provide very good frequency resolution; the only drawback is that it is computationally demanding. CWT is adopted in this paper for harmonic analysis because of its ability to preserve phase information [5-6] and to provide adaptive frequency resolution. Computational speed can be improved by frequency banding as discussed in Section VII.

The wavelet transform of a continuous signal, f(t), is defined as [5]

$$Wf(u,s)=\langle f,\psi_{u,s}\rangle=\int_{-\infty}^{+\infty} f(t)\frac{1}{\sqrt{s}}\Psi^{*}\left(\frac{t-u}{s}\right)dt, \qquad (1)$$

where $\psi^*(t)$ is the complex conjugate of the wavelet function $\psi(t)$;
s is the dilation parameter (scale) of the wavelet; and
u is the translation parameter (location) of the wavelet.

The wavelet function must satisfy certain mathematical criteria [7]. These are

- a wavelet function must have finite energy; and

- a wavelet function must have a zero mean, i.e., has no zero frequency component.

The simplified Complex Morlet Wavelet (CMW) [8-9] is adopted in the algorithm for harmonic analysis, defined as

$$\Psi(t) = \frac{1}{\sqrt{\pi f_b}} e^{\frac{-t^2}{f_b}} e^{j2\pi f_c t}, \tag{2}$$

where f_b is the bandwidth parameter and;
f_c is the centre frequency of the wavelet.

The CMW is essentially a modulated Gaussian function. It is particularly useful for harmonic analysis due to its smoothness and harmonic-like waveform. Because of the analytic nature, CMW is able to separate amplitude and phase information.

Strictly speaking, the mean of the simplified CMW in (2) is not equal to zero as illustrated in (3).

$$\int_{-\infty}^{+\infty} \Psi(t)dt = \frac{1}{\sqrt{\pi f_b}} \int_{-\infty}^{+\infty} e^{j2\pi f_c t} e^{\frac{-t^2}{f_b}} dt = e^{\frac{-f_b}{4}(2\pi f_c)^2} \tag{3}$$

However the mean of the CMW can be made arbitrarily small by picking the f_b and f_c parameters large enough [9]. For example, the mean of the CMW in (3) with f_b=2 and f_c=1 is 2.6753×10^{-9} which is practically equal to zero. The frequency support of the CMW in (2) is not a compact support but the entire frequency axis.

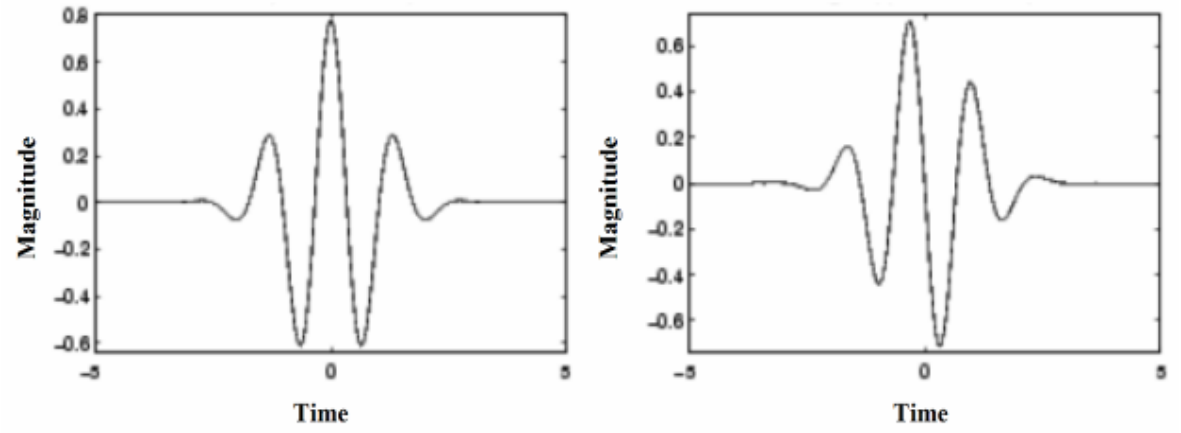

Real part Imaginary part

Fig. 1. The real part and imaginary part of the Complex Morlet Wavelet.

From the classical uncertainty principle, the time-frequency localization is measured in the mean squares sense and is represented as a Heisenberg box. The area of the Heisenberg box is limited by

$$\delta\omega\,\delta t \geq \frac{1}{2}, \tag{4}$$

where $\delta\omega$ is the frequency resolution, and δt is the time resolution.

For a dilated Complex Morlet Wavelet,

$$\delta\omega = \frac{1}{s\sqrt{f_b}}, \text{ and } \delta t = \frac{s\sqrt{f_b}}{2}. \qquad (5)$$

Complex Morlet Wavelet achieves a desirable compromise between time resolution and frequency resolution, with the area of the Heisenberg box equal to 0.5. From (5), the frequency resolution is dependent on the selection of f_b and the dilation. The dilation is dependent on f_c.

III. HARMONICS FREQUENCY DETECTION

Given a signal f(t) represented as

$$f(t) = a(t)\cos\phi(t), \qquad (6)$$

the wavelet function in (2) can be represented as [10]

$$\Psi(t) = g(t)e^{j\omega t}. \qquad (7)$$

The dilated and translated wavelet families [10] are represented as

$$\Psi_{u,s}(t) = \frac{1}{\sqrt{s}}\Psi\left(\frac{t-u}{s}\right) = e^{-j\xi u} g_{s,u,\xi}(t), \qquad (8)$$

where $g_{s,u,\xi}(t) = \sqrt{s}\, g\left(\frac{t-u}{s}\right)e^{j\xi t}$; and $\xi = \frac{\omega}{s}$.

The wavelet transform of the signal function f(t) in (6) is given as [10]

$$Wf(u,s) = \frac{\sqrt{s}}{2}a(u)e^{j\phi(u)}\left(\hat{g}(s[\xi - \phi'(u)]) + \varepsilon(u,\xi)\right). \qquad (9)$$

where $\hat{g}(\omega)$ represents the Fourier Transform of the function g(t).

The corrective term $\varepsilon(u,\xi)$ in (9) is negligible if a(t) and $\phi'(t)$ in (6) have small variations over the support of $\psi_{u,s}$ in (8) and if $\phi'(u) \geq \frac{\Delta\omega}{s}$ [10].

The instantaneous frequency is measured from wavelet ridges defined over the wavelet transform. The normalised scalogram defined by [10]

$$\frac{\xi}{\eta}P_W f(u,\xi) = \frac{|Wf(u,s)|^2}{s} \qquad (10)$$

is calculated with

$$\frac{\xi}{\eta}P_W f(u,\xi) = \frac{1}{4}a^2(u)\left|\hat{g}\left(\eta\left[1 - \frac{\phi'(u)}{\xi}\right]\right) + \varepsilon(u,\xi)\right|^2. \qquad (11)$$

Since $|\hat{g}(\omega)|$ in (11) is maximum at $\omega = 0$, if one neglects $\varepsilon(u,\xi)$, (11) shows that the scalogram is maximum at

$$\frac{\eta}{s(u)} = \xi(u) = \phi'(u). \qquad (12)$$

The corresponding points $(u, \xi(u))$ calculated by (12) are called wavelet ridges [11-13]. For the Complex Morlet Wavelet, g(t) in (7) is a Gaussian function. Since the Fourier Transform of a

Gaussian function is also a Gaussian function, the wavelet ridge plot exhibits a Gaussian shape (Fig. 2).

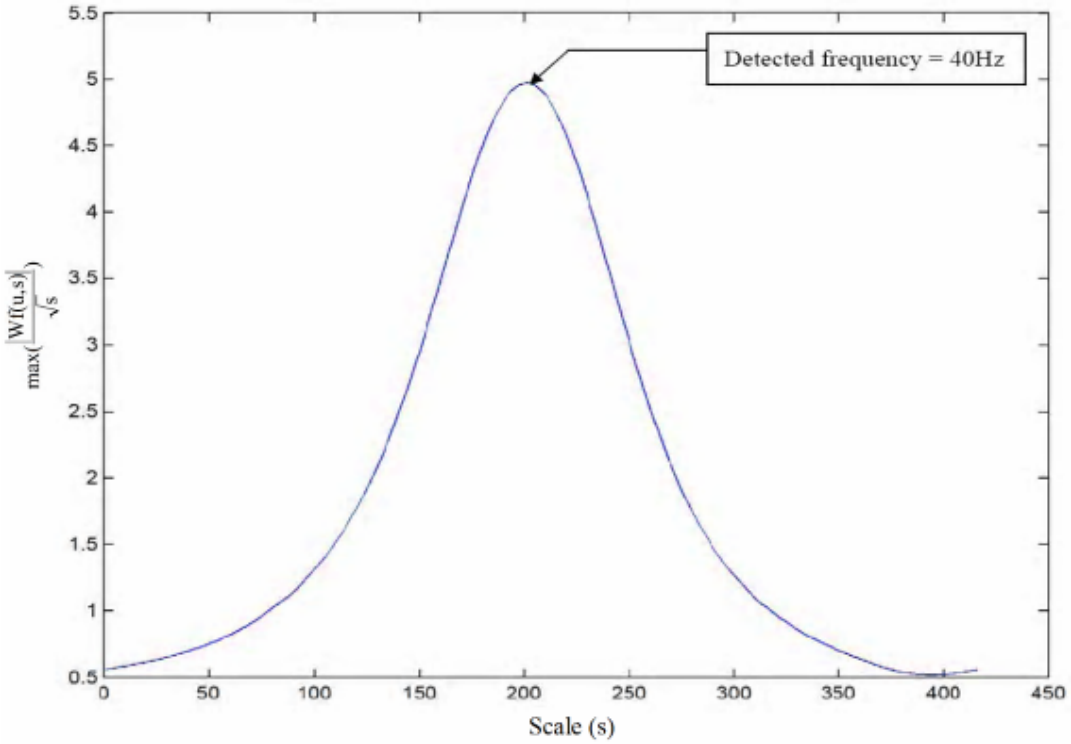

Fig. 2. Wavelet ridges plot showing a Gaussian shape.

IV. DISCRIMINATION OF ADJACENT FREQUENCIES

The Fourier Transform of a dilated CMW in (8) is represented as [10]

$$\Psi(sf)=\sqrt{s}e^{-\pi^2 f_b(sf-f_c)^2}. \tag{13}$$

The function $\Psi(sf)$ can be regarded as a bandpass filter centered at the frequency f_c. The bandwidth of the bandpass filter can be adjusted by adjusting f_b. The CWT of a signal is the convolution of the signal with a group of bandpass filters which are produced by the dilation of the CMW.

Suppose that (13) is represented as

$$\Psi(sf)=x, \tag{14}$$

where x represents an arbitrary magnitude to be defined later.

Combining (13) and (14) gives

$$f=\frac{f_c}{s}\pm\frac{1}{s\pi\sqrt{f_b}}\sqrt{\left|ln\left(\frac{x}{\sqrt{s}}\right)\right|}, \tag{15}$$

where $\frac{f_c}{s}$ is the centre frequency of the dilated bandpass

filter; and the bandwidth is $\frac{2}{s\pi\sqrt{f_b}}\sqrt{\left|ln\left(\frac{x}{\sqrt{s}}\right)\right|}$.

Fig. 3 shows the plot of the frequency support of two dilated CMW at scales S_1 and S_2 respectively.

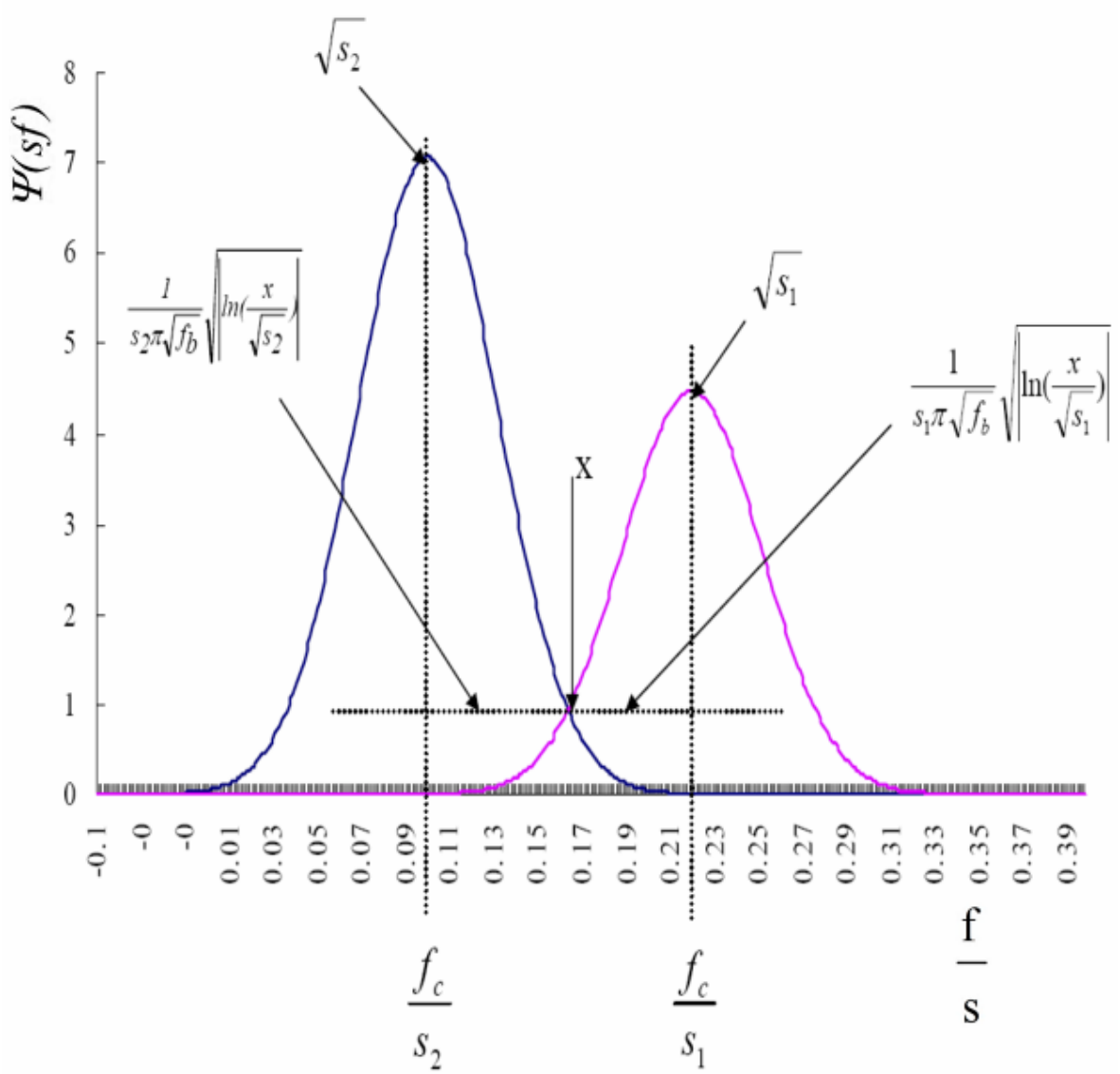

Fig. 3. Frequency plot of (15) for two CMWs at scales S_1 and S_2 respectively.

If the two dilated CMWs are used to detect two adjacent frequencies in a signal, with their frequencies represented as [14]

$$f_1 = \frac{f_s f_c}{S_1} \;\&\; f_2 = \frac{f_s f_c}{S_2}, \tag{16}$$

where f_s represents the sampling frequency, then

$$\frac{f_c}{S_1} - \frac{f_c}{S_2} = \frac{1}{S_1\pi\sqrt{f_b}}\sqrt{\left|ln(\frac{x}{\sqrt{S_1}})\right|} + \frac{1}{S_2\pi\sqrt{f_b}}\sqrt{\left|ln(\frac{x}{\sqrt{S_2}})\right|}. \tag{17}$$

Assume that $S_2 > S_1$, (17) is simplified to

$$f_c\sqrt{f_b} > \frac{1}{\pi}\sqrt{\left|ln(\frac{x}{\sqrt{S_1}})\right|}x\frac{f_2+f_1}{f_2-f_1}. \quad (18)$$

For $S_1 = 1$ and $x = 0.3$,

$$\frac{1}{\pi}\sqrt{\left|ln(\frac{x}{\sqrt{S_1}})\right|} = 0.35. \quad (19)$$

Substituting (19) into (18) gives

$$f_c\sqrt{f_b} > 0.35\,x\,\frac{f_2+f_1}{f_2-f_1};\ S_1 \le 1 \text{ and } x \le 0.3. \quad (20)$$

Equation (20) is used to determine the values of f_b and f_c in (2) for the continuous wavelet transform with Complex Morlet Wavelet which is a necessary condition to discriminate adjacent frequencies contained in the power signal. In the proposed detection algorithm, a separation of 25Hz between adjacent frequencies is used, i.e. the algorithm can be used to detect integer harmonics as well as non-integer harmonics.

V. HARMONICS AMPLITUDE DETECTION

Once the algorithms developed in Sections III and IV detect the harmonics contained in the power signal the corresponding harmonics amplitudes would be determined readily by

$$a(u) = \frac{2\sqrt{\frac{\xi}{\eta}P_W f(u,\xi)}}{|\hat{g}(0)|} = \frac{2\sqrt{\frac{|Wf(u,s)|^2}{s}}}{1} = \frac{2|Wf(u,s)|}{\sqrt{s}}. \quad (21)$$

The values of $2\sqrt{\frac{|Wf(u,s)|^2}{s}}$ in (21) are produced readily in the process of generating the scalogram.

VI. THE PROPOSED HARMONICS DETECTION ALGORITHM

Since convolution in time domain is equivalent to dot product in Fourier frequency domain, the algorithm can be implemented by Fast Fourier Transform (FFT) to reduce the computation time. The proposed detection algorithm is therefore implemented by FFT [5,13]. The flow chart of the algorithm is shown in Fig. 4. The proposed detection algorithm is implemented with Matlab software.

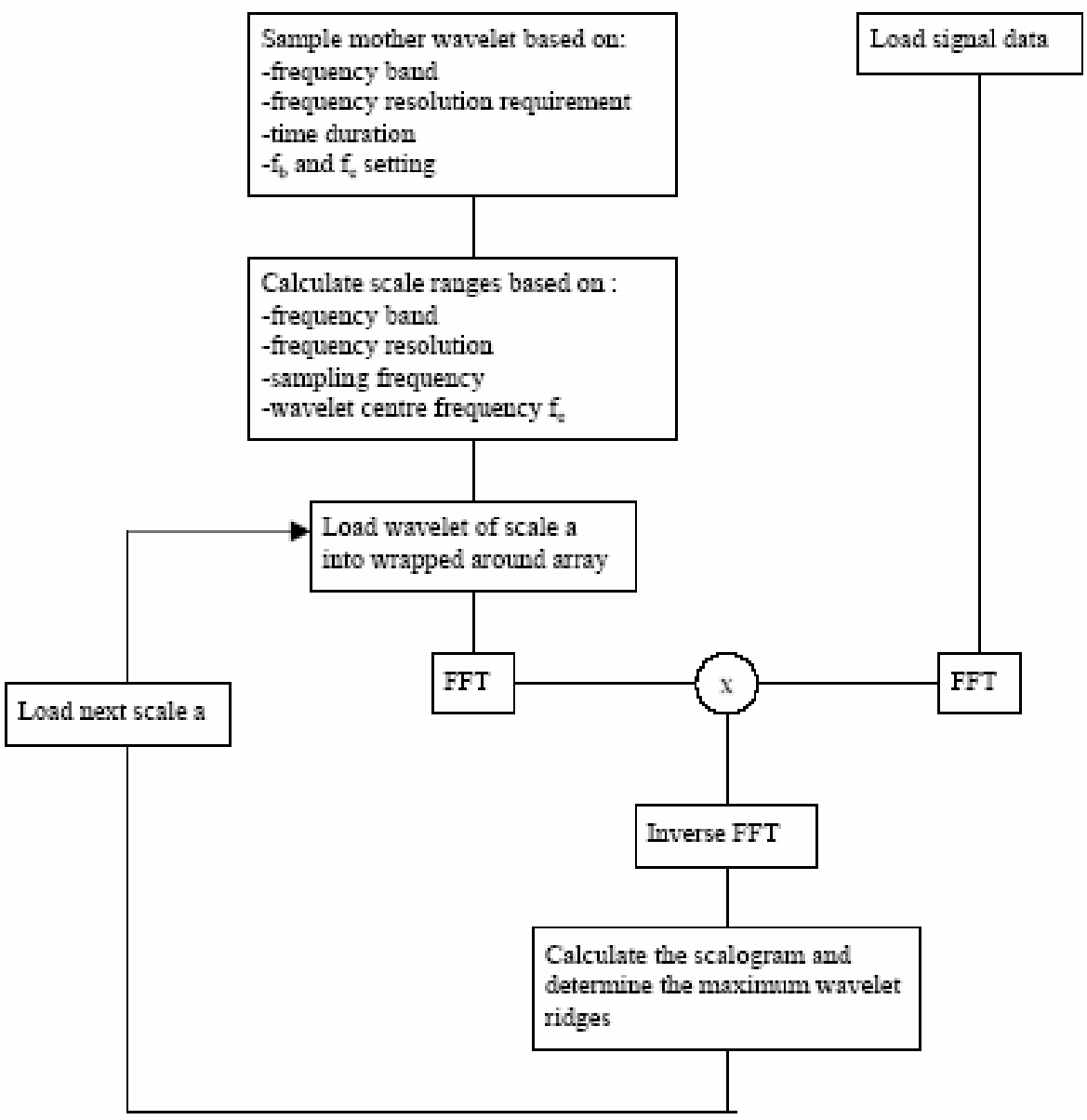

Fig. 4. The Flow chart of the proposed harmonics detection algorithm.

VII. SETTINGS OF THE DETECTION ALGORITHM

A simulated signal is used to test the proposed harmonics detection algorithm. The simulated signal contains signal frequency components as shown in Table I and an oscillatory transient.

TABLE I
HARMONICS IN THE SIMULATED SIGNAL

Harmonics (Hz)	Amplitude	Phase Angle (Degree)	Sampling Frequency (Hz)
45	100	0	6000Hz
99	77	-5	
249	35	-20	
401	20	-30	

The simulated oscillatory transient has the following properties:

- 2000Hz oscillating frequency;
- time duration is 2.16ms;
- 13 data points long sampled at 6000Hz;
- sampled peak value is equal to 93;
- peak value at data point 962 in the simulated signal.

Figs. 5 and 6 show the oscillatory transient and the simulated signal respectively.

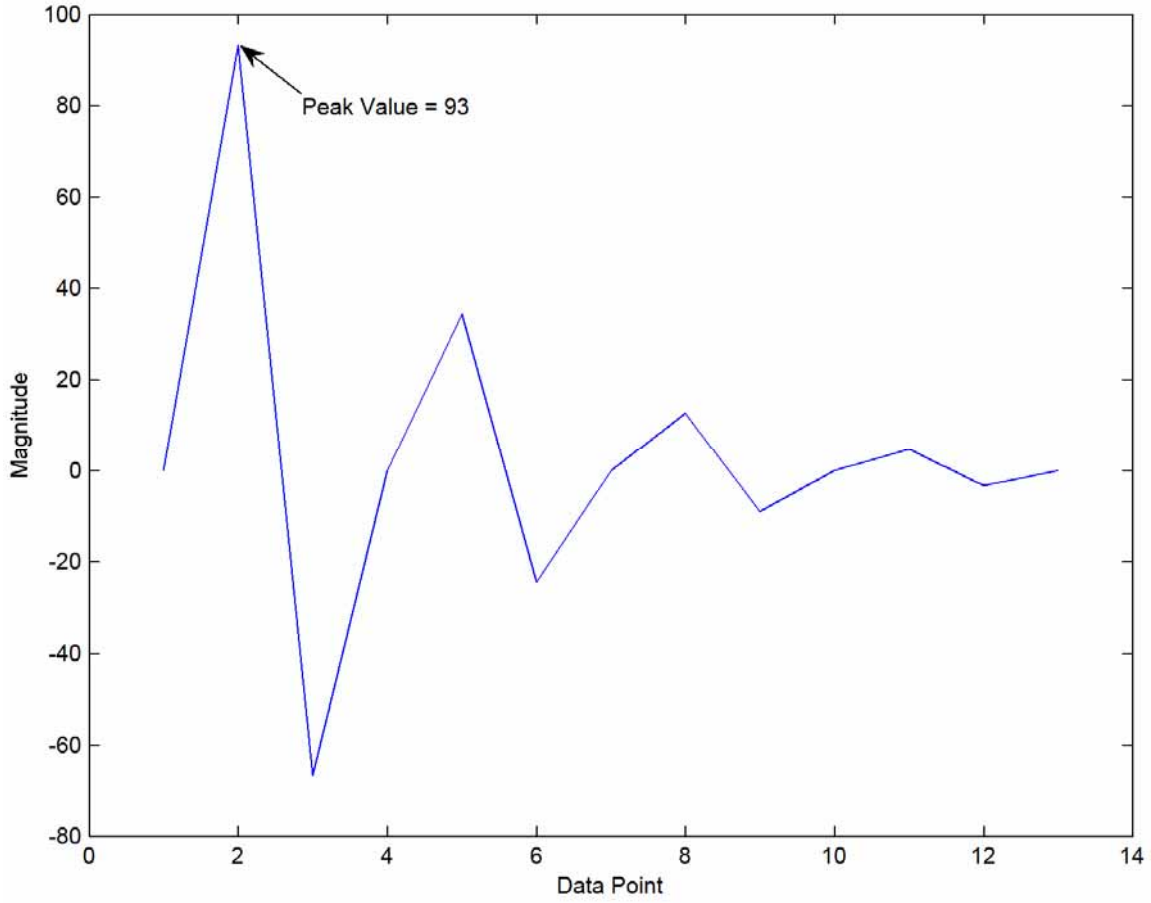

Fig. 5. The Oscillatory Transient.

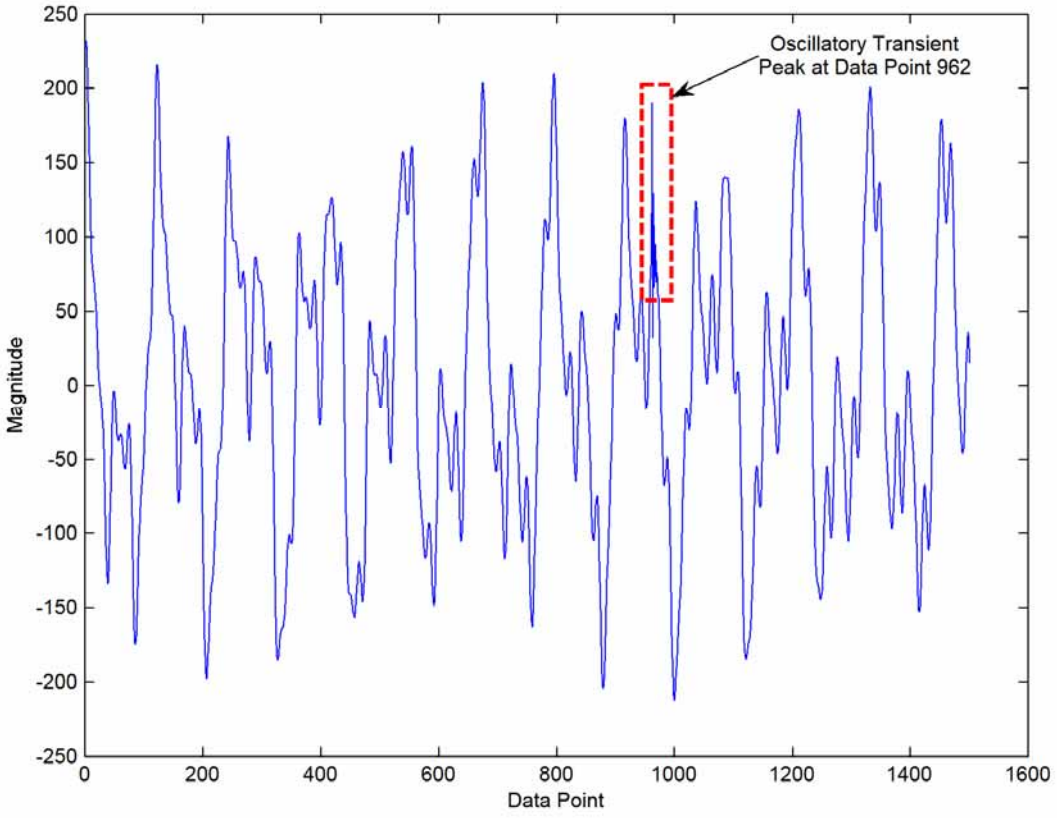

Fig. 6. The Simulated Signal.

From (5) and (16), the frequency resolution is dependent on the bandwidth parameter f_b and the centre frequency f_c of the dilated Complex Morlet Wavelet. Instead of using continuous scales for the wavelet dilation, adaptive scales are estimated from the frequency range in each frequency band by (16). The method not only can reduce computation time, but also provide an option in frequency resolution selection.

Table II shows the frequency band, the sampling frequency, time duration of the wavelet, and f_b & f_c settings. The frequency resolution is set at 1Hz.

TABLE II
SETTINGS OF THE PROPOSED DETECTION ALGORITHM

Frequency Range (Hz)	Sampling Frequency (Hz)	Time Duration (seconds)	fb - fc
30 - 60	6000	0.25	10000 - 0.0134
61 - 110	6000	0.25	10000 - 0.0275
111 - 175	6000	0.25	10000 - 0.046
176 - 275	6000	0.25	10000 - 0.074
276 - 425	6000	0.25	10000 - 0.116

For the detection of the oscillatory transient, the setting of the proposed detection algorithm is as shown in Table III.

TABLE III
SETTINGS OF THE PROPOSED DETECTION ALGORITHM FOR TRANSIENT DETECTION

Frequency Range (Hz)	Sampling Frequency (Hz)	Time Duration (seconds)	fb - fc
1500-2500	6000	0.25	10000 - 0.68

VIII. SIMULATION RESULTS

The simulation results for harmonics detection and oscillatory transient detection are shown in Table IV and V respectively. Fig. 7 shows the ridges plot and Fig. 8 to 11 show the amplitude plots of the harmonics frequencies. It can be seen that the accuracy of the proposed detection algorithm is extremely high. As can be seen in Fig. 8 to 11, the small errors in the amplitude detection are due to the presence of the oscillatory transient in the simulation signal.

The detected frequency of the oscillatory transient is 2131Hz. Comparing to the actual oscillatory frequency of 2000Hz, the detection error is 1.55% only. The actual transient peak is at data point 962 while the detected peak is at data point 964, i.e., an error of 0.33ms in time as compared to time duration 2.16ms of the oscillatory transient.

TABLE IV
HARMONICS DETECTION RESULTS

Detected Frequency (Hz)	Frequency Error	Detected Amplitude	Amplitude Error	Detected Phase (deg)	Phase Error
45	0%	100	0%	0.04^{o}	0.4%
99	0%	77.03	0.04%	-4.96^{o}	0.8%
249	0%	35.02	0.06%	-19.89^{o}	0.55%
401	0%	20.06	0.3%	-30.11^{o}	0.37%

TABLE V
OSCILLATORY TRANSIENT DETECTION RESULTS

Dominant frequency (Hz)	Peak location
2131	Data point 964

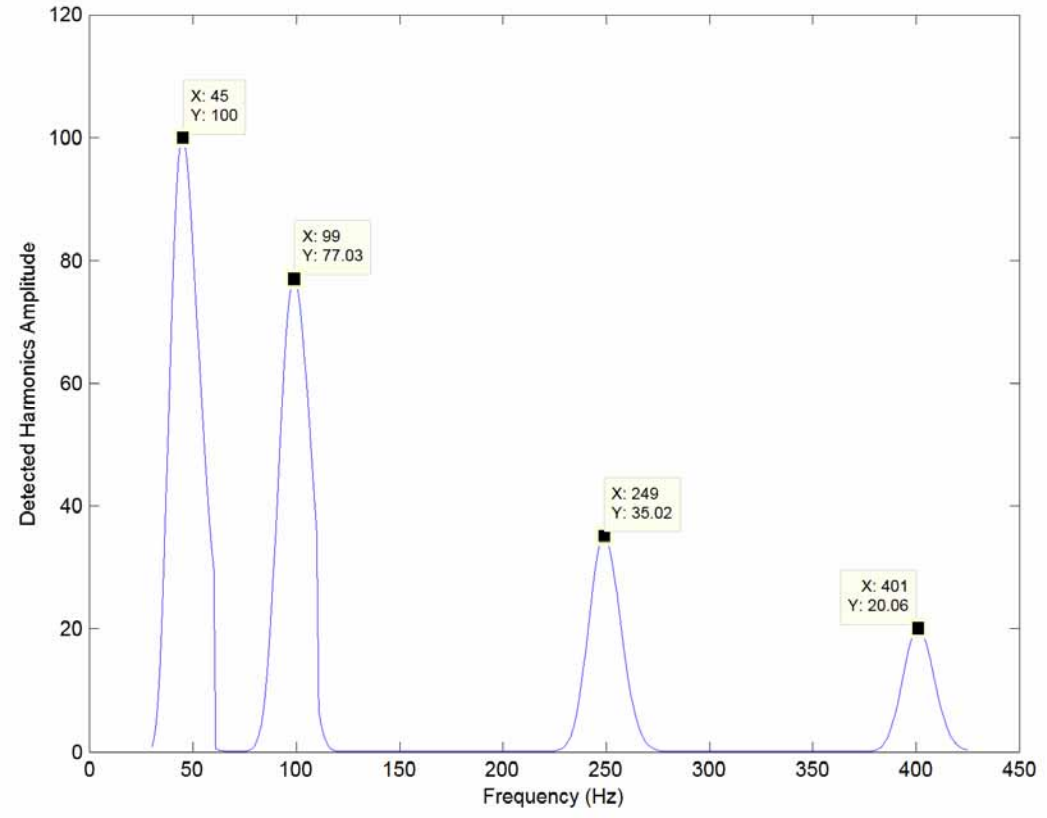

Fig. 7. The Wavelet Ridges Plot for Harmonics Frequency Detection.

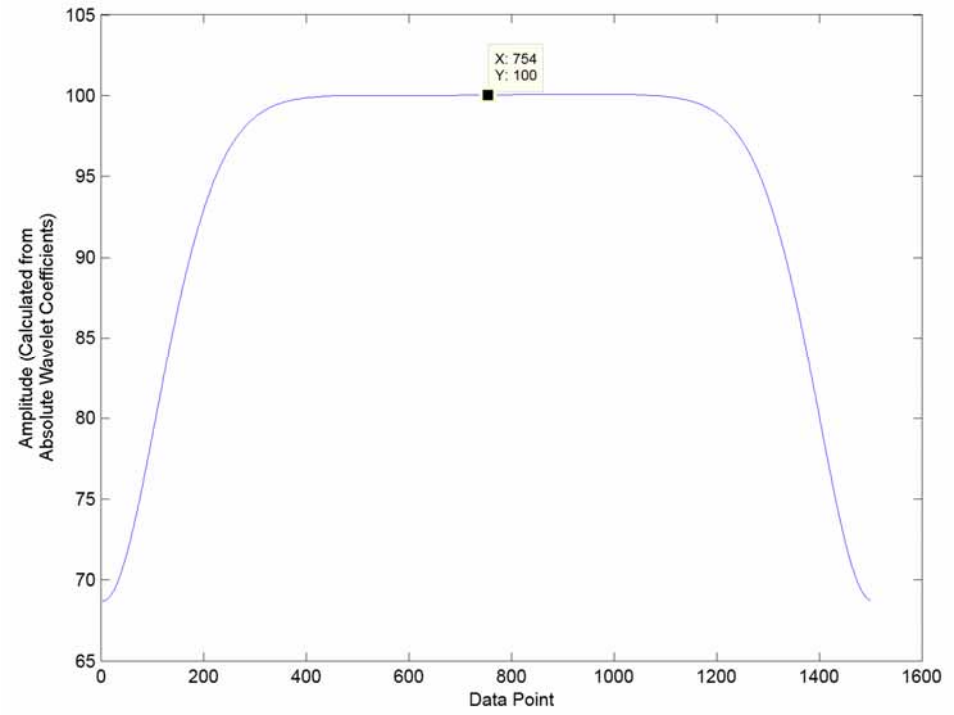

Fig. 8. The Amplitude Plot for 45 Hz Harmonics.

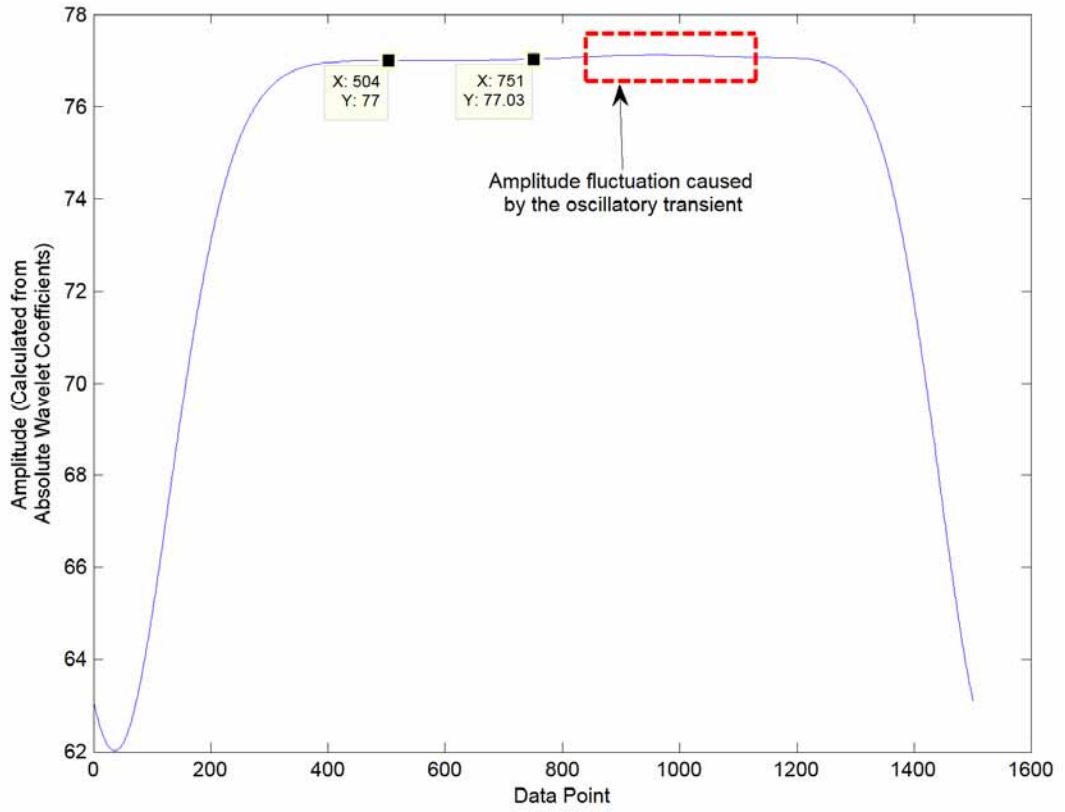

Fig. 9. The Amplitude Plot for 99 Hz Harmonics.

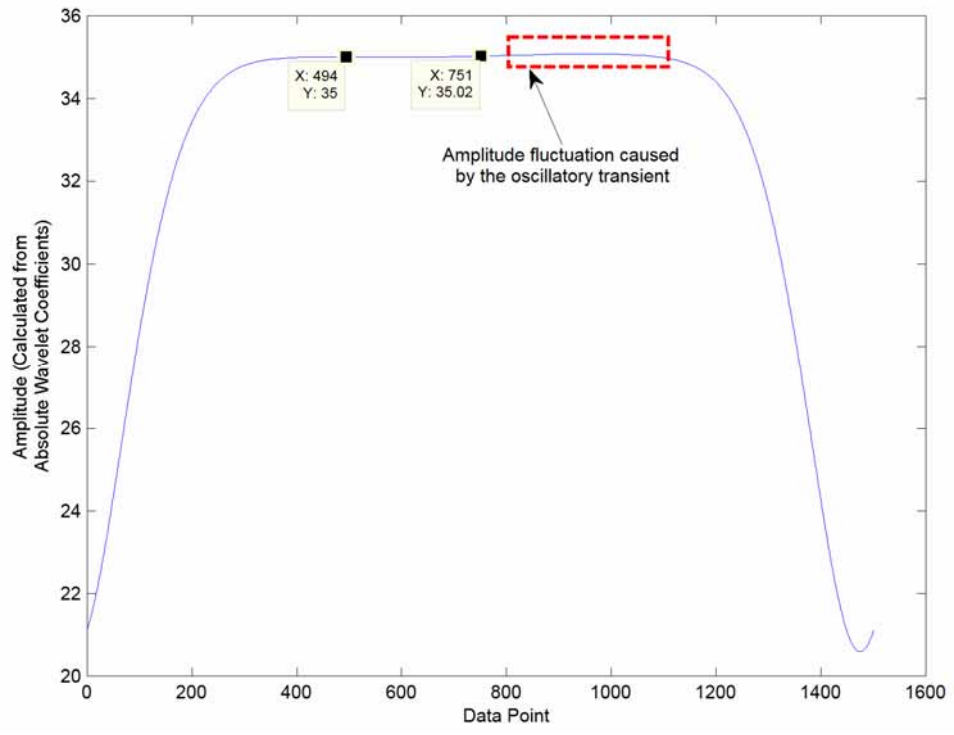

Fig. 10. The Amplitude Plot for 249 Hz Harmonics.

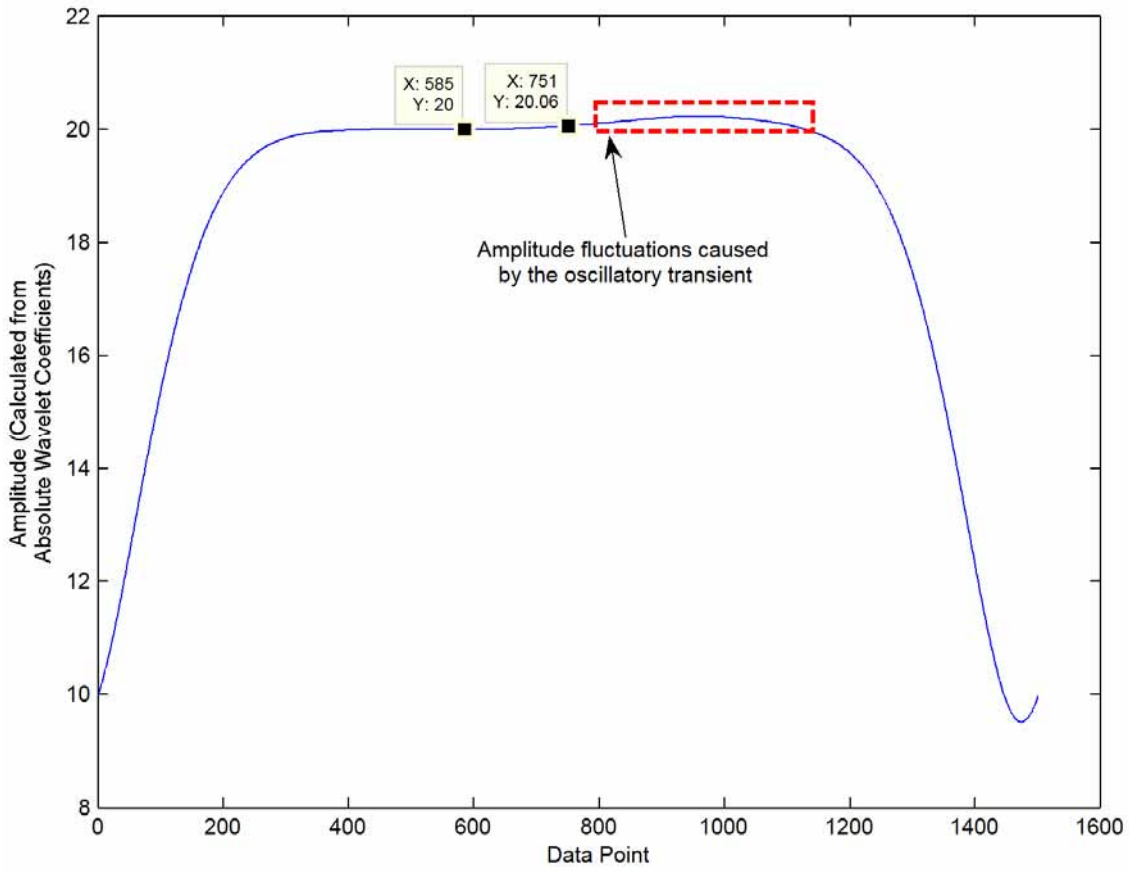

Fig. 11. The Amplitude Plot for 401 Hz Harmonics.

IX. CONCLUSIONS

The proposed harmonics detection algorithm is able to identify the frequency, amplitude and phase of harmonics in a power signal to a very high accuracy. The accuracy in the frequency estimation and peak location identification of an oscillatory transient is quite satisfactory.

Firstly a necessary condition for discrimination of adjacent frequencies is proposed which is used to select the bandwidth parameter f_b and centre frequency f_c of the Complex Morlet Wavelet. The Complex Morlet Wavelets thus specified for various frequency bands are capable to detect signal frequencies and amplitudes.

Secondly, the proposed detection algorithm makes use of frequency bands and selective scales for each frequency band to reduce the computation time. The computation time is greatly reduced by adaptive scales calculated from the frequency band and frequency resolution, as compared to continuous scales for the continuous wavelet transform. The computation time is further reduced by implementing the algorithm through FFT.

X. FURTHER WORK

Further experimental tests would need to be conducted for field data. A future paper will show simulation results that the proposed harmonic detection algorithm could be used to detect other transients.

XI. REFERENCES

[1] *IEEE recommended practice for monitoring electric power quality*, IEEE Standards Board, June 1995.
[2] L L Lai, W L Chan, C T Tse and A T P So, Real-time frequency and harmonic evaluation using artificial neural networks, *IEEE Transactions on Power Delivery*, Vol. 14, No. 1, January 1999, pp. 52-59.
[3] W L Chan, A T P So and L L Lai, Harmonics load signature recognition by wavelets transforms, *Proceedings of the International Conference on Electric Utility Deregulation, Restructuring and Power Technologies DRPT2000*, IEEE Catalog Number 00EX382, April 2000, pp. 666-671.
[4] Norman C F Tse, Practical application of wavelet to power quality analysis, *Proceedings of the 2006 IEEE Power Engineering Society General Meeting,,* IEEE Catalogue Number 06CH37818C, June 2006, CD ROM.
[5] Paul S Addison, *The Illustrated Wavelet Transform Handbook*, Institute of Physics Publishing Ltd., Bristol and Philadelphia, 2002.
[6] V. L. Pham and K. P. Wong, Wavelet-transform-based algorithm for harmonic analysis of power system waveforms, *IEE Proc. – Gener. Transm. Distrib*., Vol. 146, No. 3, May 1999.
[7] Gilbert Strang and Truong Nguyen, *Wavelets and Filter Bank*s, Wellesley-Cambridge Press, Wellesley, MA, January, 1996.
[8] Shyh-Jier Huang, Cheng-Tao Hsieh and Ching-Lien Huang, Application of morlet wavelets to supervise power system disturbances, *IEEE Trans. On Power Delivery*, Vol. 14, No. 1, Jan., 1999.
[9] Teolis, A., *Computational signal processing with wavelets*, Birkhauser, 1998.
[10] Stephane Mallet, *A Wavelet Tour of Signal Processing*, Academic Press, 1998.
[11] Rene A. Carmona, Wen L. Hwang and Bruno Torresani, Multiridge detection and time-frequency reconstruction, *IEEE Trans. on signal processing*, Vol. 47, No. 2, Feb., 1999.
[12] Rene A. Carmona, Wen L. Hwang and Bruno Torresani, Characterization of signals by the ridges of their wavelet transforms, *IEEE Trans. on signal processing*, Vol. 45, No. 10 Oct., 1997.
[13] D. Jordan, R. W. Miksad and E. J. Powers, Implementation of the continuous wavelet transform for digital time series analysis, *Rev. Sci. Instrum.* 68(3), March 1997, pp. 1484-1494.
[14] Misiti, M., Misiti, Y., Oppenheim, G., : '*Wavelet Toolbox for use with Matlab*,' (The Mathworks Inc., March 1996), pp. 6-43.

XII. BIOGRAPHIES

Norman, C. F. Tse was born in Hong Kong SAR, China on February 7, 1961. He graduated from the Hong Kong Polytechnic University (then Hong Kong Polytechnic) in 1985 holding an Associateship in Electrical Engineering. He obtained MSc degree from the University of Warwick in 1994. He is a Chartered Engineer, a Corporate member of the IET, UK (formerly IEE, UK) and the Hong Kong Institution of Engineers. He is now working with the City University of Hong Kong as a Senior Lecturer majoring in building LV electrical power distribution systems. His research interest is in power quality measurement, web-based power quality monitoring, and harmonics mitigation for low voltage electrical power distribution system in buildings.

Received January 29 2007

4. MANAGEMENT OF DISTRIBUTED GENERATION UNITS UNDER STOCHASTIC LOAD DEMANDS USING PARTICLE SWARM OPTIMIZATION (PAPER 07GM0751).

V. S. Pappala and I. Erlich (University of Duisburg-Essen, Germany).

***Abstract*—**This paper presents a Particle Swarm Optimization (PSO) approach to manage the daily electricity and heat generation in proton exchange membrane (PEM) fuel cells for residential applications under electrical demand uncertainties. The stochastic load processes are modelled as scenario trees using adaptive PSO. The resulting multistage nonlinear stochastic cost model aims to minimize the average operating costs over this scenario tree. Adaptive PSO is used to solve this model and the results are compared with the deterministic model.

Keywords - Distributed generation, particle swarm, stochastic optimization, uncertainty modeling

I. INTRODUCTION

DUE to the deregulation of the energy market, distributed generation (DG) has a huge impact on electric power market. The main idea behind the use of DG [1] for residential applications is to supply electricity to customers at a competitive price. The other benefits include efficient use of electrical and thermal energy, improved power quality, increased reliability and reduced emission. Out of the many DG units such as micro turbines, wind turbines, photovoltaic cells, combustion engines and diesel engines, fuel cells have become the most competitive [2]. As fuel cells are capable of generating electrical as well as thermal energy they are a good choice for residential utilization. However the high cost of electricity generated by fuel cell has restricted its use in DG. Many researchers have proved that the operating costs of the fuel cells can be drastically decreased by appropriate settings of the unit for optimal operation.

This paper presents an approach to reduce the daily total operating costs of a proton exchange membrane (PEM) fuel cell supplying a residential load under electrical demand uncertainty. A cost model [3] is developed to minimize the daily total operating costs of a fuel cell taking into account the various operating and technical constraints associated with the unit. The major issue in developing such a cost model is the representation of the underlying uncertainties. The significant uncertainties in the cost model include the electrical demand, thermal demand, cost of purchased electricity and cost of sold electricity. In this paper the fuel cell is modelled taking into account just the stochastic electrical demand. Even a slight variation of the temperature results in a huge variation of the electrical demand. So the electrical load demand cannot be forecasted accurately and is therefore a random process. The evolution of this random process i.e. all future realizations of the electric demand, is modelled as a scenario tree [4], where each scenario represents an instance of the future realizations. The scenario tree is visualized as a set of nodes. It starts with a root node at stage one. The information at this node is completely defined. The root node then branches of into several successor nodes. The tree progresses until the end of the planning horizon. The nodes at this stage are called the leaf nodes. The number of scenarios corresponds to the number of leaf nodes. The scenarios together with the node probabilities thus form a good discrete approximation of the uncertain load demand. The conventional scenario tree generation methods pose a restriction on the number of branching stages and the number of samples at each stage. Due to the restriction on these key parameters the stochastic model does not replicate the real model and there is a huge modelling error. To overcome these barriers a new approach of generating scenario trees using adaptive Particle Swarm Optimization (PSO) is presented. The conventional methods start with an initial bulk tree and then reduce the insignificant branches to reduce the tree. In the new approach the tree generation starts with a single scenario and then adds the best branches to generate the scenario tree. There is no need for the initial bulk tree and hence no restrictions on the

key parameters.

The scenario tree modelling transforms the cost model to a stochastic multistage nonlinear mixed integer model. Such a model can be solved without decomposition using adaptive PSO technique. PSO is an efficient tool for handling nonlinear, non-differentiable and multi-model problems. It can handle continuous as well as discrete variables. It has been successfully tested on numerous applications such as function minimization, training Neural Network weights etc.

The paper is organized as follows. The next section presents the deterministic economic model of the PEM fuel cell. A PSO algorithm is introduced in section III. In section IV, fuel cell modelling under stochastic load demands is discussed. The optimization results are presented in section V.

II. PEM FUEL CELL: DETREMINISTIC ECONOMIC MODEL

A. Objective Function

The following fuel cell model has been taken from [3]. The objective is to minimize the daily total operating costs of a fuel cell taking into account the following assumptions:

- The fuel cell will supply both electrical and thermal power to the load
- There is a possibility to sell back the excess electricity at different tariffs. These tariffs are always lower than those of the purchased electricity
- A part of the generated power is utilized by the auxiliary devices.

The objective function is developed according to the above mentioned assumptions in the following form.

$$DOC=DFC+DCPE-DISE+DCPG+O\&M+STC \tag{1}$$

- where:

- *DOC* :Daily total operating cost ($)
- *DFC* :Daily fuel cost for the fuel cell ($)
- *DCPE* Daily cost of purchased electricity if the demand exceeds the produced electrical power ($)
- *DISE* :Daily income on sold electricity if the unit electrical output power exceeds the electrical demand ($)
- *DCPG* :Daily cost of purchased gas for residential loads if the produced thermal power is not enough to meet the thermal demand ($)
- *O&M* :Daily operating and maintenance cost ($)
- *STC* :Daily start up cost ($)
-

The dependence of DFC on the generated electrical power and efficiency is given as:

$$DFC = C_{nFC} T \sum_{J} U_J \frac{P_J + P_a}{\eta_J} \tag{2}$$

where:

- C_{nFC} : Natural gas price for fuel cell ($/kWh)
- T : Time duration (h)
- P_J : Net electrical power produced at interval “J” (kW)
- P_a : Power for auxiliary devices (kW)
- η_J : Cell efficiency at interval “J”

- U_J : Unit commitment at interval "J"
-

The efficiency of the fuel cell depends on the active power [5] and hence, a typical efficiency curve (3) is developed as a function of the electrical power and is used in (2).

-

$$\eta_J = 0.4484 - 0.05359\, P_J + 0.01267\, P_J^2 - 0.00182\, P_J^3 \tag{3}$$

The main grid system is assumed to balance the difference between the load demand and the net output from the fuel cell.The cost of electricity purchased from and sold back to the network is given by:

$$DCPE = C_{elp}\, T \sum_J U_J \max(D_{el,J} - P_J, 0) \tag{4}$$

$$DISE = C_{els}\, T \sum_J U_J \max(P_J - D_{el,J}, 0) \tag{5}$$

where:

C_{elp}, C_{els} :Tariffs of purchased and sold electricity respectively ($/kWh)
$D_{el,J}$:Electrical demand at interval "J" (kW)

The thermal output power from the fuel cell depends on the electrical power. The relation is almost linear at the lower values, while the ratio of the thermal power is relatively higher at the upper operating limits [5]. A nonlinear equation is developed to give the thermal output power of the unit as a function of the produced electrical power. The daily cost of purchased natural gas for residential applications when the thermal power from the fuel cell is not enough to meet the thermal load requirements is given as:

$$DCPG = C_{n2} T \sum_J U_J \max(D_{th,J} - P_{th,J}, 0) \tag{6}$$

where:

C_{n2} : Fuel price for residential loads ($/kWh)
$D_{th,J}$: Thermal load demand at time interval "J" (kW)
$P_{th,J}$: Thermal power produced at interval "J" (kW)

The operating and maintenance (O&M) cost is assumed to be constant per kWh and hence O&M is proportional to the produced energy. The start up cost depends on the temperature of the unit and hence on the time the unit has been switched off before start up:

$$STC = \sum_J U_J (1 - U_{J-1})(\alpha + \beta(1 - e^{\frac{-T_{J,off}}{\tau}})) \tag{7}$$

where:

α, β : Hot and cold start up costs respectively
$T_{J,off}$: The time the unit has been switched off till current interval J(h)
τ : The fuel cell cooling time constant (h)

B. Constraints

The minimization of the objective function (1) is restricted by many constraints. The main operational and technical constraints associated with the PEM fuel cell are listed below:

- Unit capacity constraints : $P_J^{\min} U_J \le P_J \le P_J^{\max} U_J$ (8)
- Ramp rate constraints : $P_J U_J - P_{J-1} U_{J-1} \le \Delta P_U$ (9)
- $P_{J-1} U_{J-1} - P_J U_J \le \Delta P_D$ (10)

In the above equations, $P_J^{\min}$ and $P_J^{\max}$ are the minimum and maximum limits of the generated power, ΔP_U and ΔP_D are the upper and lower limits of the ramp rate, and P_{J-1} is the power generated at interval (J-1).At the same time, the minimum up/down time limits (continuous running-stop time constraint) must not be violated:

$$(T_{J-1}^{on} - MUT)(U_{J-1} - U_J) \ge 0 \quad (11)$$

$$\left(T_{J-1}^{off} - MDT\right)\left(U_J - U_{J-1}\right) \ge 0 \quad (12)$$

Where T_{J-1}^{on}, T_{J-1}^{off} are the unit on and off times at interval (J-1), MUT, MDT are the minimum up and down time limits and U is the unit on/off status: U=1 for running mode and 0 for stop mode. Finally, the daily number of start-stop times ($n_{start-stop}$) should not exceed a certain maximum number (N_{max}).

$$n_{start-stop} \le N_{\max} \quad (13)$$

III. PARTICLE SWARM OPTIMIZATION

Particle swarm optimization [6]-[7] is an evolutionary computational technique developed by Kennedy and Eberhart in 1995.Unlike the other search algorithms PSO finds the optimal solution not by survival of the fittest but by a process motivated by the simulation of social behavior such as fish schooling and birds flocking in search of food. It is a population based search algorithm. It is initialized by a population of random solutions called particles and the group of particles is called a swarm. Each particle in the swarm moves over the search space with a certain velocity. The velocity of each particle as given by (14) is influenced by the particles own flying experience as well as its neighbors flying experience. The velocity of each particle depends on three terms. The first term is the inertia velocity which carries information regarding the particles previous history of velocities. The second term is the cognitive part which reflects the particles behavior with respect to its own previous experiences. The final term is the social parameter which indicates the particles behavior with respect to the experience gained from the other members of the swarm. This velocity when added to the previous position generates the current position of the particle (15). PSO solves a highly constrained problem as an unconstrained one by adding a suitable penalty function to the main objective function.

$$V_i^{k+1} = \chi(wV_i^k + c_1 r_1 (P_i - X_i^k) + c_2 r_2 (P_g - X_i^k)) \quad (14)$$

$$X_i^{k+1} = X_i^k + V_i^{k+1} \quad (15)$$

Adaptive particle swarm optimization technique [8] is used for all the simulations presented in this paper. An adaptive version of PSO is used for uncertainty modeling to generate the scenario tree and is also used for solving the multi-stage stochastic optimization problem. The significant feature of this algorithm is that the optimization algorithm can be used as a black box; the user has to specify just the search space, the objective function to be minimized and stopping criteria for the algorithm.

The user is totally free from parameter tuning and also from the burden of selecting the most appropriate swarm (population) size.

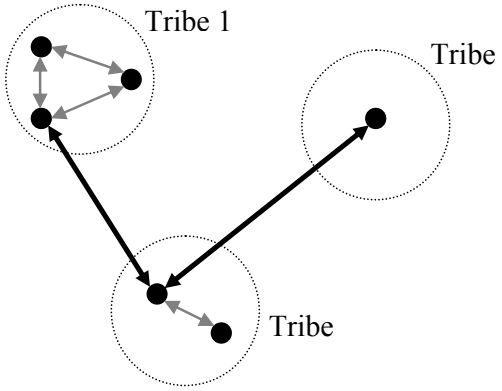

Fig. 1. Tribes of different sizes and the information links among them.

In this algorithm, different sized groups of particles called "*Tribes*" move about in an unknown environment in search of an optimal solution. Information links exist among the particles in a tribe. These particles collectively explore the search space to find a local minimum. Each such tribe succeeds in finding a local minimum. Information links also exist among the different tribes through which they exchange information regarding their local minimums to collectively decide the global minimum. The optimization process starts with a single particle representing a single tribe .After a few iterations if this particle does not improve its fitness, it generates a new particle forming a new tribe .After further iterations if neither of these particles improve their fitness ,each of these particles generate a particle simultaneously forming a new tribe with two particles. The process of evolution continues until the stopping criterion is met.

PSO has been chosen because it has many prominent merits over the other evolutionary algorithms. It has a high probability of finding a global minimum. The search process is faster and robust. It does not require parameter tuning.

IV. PEM FUEL CELL: STOCHASTIC ECONOMIC MODEL

A. Uncertainty Modeling

The first step in solving the stochastic cost model of the fuel cell is to model the underlying stochastic electric load demands. In this case study the fuel cells supplies power to a small residential load. One cannot exactly predict when the resident will switch on the air-conditioner (peak load) or for how long the lights will be switched on. These utilizations depend totally on the weather conditions. Therefore the electric load demands of a residential utilization shows huge variations even with minute changes in the weather conditions. Hence while forecasting such load demands, they have to be analyzed quite frequently (Three to four times an hour). The uncertainty in the electrical demand increases with time. We assume that the increase is as shown in the following figure.

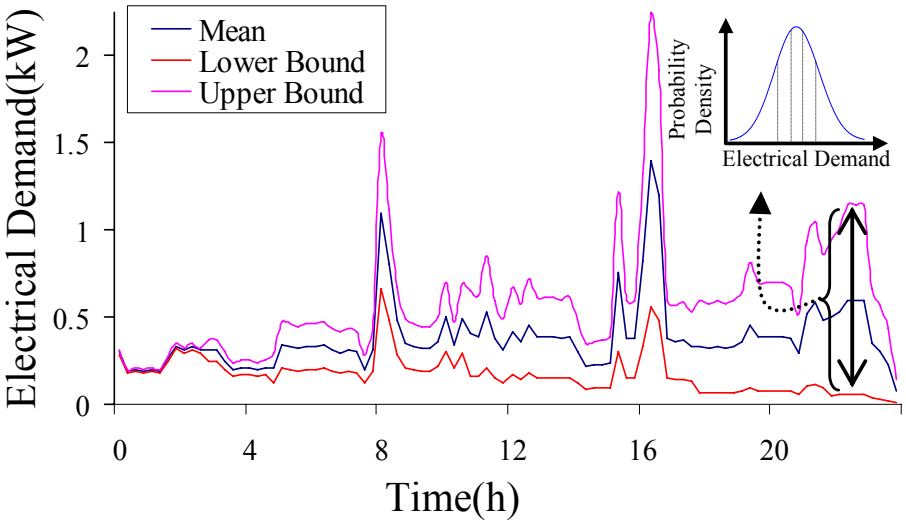

Fig. 2. Evolution of uncertainty over time.

We assume that the uncertainty evolve as a discrete random process. The evolution of this random process over time i.e. all possible future demands is realized in the form of a scenario tree with finite set of nodes as shown below.

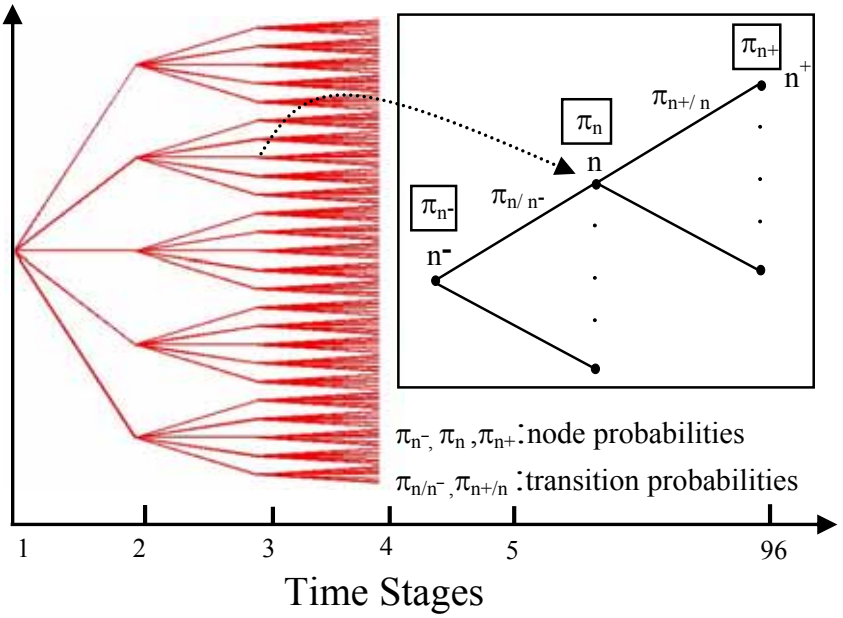

Fig. 3. Standard scenario tree with 95 branching stages and 5 branches at each stage.

Each node of the scenario tree is a decision making point. A decision involves in selecting one of the discrete approximation (e.g. the number of approximations are five for time period t=2) of the stochastic random process (Electric load demand) at that time stage. Once a decision is made at time t, the information regarding the uncertainty at time t is known only at the beginning of the next time stage t+1.The decision making process over the whole planning horizon is presented as a scenario tree. For the optimal operation of the fuel cell, the settings have to be updated every 15 minutes and hence for a planning horizon of 24 hours, there are 96 decision making stages. We

assume that the information at stage 1(root node) is completely known. Hence there are 95 decision making stages. The uncertainty at each stage is approximated to a Gaussian distribution as shown below.

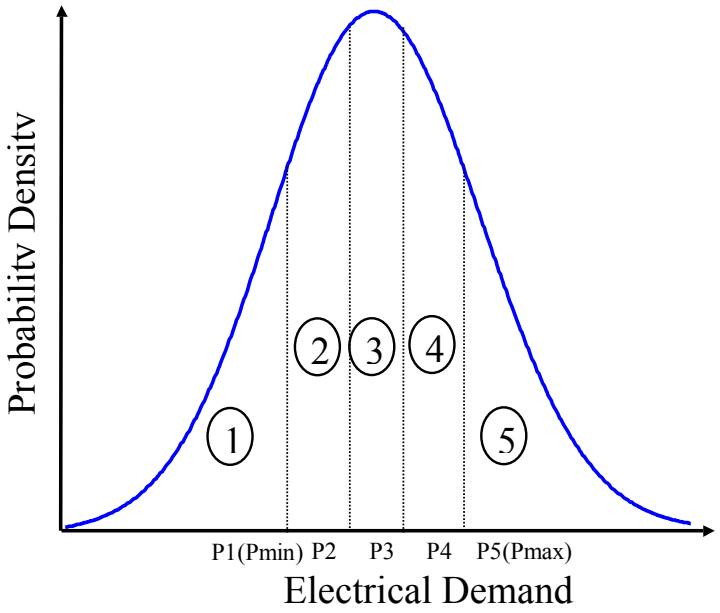

Fig. 4. Gaussian distribution of the stochastic electrical demand at a given time stage.

The distribution has a mean equal to the mean electrical demand at that stage and standard deviation corresponds to that shown in Fig. 2. The Gaussian distribution is normalized so that the sum over all possible instances of the electrical demand gives a probability of 1. The area under the curve is divided into five equal blocks. All values of the electrical demand in one region are approximated to their corresponding P value (mean value of that region) as shown in Fig. 4. For example all the values in region 2 are approximated to P2. Therefore the random electrical demand at any given node of the scenario tree is discretized into five samples of equal probability.

Each node (n) of the scenario tree has a unique predecessor node (n-) and a transition probability $\pi_{n/n-}>0$, which is the probability of n being the successor of n-. The probability π_n of each node n is given recursively by $\pi_1=1$, $\pi_{n/n-}*\pi_{n-}$ for $n\neq1$.The probabilities of all the nodes at any given time stage add to one. The future research will try to associate appropriate transition probabilities for each of these samples. The scenario tree therefore consists of 595 scenarios. Although this huge number of scenarios completely represents the randomness of the stochastic variable, it is quite cumbersome to solve the stochastic model. The conventional scenario reduction schemes can be used to prune the original tree but as there are more branching stages, the process is very complex and time consuming. Hence a method which is totally free from such restrictions is presented in this paper.

Adaptive PSO is used to generate the scenario tree. The particle represents a scenario. The particle is a 95 dimensional vector where each dimension represents a branching stage. The tree generation process is considered as an ordinary optimization problem whose objective is to maximize the fitness of each particle given by the following equation.

$$objective = \max_{m \in N_p} fitness(particle^m) \tag{16}$$

$$fitness(particle^m) = \min_{q \in N_p} \pi_m \left\{ \sum_{k=0}^{N_T} (\pi_k^m D_k^m - \pi_k^q D_k^q)^2 \right\}^{\frac{1}{2}} \quad (17)$$

where

N_p : Total number of particles in the swarm
N_T : Total number of branching stages
π_m : Total Probability of particle "m" from root to leaf node
π_k^m : Probability of particle m at time stage k.
D_k^m : Electrical demand corresponding to particle m at stage k

The process of generating the scenario tree can be explained by the following flowchart.

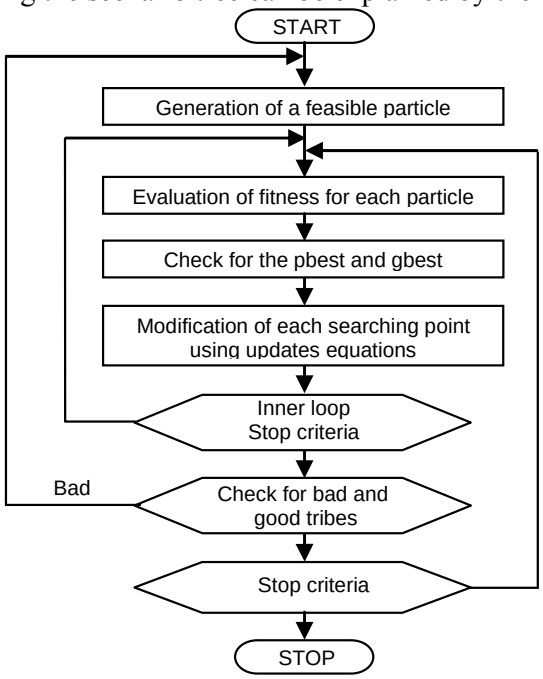

Fig. 5. Flowchart for generating the scenario tree using adaptive particle swarm approach

The process starts with the random generation of a single particle within the admissible range. The particle then enters the inner loop where a fitness value is assigned based on (17).The fitness value of a particle is the minimum weighted euclidian distance from the other particles in the swarm. Since the swarm initially has a single particle, the fitness of this particle is assumed to be the distance from a dummy particle The computational results of such a tree based stochastic cost model were very close to the true model. i.e. particle representing the mean load. The best position vector (pbest) represents the best position encountered by the particle and the global best position vector (gbest) represents the best among all the particles in the swarm. Initially these vectors are set to the current searching point. In the next step the particle searching point is updated based on (14)-(15).

The inner loop is checked for the termination condition. Outside the inner loop the tribe is evaluated. During these evaluations either a new tribe is added or an existing tribe is deleted based on the performance of the existing tribes. The tribe is considered good if it has a greater number of good particles and is considered bad if it has a greater number of bad particles. A particle is considered good if any of its previous two performances are improvements and is considered bad if

neither of its previous two performances are improvements. Such an adaptation creates competition among the particles of a tribe as well among the tribes. If a tribe happens to be bad, none of its particles could converge to local minima and therefore the tribe requires more particles to find an optimal solution. Therefore the tribe identifies the best particle in it and this particle would generate a new particle representing a new tribe. On the other hand a good tribe would identify the worst particle in it and removes it since this particle does not carry any significant information about the tribe. The outer loop is executed until the stopping criterion, which is usually the maximum number of function evaluations, is met. The probability of the deleted particle is added to its nearest neighbor. Towards the end of the process only those particles with significant fitness value survive. Since the particles represent the scenarios, we are left with only the distinct scenarios.

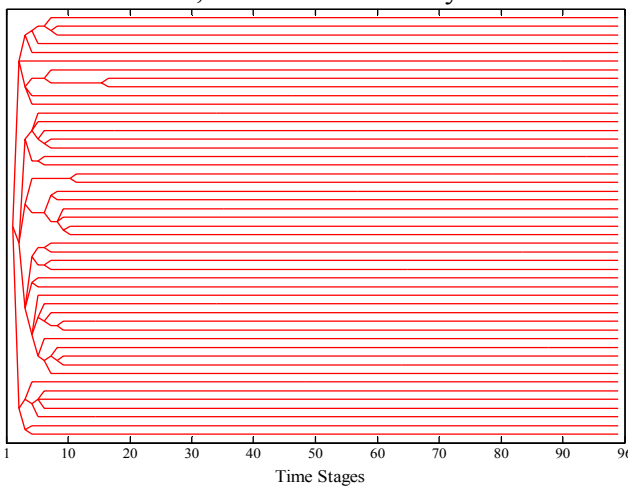

Fig. 6. Scenario tree generated by PSO for 95 branching stages and 5 branches at each stage.

B. Stochastic Optimization

With the scenario tree approach described above, the uncertainty is incorporated into the traditional cost model of the fuel cell. The cost model is solved using multistage stochastic optimization programming. The objective of the multistage stochastic optimization problem is to minimize the expectation of the daily total operating costs of a fuel cell as shown below.

$$\min E\left\{\begin{array}{l} C_{nFC}T\sum_J U_J \dfrac{P_J+P_a}{\eta_J} + C_{elp}T\sum_J U_J \max(D_{el,J}-P_J,0) \\ C_{els}T\sum_J U_J \max(P_J-D_{el,J},0) + K_{O\&M}T\sum_J U_J P_J \\ C_{nRL}T\sum_J U_J \max(D_{th,J}-P_{th,J},0) + \\ \sum_J U_J(1-U_{J-1})(\alpha+\beta(1-e^{\frac{-T_{J,off}}{\tau}})) \end{array}\right\} \quad (18)$$

The objective can be realized by minimizing the average operating costs over the scenario tree.

$$\min \sum_{n \in N} \pi_n \left\{ \begin{array}{l} C_{nFC} T \sum_J U_J^n \dfrac{P_J^n + P_a}{\eta_J^n} + \\ C_{elp} T \sum_J U_J^n \max(D_{el,J}^n - P_J^n, 0) + \\ C_{els} T \sum_J U_J^n \max(P_J^n - D_{el,J}^n, 0) + K_{O\&M} T \sum_J U_J^n P_J^n + \\ C_{nRL} T \sum_J U_J^n \max(D_{th,J}^n - P_{th,J}^n, 0) + \\ U_J^n (1 - U_{J-1}^n)(\alpha + \beta(1 - e^{\frac{-t_{off}}{\tau}})) \end{array} \right\} \quad (19)$$

where

N :Total number of nodes

P_J^n :Electrical power produced at interval "J" and node n(kW)

-

- Unit capacity constraints : $P_J^{n,\min} U_J^n \le P_J^n \le P_J^{n,\max} U_J^n$ (20)
- Ramp rate constraints : $P_J^n U_J^n - P_{J-1}^{n^-} U_{J-1}^{n^-} \le \Delta P_U$ (21)

• $P_{J-1}^{n^-} U_{J-1}^{n^-} - P_J^n U_J^n \le \Delta P_D$ (22)

$(T_{J-1}^{on} - MUT)(U_{J-1}^{n^-} - U_J^n) \ge 0$ (23)

$(T_{J-1}^{off} - MDT)(U_J^n - U_{J-1}^{n^-}) \ge 0$ (24)

$n_{start-stop} \le N_{\max}$ (25)

Note that the objective (19) and constraints of (20-25) correspond directly to (1)-(13). The tree based model for N nodes involve N binary, N continuous decision variables, N bounds and 5N inequality constraints. Table I shows how the size of the mixed integer nonlinear problem of the scenario tree model increases with the number of nodes.

TABLE I
SIZE OF THE SCENARIO TREE MODEL DEPENDING ON THE NUMBER OF SCENARIOS (S) AND NODES (N)

S	N	Variables		Constraints	*Bounds*
		Continuous	Binary		
1	96	96	96	480	*96*
15	504	504	504	2520	*504*
46	978	978	978	4890	*978*
125	*1548*	*1548*	*1548*	*7740*	*1548*

The stochastic cost model is solved using adaptive particle swarm optimization approach. Each node of the scenario is associated with two decision variables (1: optimal power generation, 2: unit commitment). Hence for a N node scenario tree, the particle represents a 2N-dimensional vector. The fitness of each particle is given by (19). The objective of the optimization process is to minimize the fitness of each particle.

$$objective = \min_{m \in N_p} fitness(particle^m) \quad (26)$$

The optimization process is the same as described by the flowchart in Fig. 4.

V. RESULTS OF THE OPTIMIZATION PROCESS

The adaptive PSO for scenario tree generation and stochastic optimization was implemented using visual C language. The results were computed on an Intel Pentium 4 CPU 3.00 GHz 1GB RAM. The basic C program for adaptive PSO was taken from *http://clerc.maurice.free.fr/pso/#Tribes*. In order to evaluate the performance of the scenario tree generation using the evolutionary algorithm, several numerical tests were conducted. Since it is quite difficult to solve the stochastic model with 595 scenarios, the dominant (peak demand) branching stages t_1=33, t_2=66, t_3=90 are considered. These accounts to 53 scenarios. The stochastic model was solved with this standard tree and the results are compared to the scenario tree generated by PSO. The results are presented in table II. The results show that this approach is a good alternative to the conventional method.

TABLE II
COMPARISON OF THE INITIAL TREE WITH THE PRUNED TREE

Type	S	N	Objective
Pruned Tree	7	294	2.165
Pruned Tree	15	504	2.180
Pruned Tree	22	624	2.200
Pruned Tree	46	978	2.252
Initial Tree	125	1548	2.327

The deterministic cost model of a 4 kW fuel cell unit was solved for the load curve in Fig. 2. The tests were carried out with C_{nFC} =0.05$, C_{elp} =0.16$, C_{els}=0.10$,$C_{nRL}$=0.09$. Under the optimal operation, the daily operating costs amount to 2.098$ while non-optimal operation (operating at 4 kW) costs 7.623$. There is a reduction of 5.525$ per day which amounts to 2016.6$ per year. In order to check the influence of uncertainty on the operating cost, the stochastic model was solved for the same set of conditions. The uncertainty was modeled as a scenario tree with 95 branching stages and 5 branches at each stage. (The initial scenario tree with 595 scenarios is reduced to a tree with 49 scenarios and 4468 nodes as shown in Fig. 6. The stochastic model is solved over the scenario tree. The operating cost under these conditions was 2.757$.The reduction is approximately 4.866$ per day and 1776.1$ per year. The value of stochastic solution which measures the advantage of using the stochastic model is 240.5$/year.

TABLE III
COMPARISON OF THE PRODUCTION COSTS FOR DIFFERENT MODELS

Model	Production Cost($/day)
Full capacity generation model	7.623
Deterministic mean model	2.098
Stochastic model	2.757
Non-optimal generation to meet electrical demand	2.585

The results show that considerable reduction can be made in the operating costs of the fuel

cell. Hence fuel cells can be a competitive energy source for distributed generation. .

VI. CONCLUSION

This paper presented an evolutionary based approach to model the uncertainties prevailing in the cost model of the fuel cell. A new scenario tree generation algorithm using adaptive PSO is proposed. This approach is proved to be more efficient than the conventional tree generation as it has no restriction on the evolution of the scenario tree. For computational simplicity, the current model considered only the electrical demand as an uncertain variable. However the proposed approach can be extended to any number of uncertainties.

Secondly, adaptive particle swarm optimization was successfully applied to solve the multistage mixed-integer nonlinear cost model without any decomposition techniques. PSO algorithm is more efficacious in handling mixed-integer nonlinear problems. It was observed that the uncertainties had a significant impact on the daily operating costs. The computational results of such a tree based stochastic cost model were very close to the true model. Further research is required to investigate the effect of all the other uncertainties on the operating costs.

VII. References

[1] Electric Power Research Institute.Distributed Generation.Webpage www.epri.com.
[2] Review of State-of-the Art Fuel Cell technologies for distributed Generation (ECW report number 193-2).
[3] Ahmed M. Azmy ,B.P. Wachholz and I.Erlich , "Management of PEM Fuel Cells for Residential Applications using Genetic Algorithms" The ninth International Middle-east Power systems conference(MEPCON) ,Egypt,December,16-18,2003
[4] Kjetil Hoyland and Stein W. Wallace, "Generating Scenario Trees for Multistage Decision Problems" Management Science 2001 INFORMS Vol. 47,No 2,February 2001 pp. 295-307
[5] F. Barbir and T. Gomez "Efficiency and Economics of Proton Exchange Membrane (PEM) Fuel Cell", Int. J. Hydrogen Energy,Vol 21, No 10, pp 891-901,1996.
[6] J.Kennedy and R.C. Eberhart. "Particle Swarm Optimization" International Conference on Neural Networks IV, pages 1942-1948, Piscataway, NJ, 1995. IEEE E Service Center.
[7] J.Kennedy and R.C. Eberhart. *Swarm Intelligence*, Morgan Kaufmann Publishers, 2001.
[8] Maurice Clerc, "TRIBES, a Parameter Free Particle Swarm Optimizer" French version: 2003-10-02.Presented at OEP'03, Paris, France.
[9] T.O. Ting, M.V.C.Rao, and C.K.Loo, "A Novel Approach for Unit Commitment Problem via an Effective Hybrid Particle Swarm Optimization". *IEEE Transactions on Power Systems, vol.21,no.1, February 2006.*
[10] http://www.swarmintelligence.org
[11]

VIII. BIOGRAPHIES

Venkata Swaroop Pappala (1981) received the B.E degree in electrical engineering from Faculty of Electrical engineering, S.V.H College of engineering, India in 2002, and M.Sc. degree in electrical engineering with emphasis on power and automation from University Duisburg-Essen, Germany in 2005. He is currently a Ph.D. student at the University of Duisburg-Essen, Germany. His research interests include stochastic optimization under uncertainty using evolutionary algorithms.

Istvan Erlich (1953) received his Dipl.-Ing. degree in electrical engineering from the University of Dresden/Germany in 1976. After his studies, he worked in Hungary in the field of electrical distribution networks. From 1979 to 1991, he joined the Department of Electrical Power Systems of the University of Dresden again, where he received his PhD degree in 1983. In the period of 1991 to 1998, he worked with the consulting company EAB in Berlin and the Fraunhofer Institute IITB Dresden respectively. During this time, he also had a teaching assignment at the University of Dresden. Since 1998, he is Professor and head of the Institute of Electrical Power Systems at the University of Duisburg-Essen/Germany. His major scientific interest is focused on power system stability and control, modelling and simulation of power system dynamics including intelligent system applications. He is a member of VDE and senior member of IEEE.

Received January 26 2007

5. THE EFFECT OF ISLAND INTERCONNECTIONS ON THE INCREASE OF WIND POWER PENETRATION IN THE GREEK SYSTEM (PAPER 07GM1075).

Nikos Hatziargyriou[#], Zoe Vrontisi, and Antonis G. Tsikalakis {National Technical University of Athens, Greece), and Vasilis Kilias (Center of Renewable Energy (CRES), Athens, Greece).

Abstract: Greece is a country with many dispersed islands where favorable conditions for exploiting RES exist. Cyclades is a group of islands that some of them are not so far away to be interconnected with the mainland and among them. This interconnection will reduce the need for operating the local oil-fired stations and extending the area they occupy to meet future needs.

This paper presents an additional benefit from the Interconnection of Cyclades to the mainland, the exploitation of the very favorable wind conditions of the area. With the use of Geographical Information Systems (GIS) the most promising locations for installing wind power have been identified with the restriction of the thermal limits of the interconnection lines. The results from investment analysis of wind power after interconnection of Cyclades show clear financial benefits for the potential investors even without subsidy.

Index Terms— Wind Power, Geographical Information Systems (GIS), Autonomous power systems, economic analysis

I. INTRODUCTION

Greece is a country with many dispersed islands especially in its eastern part. In the western part of Greece, all islands of the Ionian Sea are interconnected to the mainland Hellenic Transmission System (HTS) [1] with the exception of two tiny islands near northern Corfu. Saronic Gulf islands and few islands near Magnisia, Central Greece, are interconnected as well. On the contrary, most of the Aegean Sea islands are not interconnected to the mainland network mainly due to their significant distance from the mainland. The population on these islands is roughly 1,000,000 citizens and electricity consumption is about 4% of the total electricity consumption in Greece. The annual electricity demand is increasing by 8 %, which is almost double of the annual demand increase in the mainland (4.2 %).

As it is common for many other islands around the world, electricity production is mainly based on the consumption of imported oil; resulting in increased cost on the energy produced and increased dependency on imported fuel with fluctuating price. Moreover, oil-fired stations are one of the main detrimental installations both environmentally and aesthetically in the sensitive environment of the islands. This leads to intense reactions from the local communities, especially when existing thermal plants need extension of their installations.

On the islands of the Aegean Sea and especially on Cyclades high wind potential exists with average winds usually exceeding 8 m/sec. The legal framework, has given since 1994 a significant motivation to the private sector to invest and develop wind parks 180MW of 661MW of the installed capacity in Greece while further proposals up to 221MW for installing wind parks on most Greek islands have been positively qualified [2].. However, technical constraints due to the autonomous power system operation limits bring problems of co-operation of wind power with the existing power stations, limiting the potential for installing wind power [3].

[#] N. D. Hatziargyriou, Z.Vrontisi A. Tsikalakis are with the School of Electrical and Computer Engineering, National Technical University of Athens, Athens, Greece,9 Heroon Polytechniou Str , GR 15773,Athens,Greece. E-mail: nh@power.ece.ntua.gr zvrontisi@gmail.com, atsikal@power.ece.ntua.gr)

V.Kilias is with the Centre of Renewable Energy Sources(CRES), 19thkm Marathonos Ave, Pikermi,Athens,GR19009,vkillias@cres.gr)

The distance among the Cycladic islands is rather short, allowing the interconnection between them without significant technical problems. Some of them are not so far away for interconnecting them to the HTS taking into account the technological improvement in interconnections via HVAC or HVDC technology [4].

Implementing such an inter-connection, helps in increasing the reliability of supply in the islands, reducing significantly the operating hours of the local oil-fired power stations and thus the local pollution of their fragile environment. Furthermore, interconnection can help in alleviating the need for extending the area that existing power stations on the islands use, to meet the future needs of the islands. Moreover, it can help in exploiting the favorable wind regime that exist on Cyclades, either meeting the local demand or injecting energy to the HTS near the centre of consumption, Athens helping in meeting the EC directive requirements [5].

The scope of this paper is to identify, with the aid of Geographical Information Systems (GIS), the financially promising sites on the islands to be interconnected for exploitation of wind parks taking into account a) environmental and other site-specific restrictions and b) the thermal limits of the submarine cables to be used for the islands interconnections.

The structure of the paper is as follows. In section II, the current situation regarding the electricity sector on the islands to be interconnected is described. In the same section the plans for interconnections of the Cycladic islands according to the studies conducted by the HTS Operator [6] are described. In section III the parameters used for the GIS studies are presented while in Section IV the energy output calculations are presented. Finally, the economic analysis is presented in Section V and conclusions are drawn in Section VI.

II. EXISTING AND FUTURE INTERCONNECTIONS OF THE CYCLADIC ISLANDS WITH THE MAINLAND

A. EXISTING INTERCONNECTIONS AND INSTALLATIONS

The islands to be interconnected with the mainland are Andros, Tinos, Syros, Mykonos, Paros and Naxos. On these islands only a minor part of the wind energy potential of the region has actually been exploited and the energy production is mainly based on the diesel units existing on these islands. The current installation of thermal power stations and wind power is presented in Table [6,7]

TABLE I. INSTALLED RES CAPACITY ON THE GREEK CYCLADIC ISLANDS

Islands to be connected to H.T.S	Installed Thermal Capacity (MW)	Installed W/P Capacity (MW)
Naxos	0	1.75
Syros	24	3.05
Paros	54	0.11
Mykonos	34	0.3
Andros	12.3	1.575
Tinos	0	0.4
Total	**124.3**	**7.185**

The following interconnection projects concerning the examined islands have already been completed [1].

- Evia island is interconnected with Attica via submarine (u/w) cable HV transmission line (400kV)
- Andros is interconnected with Evia via 150 kV u/w line.

- Andros is interconnected with Tinos (the existing Medium voltage u/w line of 150kV operates at 20kV)
- Tinos is interconnected with Syros and Mykonos (66kV existing u/w lines operate at 20kV)

The necessity for further interconnection of these islands has already been a matter of study of a joint commission with members from Public Power Corporation (PPC), currently the operator of the power system of the islands, the HTSO and the Regulatory Authority of Energy [8]. According to this report the interconnection project is bound to begin around 2010. The main objective of this project is to ensure the reliable supply of the islands as well as the gradual decommissioning of the autonomous diesel stations. As it can be concluded from the current research, the Interconnection of Cyclades will result in a much higher penetration of wind energy installed in the examined area, constituting also a solution to the continuously increasing energy demand of this region. Moreover, the combination of the Interconnection and the growth of Wind Parks enable the progressive decommissioning of the diesel power stations, ensuing in numerous environmental and financial profits.

B. FUTURE INTERCONNECTIONS

The proposed interconnection topology is presented in Fig. 1. According to the legal framework, the project should be accomplished in such a way that environmental impacts will be minimal. More specific, the construction of new overhead High Voltage transmission lines (150kV) on the islands is prohibited and the new substations (in Syros, Mykonos, Paros and Naxos) will be constructed in carefully selected areas.

As it is proposed, the islands to be connected with submarine 150kV line are Syros, Andros, Tinos, Mykonos, Paros and Naxos. The existing interconnections will be used and Syros will be interconnected to Lavrio, Attica Coast, with submarine cable. Possible interconnection with Milos, where favourable geothermal potential exist, is under study by the committee. Regarding the technology that will be applied for the Syros-Lavrio inter-connection, there has been no decision on whether HVDC or HVAC cables will be used. No matter what the interconnection capacity technology may be, its capacity will not be higher than 400MW, due to restrictions of transmission system on the mainland. The HVAC technology has many former applications that provide experience (the know-how of the technology) and reliability, and HVDC technology is an emerging technology that requires D.C/A.C inverters to be installed on Syros Island. However, the latter can ensure that the voltage imbalances and the harmonics are within the standard thresholds, as are used and hence no need for many other power electronics devices exists to alleviate such problems [4].

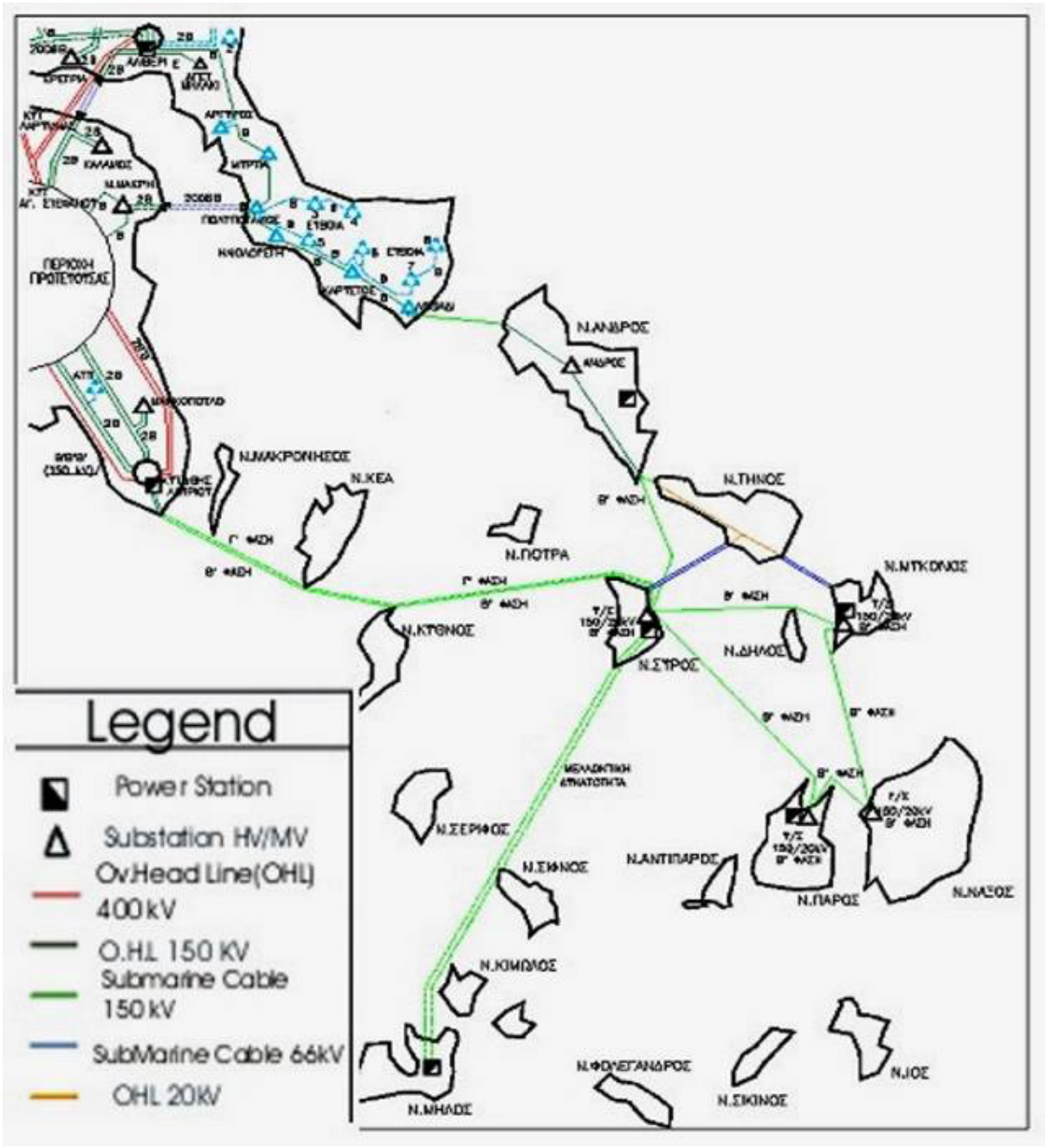

Fig.1: Distribution of RES installations in Greece [8]

III. The Use of Geographical Information System (GIS)

A. GEOGRAPHICAL INFORMATION SYSTEMS

In order to meet the directives of the Kyoto protocol by the year 2010 the state target of Greece is 20.1% penetration of RES in Electricity production amounting to 14.5 TWh per year [9]. As a result, a high number of RES plants have to be installed. Such an installation involves several financial and technical risks, hence apart from the purely connection and operation issues, there is the need for handling the geographical dimension of RES in a rather sensitive area like the islands. Moreover, analysis with GIS can help in identifying the distances from the substation of the island

in order to be taken into account in the financial analysis of connection of potential wind parks sites.

The ESRI ArcView GIS 3.1 [10], which is software widely used (ESRI proposes almost 30% of the world market of GIS), was selected for our application and has been used in collaboration with CRES (Center of Renewable Energy Sources) [11]. CRES provided us with the digital database, which includes information on the wind speed, the altitude, the flow accumulation, the distance from existing roads and other useful data concerning the Cycladic Islands.

The GIS software is used in order to define the possible sites for the installation of Wind Parks. Table II describes the parameters used in the GIS application, which refer to restrictions regarding security, technical, environmental and infrastructure networks. Additionally, a filter concerning the visibility of the installation with Ancient Monument Areas was enabled, which prohibits the visibility of a wind turbine (50m height) for a distance of 3km and for an observatory height equal to 2m.

TABLE II. PARAMETERS OF GIS

Parameter	**Value**
Terrain slope	<15º
Altitude	<1200m
Wind speed	>6 m/s
Max. installed MW per W/P	<20 MW
Archaeological sites Filter	Enabled
Visibility with ancient monuments	Enabled
Nature Protected Areas Filter	Enabled
Proximity to towns or villages	>1000m
Distance from coastline	>1000m

In Fig. 2 the potential Wind Parks are indicated with a purple pentagon, as they were selected in the GIS application for the island of Tinos. Fig. 2 does not include the visibility from ancient monuments restrictions, while Fig. 3 shows the actual perimeter that is barred when the filter is enabled. The island of Tinos is a specific case, where many archaeological sites exist (marked with orange color on the map). Consequently, after the activation of the filter for the visibility together with ancient monuments many possible W/P sites have been omitted (around 150MW).

One basic result of this analysis is the average wind speed of the projected Wind Park sites, which for the 290 possible sites on the islands is approximately 9.7m/s, creating together with results of the economic analysis a promising environment for investors of wind plants.

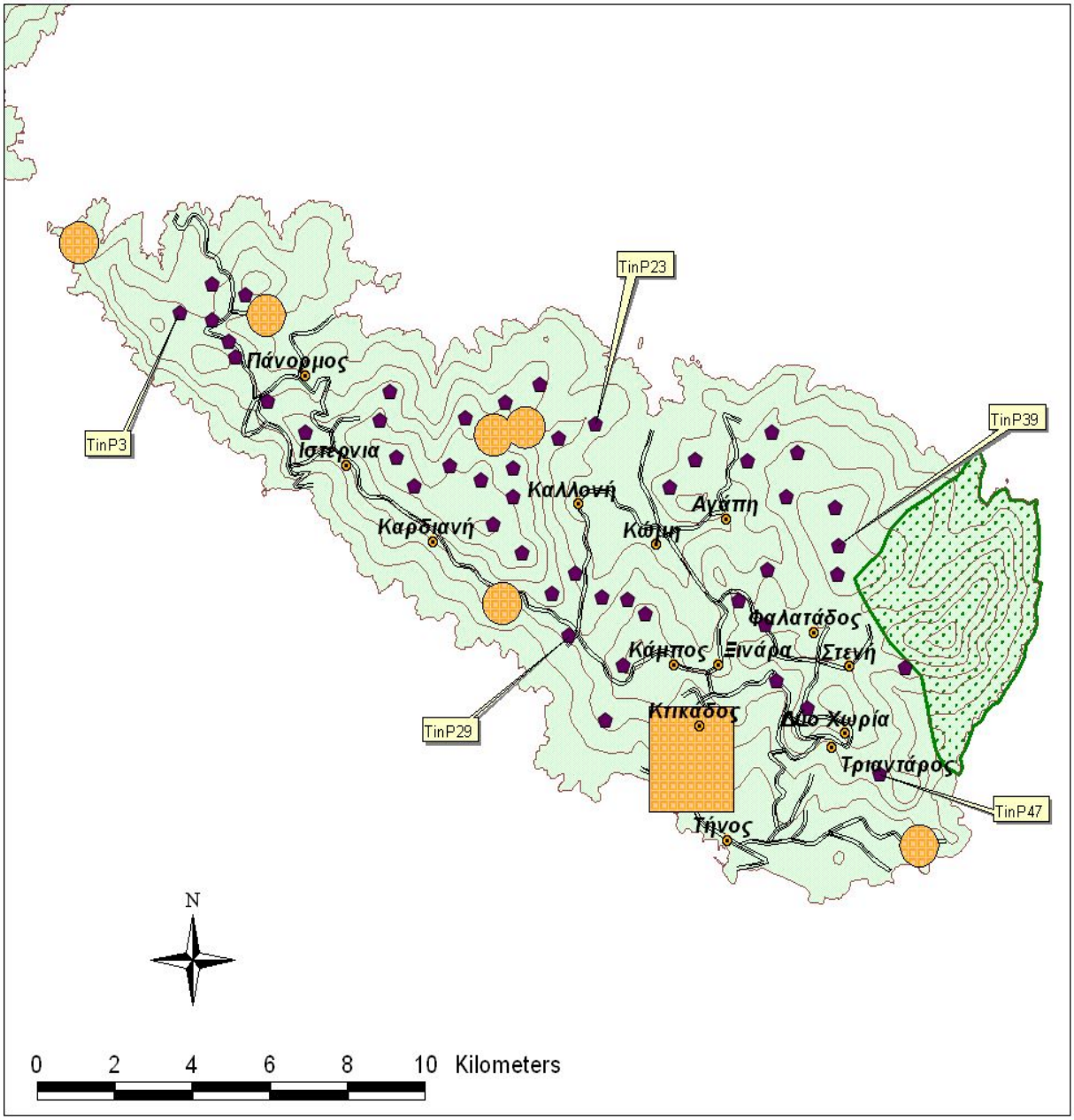

Figure 2: GIS-possible W/P on Tinos Island

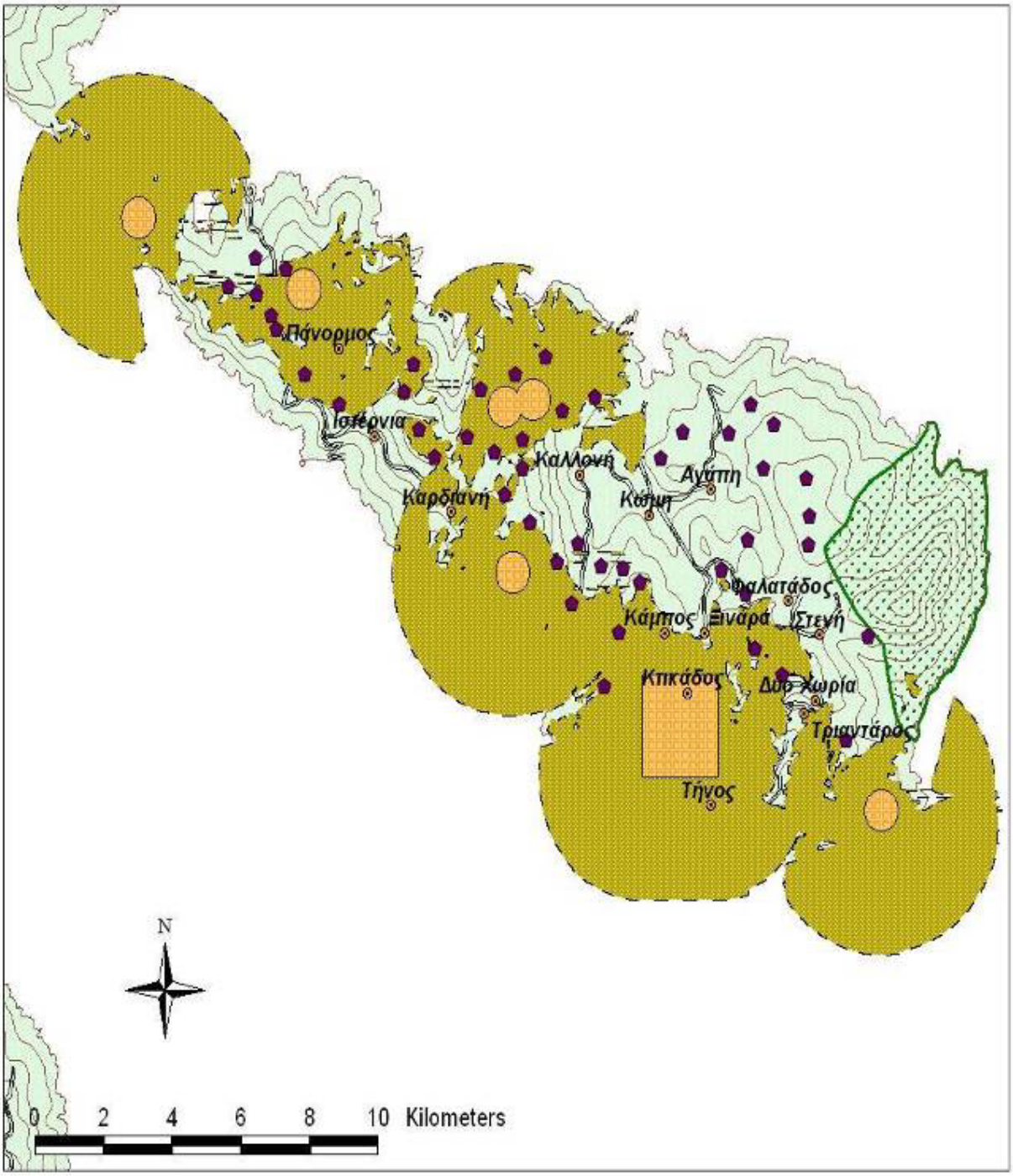

Fig 3: GIS-possible W/P on Tinos Island with visibility from ancient monuments filter enabled

IV. ENERGY PRODUCTION

Then the methodology for deriving the expected wind energy calculation and the results from such an analysis are presented.

A. WIND ENERGY CALCULATION

The annual energy output calculation for each of the selected W/P was completed with the aid of OPTIRES [12], which is a software tool developed by CRES. This tool was selected among numerous other choices, e.g.[13], as the most suitable one for this specific application. The parameters used are shown below in Table III and were carefully selected for the particular environment of the islands. For the implementation of the research the Vestas V52-850 kW Wind Turbine was selected [14]. Larger capacity wind turbines would be even more effective, but the restriction fro installations on the islands and the transportation difficulties on the narrow roads of the islands, constraints the size and height of the wind turbines to be used. Wind turbines with similar characteristics with this wind turbine can be used as well.

TABLE III. PARAMETERS FOR THE CALCULATION OF ENERGY OUTPUT

Parameter	**Value**
Wind Turbine	Vestas-V52
Mean temperature	19°C
Altitude	According to GIS data
Air density	1.255
Wind speed distribution	Weibull, k=2
Average wind speed	According to GIS data
Adjustment to height of measurement	40m
W/T Technology	Pitch control
W/T availability	95%
Hub height	44m
Roughness (rural areas)	0.055

The losses coefficient is estimated for each Wind Park considering the individual needs of the remote islands. The values of the parameters are presented in Table IV. It is shown that the considerably large value of the losses coefficient is due to the remoteness of the islands, which creates a difficulty in transportations as well as in the available staff for the W/P.

TABLE IV. PARAMETERS OF LOSSES COEFFICIENT

Parameter	**Value (% of gross energy production)**
Array losses	10
Airfoil soiling losses	5
Network availability	5
Measurements and power curve losses	5
Miscellaneous losses (off-yaw operation, transmission line losses)	5
C_L (losses coefficient)	0.7

B. RESULTS

The value for the Capacity Factor (C.F) resulting from the calculation described above is relatively high when compared to the typical value of 25-30%. 10W/P show a C.F of around 50% while the mean value of all the estimated W/P is C.F=38.77%.

Regarding the available potential capacity in MW, without taking under consideration the technical restrictions of transmission and interconnection, the astonishing number of viable W/Ps to be interconnected for all six islands to be interconnected is 1250MW. However, the above 'proved' potential cannot be exploited due to the limitations in electricity transmission. Taking into account the thermal limits of the existing and future interconnection network among the islands and the islands with the mainland network, as well as the minimum demand of each island, the maximum installed wind power capacity without violating thermal limits of the High Voltage lines is 408 MW.

The wind power capacity exceeds the peak demand of all the islands, 186.55 MW, as forecasted by PPC in 2015. Thus, for significant number of hours every year wind power will be transmitted to the mainland network providing further benefits to the Mainland system than simply switching off the local diesel generation on the islands.

V. ECONOMIC ELEMENTS OF WIND PLANTS

It is assumed that the electrical energy production cost is estimated from the public sector point of view, i.e. without taking under consideration the tax ratio, the state subsidy, and the external social and environmental benefits.

A. ENERGY PRODUCTION COST

The production cost in €/kWh C_{kWh} is divided in annual amortization cost C_{INST} for installation and operation and maintenance cost $C_{O\&M}$ as shown in (1),

$$C_{kWh} = \frac{C_{INST} + C_{O\&M}}{E(kWh)} \quad (1)$$

that are determined by the parameters of the following Tables V and VI [15]. E stands for the energy calculated in the previous section.

TABLE V. PARAMETERS OF THE INSTALLATION COST [15]

Parameter	**Value**
Total Wind Turbine cost (life cycle 15 yrs)	1000000€/MW
Infrastructure cost (life cycle 30 yrs)	5% of total wind turbine cost
Consulting cost (life cycle 15yrs)	4% of total wind turbine cost
Road Network cost (life cycle 50yrs)	100000€/km
Medium Voltage Interconnection Cost (20kV)	40000€/km

The operation& Maintenance costs (O&M) are slightly higher than in bibliography to account for the remoteness of the installation site and the cost of land in such touristic areas as shown in Table VI.

TABLE VI. PARAMETERS OF THE OPERATION& MAINTENANCE COST

Parameter	**Value (per year)**
Land hiring cost	564.3€/MW
Total Personnel payments	2€/MWh
W/T Maintenance cost	1.75% of W/T cost
Line Maintenance cost	1% of network cost
Insurance cost	1.75 ‰ of W/T cost

B. INVESTMENT ENVIRONMENT

Table VIII provides the investment environment characteristics to be used in analyzing the viability of investment provided the cost data described in the previous sub-section.

TABLE VII. PARAMETERS OF INVESTMENT INDICATORS

Parameter	**Value (per year)**
Mean Accountancy lifetime	12 yrs
Discount rate	8%
State Subsidy [16]	30% of installation cost
Loan Capital	40% of installation cost
Grace loan period	1 yr
Loan interest	5.5%
Pay Back Period years	10 yrs
Tax ratio	25%
Fixed energy price	0.073€/kWh

C. ECONOMIC ANALYSIS RESULTS

The estimated wind power cost ranges within 30.6–65 €/MWh, while 84% of the potential Wind Parks sites present cost below 50€/MWh.

Taking the average of the results of all the estimated Wind Parks (W/P) the typical W/P consists of 5.44MW, characterized by C.F equal to 38.74% and energy cost equal to 43.08 €/MWh.

In Table VIII the capacity of the potential Wind capacity with no transmission restrictions is presented. The suggested wind capacity on each island according to the thermal limits of the connection lines and ascending order of wind power cost is given in the same table. So the best sites for each island for installing wind power without violating the thermal limits of the lines have been calculated.

TABLE VIII. POTENTIAL AND FEASIBLE WIND POWER CAPACITY PER ISLAND

Island	Potential Capacity (MW)	Feasible Capacity (MW)
Anros	406.8	174.8
Mykonos	63.2	18
Naxos	418	128.4
Paros	278.4	66.4
Tinos	64	15.2
Syros	21.6	4.4
Total	**1252**	**407.2**

The investment indices, calculated to show the viability of Wind power installation on Cyclades are Internal Rate of Return (IRR) and Pay Back Period (PBP).
Table IX presents the worst-case analysis through the investment indicators of 10 W/P, which have the highest energy cost (€/MWh) among the selected W/P that are represented in Table VIII. The profitability of investing on Wind power on Cyclades is evident.

TABLE IX. INVESTMENT INDICES (WORST CASE ANALYSIS)

W/P	PBP (years)	IRR (%)
ParosP22	3.5	28.4
NaxosP43	3.5	28.3
ParosP25	3.5	28.2
NaxosP61	3	28.8
NaxosP38	3	28.6
MykonosP6	3	30.6
NaxosP53	3	28.8
ParosP10	3	31.2
SyrosP1	3	31.4
ParosP21	3	31.4

In fig. 4 the change of IRR with the wind power cost on the island of Andros, the island with the best wind power potential among Cyclades is shown. The production cost for the least efficient wind parks does not exceed 37 €/MWh and the corresponding IRR is just below 40%.

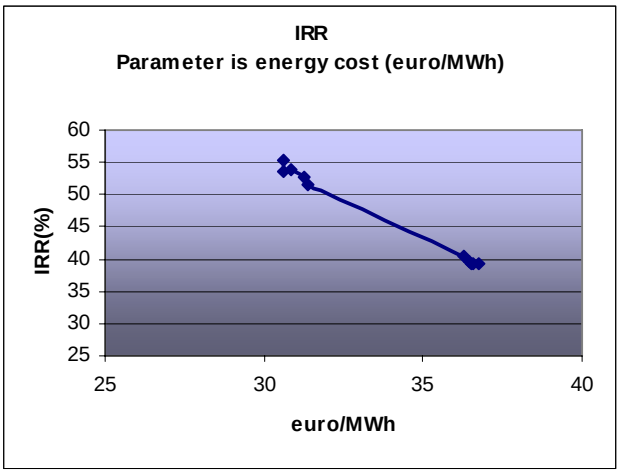

Fig. 4: IRR(%) related to Energy Production cost

Even in the sites with the highest production cost among the 290 sites studied, the IRR is above 17% making wind power installation on Cyclades rather attractive even without subsidy on the installation cost.

From the above remarks, the state subsidy is more than adequate to the actual needs of the investor. Moreover, the resulting Production cost is highly competitive when compared to the average energy cost of the conventional power plants.

VI. CONCLUSIONS

Interconnection of Cyclades to the Mainland power system will help in increasing the reliability of supply, reducing the production from local oil-fired thermal stations. Moreover, will reduce the need for extending the existing production facilities, which is usually a controversial issue for the local communities.

With the aid of GIS, the most promising sites on the islands to be interconnected, taking into account thermal limits of the lines used, have been indicated. The financial analysis for these installations has shown that Interconnection of Cyclades can be a very profitable investment for Wind power investors due to the low production cost and the favorable investment environment for wind power in Greece. The pay back time is less than 4 years and IRR is higher than 17% making investment on wind power a viable investment even without any subsidy.

Thus, not only will, the installation of Wind Parks combined with the interconnection of Cyclades, give an emission-free solution to the supply problem of the region but it will also establish the islands as power suppliers for the mainland and especially for capital area, Athens. Furthermore, the emissions avoided from local thermal plants will help Greece to make a step further in meeting the Kyoto protocol commitments.

VII. REFERENCES

[1] Hellenic Transmission System Operator http://www.desmie.gr

[2] N. D. Hatziargyriou, A. Tsikalakis, A.Androutsos, “Status Of Distributed Generation In The Greek Islands”, In proc of the 2006 IEEE PES General Meeting 18-22June2006, Montreal, Canada, PESGM2006-00368

[3] N. Hatziargyriou, et al “Security and Economic Impacts of High Wind Power Penetration in Island Systems”, 2004 Cigre Session, Paris, August 2004

[4] Papadopoulos et al. “Interconnection of Greek islands with dispersed generation via HVDC light technology”.In proc of the Cigre Symposium on Distributed Generation DG Cigre Athens, April 2005

[5] Directive 2001/77/EC of the European Parliament and of the Council of 27 September 2001 on the promotion of electricity produced from renewable energy sources in the internal electricity market.Offical Journal of the European Communities 27.10.2001
[6] Public Power Corporation S.A., Also : http://www.dei.gr
[7] Regulatory Authority of Greece, Also: http://www.rae.gr
[8] Final report of the commission for electirication of the Cyclades islands, available http://www.rae.gr/cases/C11/index.html (In Greek)
[9] M. Bechberger, D. Reiche, "Renewable energy policies in an enlarged European Union, RE in EU-28", Refocus Magazine, Issue September/October 2003
[10] ESRI, GIS software, Guide to Geographic Information Systems.www.esri.com
[11] Centre for renewable energy Sources CRES available on-line http://www.cres.gr
[12] OPTIRES- A Planning Tool for the Oprtimal Regional Intergration of Renewable Energy Sources: www.optires.info
[13] RETScreen International-Clean Energy Decision Support Centre: "Wind Energy Project Analysis", www.retscreen.net .
[14] Vestas wind turbines manufacturer web-site www.vestas.com
[15] Wind Energy: The facts. European Wind Energy Association www.ewea.org
[16] 3rd Operational program "Competitiveness", available on-line at www.antagonistikotita.gr

VIII. BIOGRAPHIES

Nikos D. Hatziargyriou was born in Athens, Greece. He received the Diploma in Electrical and Mechanical Engineering from NTUA and MSc and PhD degrees from UMIST, Manchester, UK. He is professor at the Power Division of the Electrical and Computer Engineering Department of NTUA. His research interests include Dispersed and Renewable Generation, Dynamic Security Assessment, and application of Artificial Intelligence Techniques to power systems. He is senior IEEE member, member of CIGRE SCC6 and the Technical Chamber of Greece.

Zoe N. Vrontisi was born in Athens, Greece. She received the Diploma in Electrical and Computer Engineering from NTUA. Her research interests include Dispersed and Renewable Generation, Energy Planning and Energy Economics. Ms Vrontisi is a member of the Technical Chamber of Greece.

Antonis G. Tsikalakis was born in Athens, Greece in 1979. He received his diploma in Electrical and Computer Engineering from NTUA. He is currently a Ph.D. student at Electrical and Computers Engineering Department of NTUA. His research interests include optimization of power system operation, Dispersed Generation and energy storage. Mr. Tsikalakis is a student member of IEEE and member of the Technical Chamber of Greece.

Vasillis Kilias is Head of Information Systems Department of the Centre of Reneweable Energy

Received January 18 2007

6. PERMANENT-MAGNET MACHINES FOR DISTRIBUTED POWER GENERATION: A REVIEW. (PAPER 07GM0593).

Tze-Fun Chan (Hong Kong Polytechnic University, Hong Kong)
Loi Lei Lai (City University London, UK).

Abstract— A review of permanent-magnet machines for distributed power generation is presented. Radial-flux, linear and axial-flux machine configurations are discussed with reference to generation that utilize energy resources such as wind, wave energy, and natural gas. Isolated operation and grid-connected operation are considered. Some of the authors' research work on a surface-inset permanent-magnet synchronous generator (PMSG) for autonomous power system application is also included.

Index Terms—Permanent-magnet synchronous generator, machines, distributed power generation.

I. INTRODUCTION

Conservation of energy resources, environmental protection and sustainable development are the major challenges that the modern world is facing. One important issue is to satisfy the energy needs of people without causing rapid depletion of the natural energy resources and degradation of the environment. The general consensus is that greater emphasis should be placed on the use of renewable energy resources for electric power generation. Many countries have abundant renewable energy resources, but these resources are invariably located in remote regions, thereby creating a number of obstacles for their deployment. The problem can readily be solved if the region is already served by a three-phase grid. Local, small-scale power systems that employ these distributed energy resources may be developed, thereby reducing the load to be transmitted over long distances. Autonomous (or standalone) distributed generation systems could be used when grid connection is not feasible.

Further to the several major blackouts, which affected more than 100 million persons, in the US and Europe in 2003, the possibilities in reducing large blackouts are extremely important. Distributed generation could also reduce the problem created due to terrorism if electricity supply is attacked. The global trend of privatization and deregulation is a further impetus to the development of small-scale distributed generation systems [1]. Also in recent decades carbon dioxide rose on average 1.3 parts per million (PPM) a year but went up over 2.5 PPM in 2002 and 2003. This unexplained rise in level of carbon dioxide in the Earth's atmosphere has raised fears that global warming is speeding up. It was forecasted that sea levels could rise by another 88 cm by the end of this century. Such a massive water rise will affect 100 million people around the planet now living below that level. Evidence provided by melting glaciers, declining sea ice and snow cover and increasingly frequent extreme weather events shows that climate change could cause a global catastrophe. All these point to the importance of integration of distributed generation with renewables.

For such applications, the permanent-magnet synchronous generator (PMSG) is increasingly used. A PMSG is a rotating electric machine in which the field excitation is furnished by permanent magnets. The advantages of PM machines include: brushless construction, light weight, small size, high reliability, less frequent maintenance, and high efficiency. The disadvantage, however, is that the excitation cannot be varied and hence the output voltage of the generator will vary with load.

This work was supported in part by the Hong Kong Polytechnic University under Grant A-PF89.

Tze-Fun Chan is with the Department of Electrical Engineering, The Hong Kong Polytechnic University, Hung Hom, Kowloon, Hong Kong, P.R. of China (e-mail: eetfchan@polyu.edu.hk).

Loi Lei Lai is with the Energy Systems Group, School of Engineering and Mathematical Sciences, City University, Northampton Square, London EC1V 0HB, UK (e-mail: L.L.Lai@city.ac.uk).

From practical considerations, it is desirable that the voltage regulation of the generator be minimized. This may be accomplished by capacitor compensation, electronic voltage controller, or by using a generator with inherent voltage regulation capability.

This paper gives an overview of various types of PMSG suitable for distributed power generation. Section II gives a brief review of radial-flux PMSGs. A steady-state analysis of PMSG supplying isolated loads is developed using the two-axis model. Section III presents linear PM machines suitable for short-stroke oscillatory movements, with particular emphasis on wave energy conversion system applications. Section IV presents various types of axial-flux PM machines for renewable generation, such as a wind energy conversion system. Section V presents work on grid-connected distributed generation systems and Section VI gives some conclusions.

II. RADIAL-FLUX PMSG FOR ISOLATED OPERATION

Conventional PM machines are generally of the radial-flux type. The rotor configuration may be surface-magnet type, interior type, or surface-inset type [2]. PMSGs developed in the late nineteen seventies and early nineteen eighties employed low-cost, ceramic magnets. Binns *et al.* [3] developed a permanent-magnet generator of a novel multi-stacked form. The use of capacitance to improve regulation and increase output was discussed. In another paper [4], Binns *et al.* described the performance and application of multi-stacked imbricated permanent-magnet generators. Typical characteristics were discussed and it was shown that the relatively cheap anisotropic ferrite magnets are well suited to this type of machine. For windmill applications, switched load with a fixed capacitor in parallel was used for approximate load matching between the turbine and generator power characteristics. Voltage control of PMSGs by using shunt capacitors was also studied by Rahman *et al.* [5] and Z. Chen *et al.* [6].

Y. Chen *et al.* [7] studied a radial-flux PMSG with outer- rotor construction that facilitated direct coupling to the wind turbine. The initial electromagnetic design was based on the classical magnetic circuit analysis but the finite element method (FEM) was used to obtain the detailed characteristics.

Chalmers [8] subsequently showed that a PMSG with interior magnets has an inverse saliency feature (i.e., the d-axis synchronous reactance X_d is less than the q-axis synchronous reactance X_q). Negative voltage regulation could result when the PMSG supplied an isolated resistive load.

Towards the mid-nineteen eighties, neodymium-iron-boron (NdFeB) emerged as an important class of high-energy PM material [2]. Since then it was widely used in electric machines, such as brushless dc motors and PMSGs. Chan *et al.* [9], [10] investigated voltage regulation improvement by using a PMSG with surface inset NdFeB rotor (Fig. 1). Effects of inverse saliency ratio, armature resistance, and the rotor speed on the voltage regulation characteristic were studied.

A. Steady-State Analysis

The voltage-current characteristics of a PMSG when supplying a lagging-power-factor load can be computed using the two-axis model as shown in Fig. 2. Computation of performance can be carried out by using a direct method or an iterative method.

The direct method may be used when the load impedance Z_L is given explicitly. For lagging load power factors, the following equations may be written with reference to Fig. 2(b):

$$V\cos\delta = E - I_d X_d - I_q R \tag{1}$$

$$V\sin\delta = I_q X_q - I_d R \tag{2}$$

$$I_d = I\sin(\delta + \phi) \tag{3}$$

$$I_q = I\cos(\delta + \phi) \tag{4}$$

where δ is the load angle and ϕ is the load power factor angle.

Substituting (3), (4) into (2) and using the relationship $V = I.Z_L$ for isolated operation (where Z_L is the load impedance),

$$Z_L \sin\delta = X_q \cos(\delta + \phi) - R \sin(\delta + \phi) \tag{5}$$

Expanding the right-hand side of (5) and rearranging terms, the following equation may be deduced:

$$\tan\delta = \frac{X_q \cos\phi - R \sin\phi}{Z_L + X_q \sin\phi + R \cos\phi} \tag{6}$$

For a given load impedance Z_L and load power factor angle ϕ, the load angle δ can be computed from (6). Substitution of the value of δ into (1) gives the terminal voltage V as follows:

$$V = \frac{E.Z_L}{Z_L \cos\delta + R \cos(\delta + \phi) + X_d \sin(\delta + \phi)} \tag{7}$$

The iterative method may be used when the load current I is specified. For isolated operation, the load angle δ has little practical significance and hence could be eliminated from the previous equations. Rewriting (6) in terms of the load current I and terminal voltage V,

$$\tan\delta = \frac{IX_q \cos\phi - IR \sin\phi}{V + IX_q \sin\phi + IR \cos\phi} \tag{8}$$

The load current I is given by

$$I = \sqrt{I_d^2 + I_q^2} \tag{9}$$

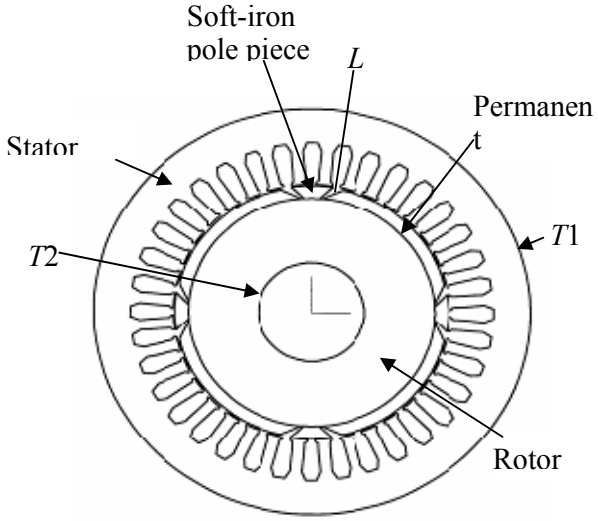

Fig. 1. Cross-section of an PMSG with inset NdFeB rotor.

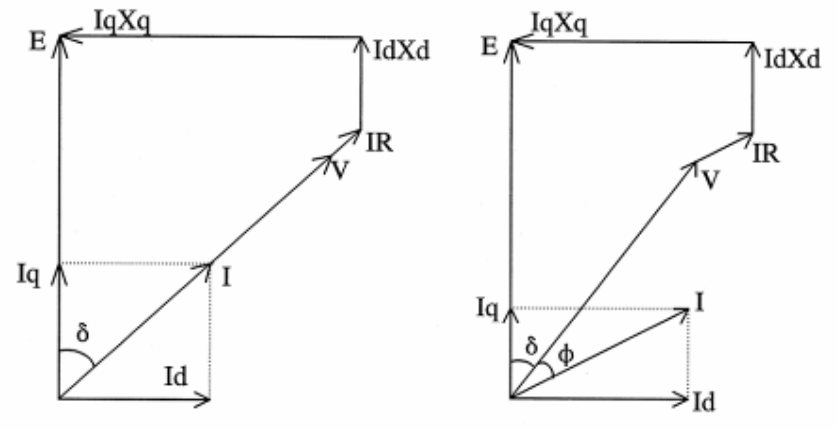

(a) **(b)**

Fig. 2. Phasor diagram of PMSG: (a) Unity-power-factor load; (b) lagging-power-factor load.

From (1)-(4) and (8)-(9), the open-circuit voltage E and the terminal voltage V are found to be related by [9]:

$$E = \frac{V^2 + 2VI.R\cos\phi + VI(X_d + X_q)\sin\phi + I^2(R^2 + X_d X_q)}{\sqrt{V^2 + 2VI.(X_q\sin\phi + R\cos\phi) + I^2(R^2 + X_q^2)}} \quad (10)$$

For a given load current I and load power factor angle ϕ, (10) may be solved iteratively to give the terminal voltage V.

B. Conditions for Zero Voltage Regulation

It is desirable to achieve zero voltage regulation when the generator is supplying an isolated load, i.e. the terminal voltage V is equal to the open-circuit voltage E. From Fig. 2(b), it can be shown that this condition is satisfied at a load angle δ given by:

$$\tan\left(\frac{\delta}{2}\right) = \frac{R + X_d\tan(\delta+\phi)}{X_q - R\tan(\delta+\phi)} \quad (11)$$

Equation (11) may be solved iteratively to give the corresponding load angle δ. For a generator with negligible armature resistance and supplying a unity-power-factor load, (11) simplifies to:

$$\tan\left(\frac{\delta}{2}\right) = \sqrt{\frac{r-2}{r}} \quad (12)$$

where r ($= X_q/X_d$) is the inverse saliency ratio.

Equation (12) implies that zero voltage regulation can be obtained when the generator has an inverse saliency ratio r exceeding 2. For practical machines, the presence of armature resistance R will require a higher value of r. It should also be noted that (11) is satisfied only for a limited range of lagging-power factor angle ϕ, i.e. a drooping load characteristic will normally be expected for lagging loads.

Fig. 3 shows the computed load characteristics of the prototype generator at nominal speed (1500 r/min) and four times of nominal speed (6000 r/min). The generator has a rated armature current of 13.3 A, and the following parameters at nominal speed [10]: E = 66.44 V, X_d = 0.88 Ω, X_q = 2.23 Ω. For easy comparison, the voltages have been normalized to the corresponding no-load voltages. At the nominal speed (1500 r/min), the full-load voltage drop is 4.7% when the load power factor is unity and 15.7% when the load power factor is 0.8 lagging. At a speed of 6000

r/min, the generator exhibits a nearly level load characteristic when the load power factor is unity, with zero voltage drop at full load. At 0.8 power factor lagging, the corresponding voltage drop is 11%. The voltage compensation due to inverse saliency thus increases with the rotor speed and is more effective for resistive loads.

C. Application of Finite Element Method

Availability of high-speed computers with large internal memory at modest costs has made it practicable to carry out electric machine performance analysis based on the electromagnetic field approach. The coupled circuit and field method, for example, is now widely used in electric machine design and analysis. It has the advantages of more precise modeling, no need for empirical formulae, and good accuracy. This method has been applied to PM synchronous motors and PMSGs [11]-[13]. Fig. 4 shows the computed radial component of full-load flux density distribution in the PMSG in Fig. 1 [13]. The contribution of the armature reaction in the q-axis is apparent. From Fig. 5, it is seen that the FEM gives a very good prediction of the experimental characteristics of the PMSG.

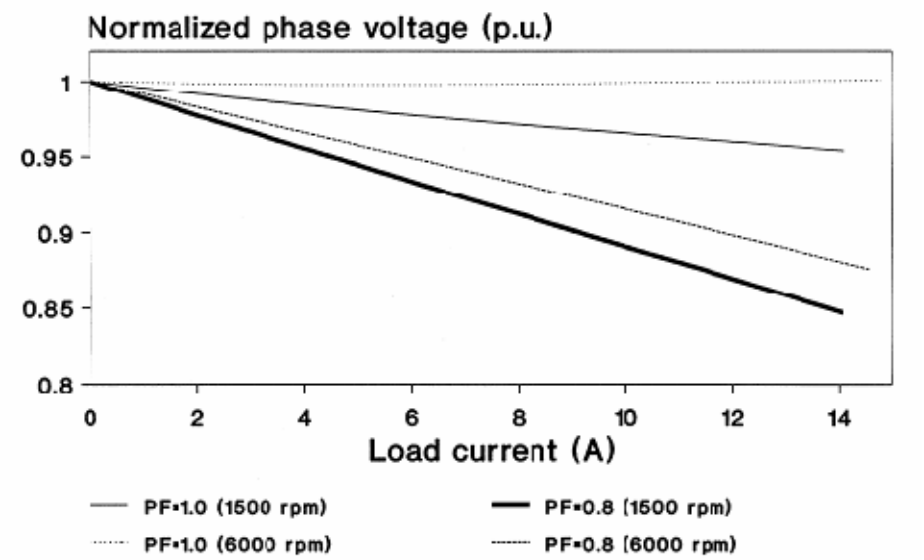

Fig. 3. Computed load characteristics of PMSG with the following machine parameters at nominal speed: E = 66.44 V, R = 0.295 Ω, X_d = 0.88 Ω, X_q = 2.23 Ω.

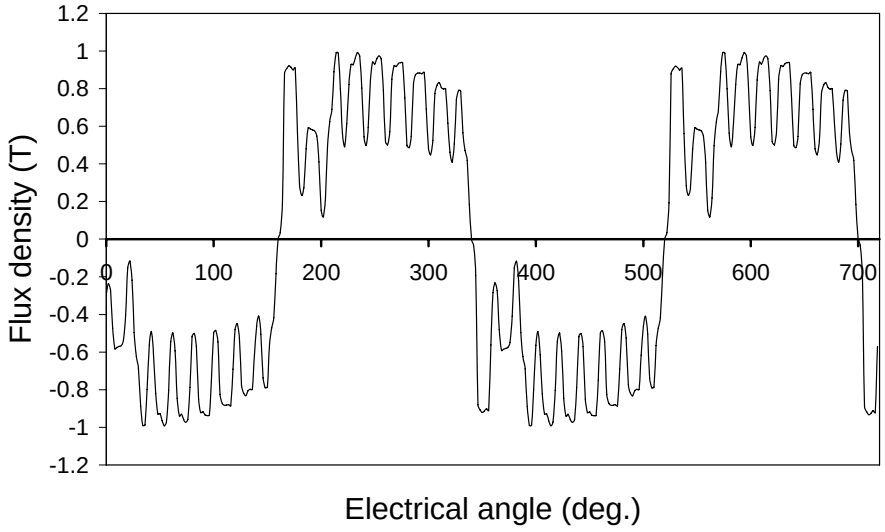

Fig. 4. Computed variation of B_n when the PMSG is supplying full-load current to a resistive load.

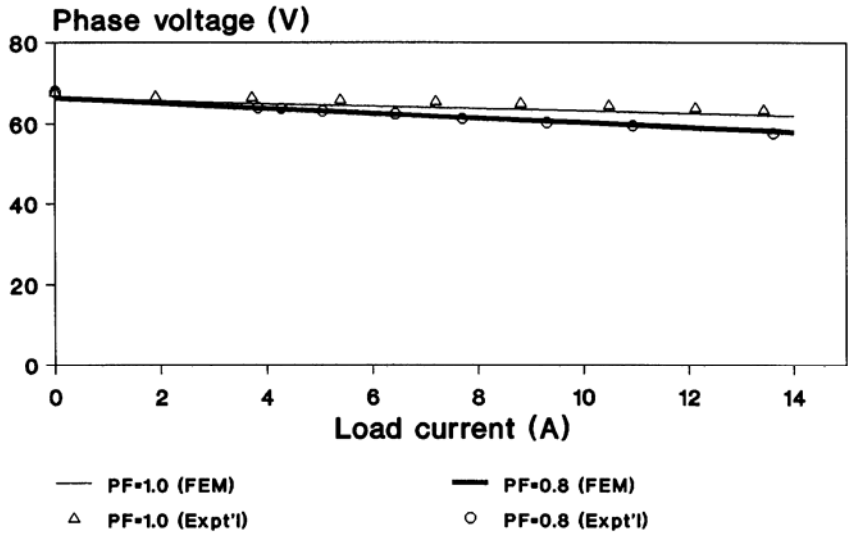

Fig. 5. Computed and experimental load characteristics of PMSG when supplying unity-power-factor and 0.8 lagging-power-factor loads at nominal speed.

D. High-Speed PMSGs

Some countries in the world are abundant in natural resources that could be exploited for distributed power generation. The western regions of China, for example, have natural gas reserves but are too remote for central grid access. Distributed generation system based on small gas turbine technology is therefore an option worthy of consideration. By using a direct-driven generator operating at very high speeds (typically above 30,000 r/min), there is significant reduction in system size and improvement in efficiency. The main technical issues [14] to be addressed are the electromagnetic designs of the PMSG for high-speed operation (such as the rotor structure and the choice of pole number), reduction of iron and stray losses, and development of high-speed bearings. Fig. 6 shows a possible rotor construction for high-speed PMSG, where the magnets are secured by a retaining ring or layers of fibre-glass bands against the centrifugal forces due to rotation.

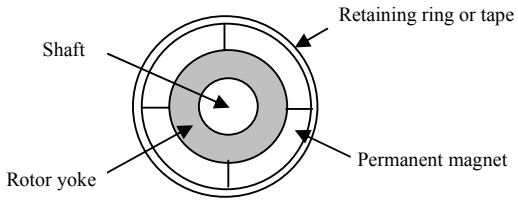

Fig. 6. Four-pole rotor for high-speed PMSG.

III. LINEAR PERMANENT-MAGNET MACHINES

Linear electric machines are electromagnetic devices that involve translational motion. In the past linear induction motors (LIMs) and linear synchronous motors (LSMs) have been developed mainly for high-speed ground transportation systems, conveyors, people movers, and propulsion system for aircraft take-off. For generator operation, the motion of the linear generator has to be of short-distance and oscillatory in nature. A brief review of the history, types and applications of linear electric actuators and generators was given by Boldea *et al*. [15]. Fig. 7 shows the construction of a simple moving PM linear generator.

Amara *et al.* [16] investigated a tubular linear permanent magnet machine that might offer the highest efficiency and power/force density. The machine studied had a nine-slot, ten-pole configuration, with a fractional number of slots per pole per phase. Since the Halbach magnetic array was used for the mover, the flux at the inner bore is quite small, permitting the use of nonmagnetic supporting tube for the magnets. The problem of eddy current reduction is the main design issue for this type of machine configuration.

A typical application of the linear permanent-magnet synchronous generator (LPMSG) is in a wave-energy to electric energy conversion system. The perpetual vertical motion of the sea waves is exploited to drive the mover of a linear generator for producing electricity. A pilot plant using this principle, namely the Archimedes Wave Swing (AWS), was designed for 4-MW peak power [17]. A three-phase linear permanent-magnet generator was designed to extract electric energy from the motion of the floater [18]. Polinder *et al.* [19] showed that the linear PM generator was cheaper than linear induction generators for such applications. Conventional LPMSG had magnets mounted on the mover, but the authors also proposed a transverse-flux PM generator (TFPMG) which had flux concentrators, magnets and conductors all on the stator, while the translator only consisted of iron. Such a machine configuration was more difficult to build and hence further investigations would be needed.

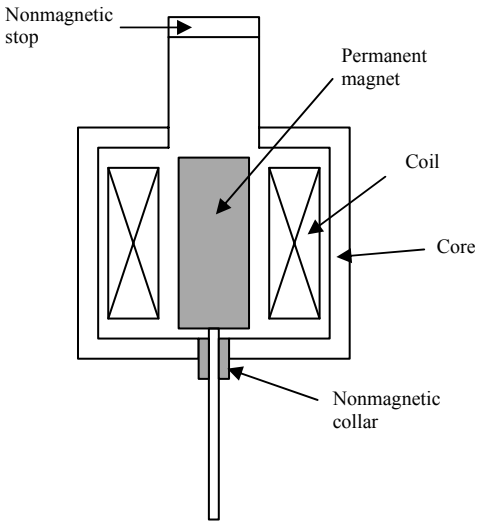

Fig. 7. A simple linear oscillatory permanent-magnet generator.

IV. AXIAL-FLUX PERMANENT-MAGNET MACHINES

Axial-flux machines are usually disk-shaped with flat, annulus air gaps. The flux is oriented in the axial direction while the effective conductors of the armature run in radial directions. Axial-flux PMSGs have recently received consideration attention, mainly in wind-energy conversion systems (WECs) as they could be designed for use with direct-coupled wind turbines. Since the bulky and expensive mechanical gearbox is eliminated, the noise level is reduced and the reliability of supply is improved. The axial-flux PMSG can be conveniently designed with a high pole number that is required for low-speed operation.

A modular PM generator with axial flux direction was proposed for a direct-drive wind turbine generator by Muljadi *et al.* [20]. Flexibility of design was achieved since each generator could be expanded to several modules. Each unit module in turn was built from simple modular poles. The stator winding was formed like a torus, linked by flux-focusing guides. The prototype built could deliver a power of 650 W at an efficiency of 75% when driven at 667 r/min.

Chalmers *et al.* [21]-[23] developed an axial-flux permanent-magnet generator called 'torus' for a gearless wind energy system. The stator armature consisted of a laminated toroidal core on which the air gap winding was wound, as in the classical Gramme-ring winding. The cogging torque was therefore eliminated by the slotless design, while the double-sided permanent-magnet rotor minimizes the magnetic pull between the stator and rotor. The experimental machine in [22] had a rating of 5-kW at 200 r/min. Output voltage was practically sinusoidal and an efficiency of 82% could be accomplished at full load. When the air gap lengths on the two sides of the torus are not the same, the resultant magnet pull in the axial direction could be significant, and special thrust bearings need to be used.

Hwang *et al.* [24] and Parvianen *et al.* [25] adopted the more conventional axial-flux machine configuration with toothed iron core. Hwang's machine [24] employed the doubled-sided configuration in which the rotor permanent- magnet disk was sandwiched between two toothed stator armature cores. The 24-pole machine was rated at 10 kVA and 380 V when operating at 300 r/min. Parvianen *et al.* [25] on the other hand developed a single-sided axial machine configuration with open slots. Various combinations of armature slot number and pole number were studied with a view of reducing the cogging torque. A 1.6-kW prototype machine was constructed and was installed in a pilot power plant. Since a single-sided configuration was used, thrust bearings had to be used to withstand the strong magnetic pull between the stator and rotor.

Spooner *et al.* [26] proposed an ironless, radial-flux, permanent-magnet direct coupled wind generator machine that employed lightweight spoke-wheel structures for both the rotor and the stator. A working flux density of about 0.25 T was produced at the winding. The generator could

have a mass typically 20-30% of equivalent designs based on iron-cored magnetic circuits, and the efficiency was greater than 90%. The experimental machine had a specification of 11.1 kW at 150 r/min.

Chan *et al.* [27] recently reported a single-sided axial-flux PMSG for small-scale wind energy systems with either vertical-axis or horizontal-axis turbines. The machine featured an outer-rotor configuration and had an air gap disk armature winding, hence there was no cogging torque and no iron loss. At a speed 600 r/min the generator could deliver a power of 350 W at rated current. Fig. 8 shows the test rig for load tests on a prototype axial-flux PMSG.

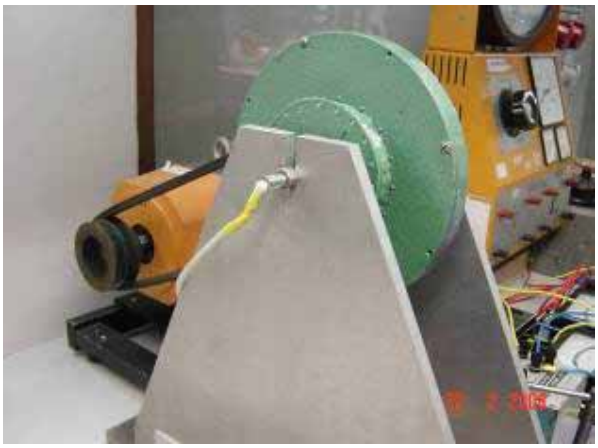

Fig. 8 Test rig for experimental investigations on a prototype axial-flux PMSG.

Summarizing, various designs of axial-flux permanent-magnet generators could be adopted for direct coupled wind turbine applications. The choice of a particular design depends upon the expertise of individual research teams, the availability of components and materials (e.g., NdFeB magnets, wound silicon cores, etc.) and the accessible manufacturing technology.

Axial-flux PMSGs could also be used for high-speed applications. For example, Wang *et al.* [28] reported the optimal design of a coreless, double-sided stator axial-flux PMSG suitable for integration with internal combustion engines (ICEs), e.g., as integrated starter-generators for use in hybrid vehicles.

V. Variable-Speed PMSG Connected to Grid

Variable-speed power generation enables the turbine generator system to operate at maximum power conditions. Since the frequency of a PMSG varies with the speed, a frequency converter has to be provided for integration with the power grid. Kimura *et al.* [29] presented a distributed power generation system that included a variable-speed turbine with a power conversion system for use in a cogeneration system. The PM generator was to be directly driven by a diesel engine operating at variable speed, while the output power was delivered to a distribution line. Experimental results were presented and some practical operational issues were discussed. Amei *et al.* [30] proposed a maximum power control strategy for a wind-driven PMSG by using a rectifier, a boost chopper circuit, and an inverter, and a theoretical analysis was carried out. Chinchilla *et al.* [31] also investigated maximum power control of a direct-coupled wind turbine generator by using a pulse-width modulated (PWM) rectifier, an intermediate dc circuit, and a PWM inverter. In addition, vector control of the grid-side inverter allows power factor regulation of the system. The dynamic system performance was analyzed and experimentally verified.

VI. CONCLUSION

Permanent-magnet synchronous machines are suitable for distributed power generation applications. Advances in PM material technology have stimulated the development of more efficient and more compact generator units. Further work on PM machines may include, but not necessarily limited to the followings: refined performance analysis, loss and thermal models, innovative machine and winding configurations, design optimization, analytic methods and finite element methods for field computations, control for grid-connected and isolated operation, and other niche application areas.

VII. REFERENCES

[1] Loi Lei Lai (Editor), *Power System Restructuring and Deregulation: Trading, Performance and Information Technology*. UK: John Wiley & Sons, Aug. 2001.

[2] J. F. Gieras and M. Wing. *Permanent Magnet Motor Technology - Design and Applications*. New York: Marcel Dekker, 1997.

[3] K. J. Binns and A. Kurdali, "Permanent-magnet a.c. generators," *Proc. Inst. Elect. Eng.—Elect. Power Appl.*, vol. 129, no. 7, pp. 690–696, Jul. 1979.

[4] K. J. Binns and T. S. Low, "Performance and application of multi-stacked imbricated permanent-magnet generators," *Proc. Inst. Elect. Eng.*, vol. 130, Pt. B, pp. 407–414, Nov. 1983.

[5] M. A. Rahman, A. M. Osheiba, T. S. Radwan and E. S. Abdin, "Modelling and controller design of an isolated diesel engine permanent magnet synchronous generator," *IEEE Trans. Energy Convers.*, vol. 11, no. 2, pp. 324–330, Jun. 1996.

[6] Z. Chen, E. Spooner, W. T. Norris and A. C. Williamson, "Capacitor-assisted excitation of permanent-magnet generators," *Proc. Inst. Elect. Eng.—Elect. Power Appl.*, vol. 145, no. 6, pp. 497–507, Nov. 1998.

[7] Jian Yi Chen, Chern Nayar and Longya Xu, "Design and FE analysis of an outer-rotor PM generator for directly-coupled wind turbine applications," in *Proc. IEEE–IAS 33rd Annu. Meeting*, vol. 1, 1998, pp. 387–394.

[8] B. J. Chalmers, "Performance of interior type permanent-magnet alternator," *Proc. Inst. Elect. Eng. —Elect. Power Appl.*, vol. 141, no. 4, pp. 186–190, Jul. 1994.

[9] T. F. Chan, Lie-Tong Yan, and L. L. Lai, "Performance of a three-phase a.c. generator with inset NdFeB permanent-magnet rotor," *IEEE Trans. Energy Convers.*, vol. 19, no. 1, pp. 88–94, Mar. 2004.

[10] T. F. Chan, L.-T. Yan and L. L. Lai, "Permanent-magnet synchronous generator with inset rotor for autonomous power-system applications," *Proc. Inst. Elect. Eng.—Gen., Transm. and Distrib.*, vol. 151, no. 5, pp. 597–603, Sept. 2004.

[11] P. Zhou, M. A. Rahman and M. A. Jabbar, "Field circuit analysis of permanent magnet synchronous motors," *IEEE Trans. Magn.*, vol. 30, no. 4, pp. 1350–1359, Jul.1994.

[12] S. L. Ho and H. L. Li, "Dynamic modeling of permanent magnet synchronous machines using direct-coupled time stepping finite element method," in *Proc. IEEE International Electric Machines and Drives Conference (IEMDC '99)*, Seattle, Washington, USA, May 9-12, 1999, pp. 113–115.

[13] T. F. Chan, L. L. Lai and L.-T. Yan, "Analysis of a stand-alone permanent-magnet synchronous generator using a time-stepping coupled field-circuit method," *Proc. Inst. Elect. Eng.—Elect. Power Appl.*, vol. 152, no. 6, pp. 1459–1467, Nov. 2005.

[14] Fengxiang Wang, Wenpeng Zheng, Ming Zhong and Baoguo Wang, "Design considerations of high-speed PM generators for micro turbines," in *Proc. International Conference on Power System Technology 2002*, vol. 1, 13-17 Oct. 2002, pp. 158–162.

[15] I. Boldea and S. A. Nasar, "Linear electric actuators and generators," *IEEE Trans. Energy Convers*., vol. 14, no. 3, pp. 712–717, Sept. 1999.

[16] Yacine Amara, Jiabin Wang and David Howe, "Analytical prediction of eddy-current loss in modular tubular permanent-magnet machines," *IEEE Trans. Energy Convers*., vol. 20, no. 4, pp. 761–770, Dec. 2005.
[17] Mats Leijon, Hans Bernhoff, Olov Agren, Jan Isberg, Jan Sundberg, Marcus Berg, Karl Erik Karlson and Arne Wolfbrandt, "Multiphysics simulation of wave energy to electric energy conversion by permanent magnet linear generator," *IEEE Trans. Energy Convers*., vol. 20, no. 1, pp. 219–224, Mar. 2005.
[18] H. Polinder, M.E.C. Damen and F. Garder, "Linear PM generator for wave energy conversion in the AWS," *IEEE Trans. Energy Convers*., vol. 19, no. 3, pp. 583–589, Sept. 2004.
[19] H. Polinder, Barrie C. Mecrow, Alan G. Jack, Phililip G. Dickinson and Markus A. Mueller, "Conventional and TFPM linear generators for direct-drive wave energy conversion," *IEEE Trans. Energy Convers*., vol. 20, no. 2, pp. 260–267, Jun. 2005.
[20] E. Muljadi, C. P. Butterfield and U. H. Wan, "Axial-flux modular permanent-magnet generator with a toroidal winding for wind-turbine applications," *IEEE Trans. Ind. Appl.*, vol. 35, no. 4, Jul./Aug. 1999, pp. 831–836.
[21] W. Wu, E. Spooner and B. J. Chalmers, "Design of slotless TORUS generators with reduced voltage regulation," *Proc. Inst. Elect. Eng.—Elect. Power Appl.*, vol. 142, no. 5, pp. 337–343, Sept. 1995.
[22] B. J. Chalmers, W. Wu and E. Spooner, "An axial-flux PM generator for gearless wind energy system," *IEEE Trans. Energy Convers.*, vol. 14, no. 2, pp. 251–257, Jun. 1999.
[23] J. R. Bumby, R. Martin, M. A. Mueller, E. Spooner, N. L. Brown and B. J. Chalmers, "Electromagnetic design of axial-flux permanent magnet machines," *Proc. Inst. Elect. Eng.—Elect. Power Appl.*, vol. 151, no. 2, pp. 151–159, Mar. 2004.
[24] D. Hwang, K. Lee, D. Kang, Y. Kim, K. Choi and D. Park, "An modular-type axial-flux permanent magnet synchronous generator for gearless wind power systems," in *Proc. IEEE-IES 30th Annual Conference (IECON 2004)*, Nov. 2-6, 2004, Pusan, Korea, vol. 2, pp. 1396–1399.
[25] A. Parvianen, J. Pyrhonen and P. Kontkanen, "Axial flux permanent magnet generator with concentrated winding for small wind power applications," in *Proc. 2005 IEEE International Conference on Electric Machines and Drives*, San Antonio, Texas, USA, May 2005, pp. 1187–1191.
[26] E. Spooner, P. Gordon, J. R. Bumby and C. D. French, "Lightweight ironless-stator PM generators for direct-drive wind turbines," *Proc. Inst. Elect. Eng.—Elect. Power Appl.*, vol. 152, no. 1, pp. 17–26, Jan. 2005.
[27] T. F. Chan and L. L. Lai, "An axial-flux permanent-magnet synchronous generator for a direct-coupled wind turbine system," *IEEE Trans. Energy Convers.*, to be published.
[28] Rong-jie Wang, Maarten J. Kamper, Kobus Van der Westhuizen and Jacek F. Gieras, "Optimal design of a coreless stator axial-flux permanent-magnet generator," *IEEE Trans. Energy Convers.*, vol. 41, no. 1, pp. 55–63, Jan. 2005.
[29] M. Kimura, H. Koharagi, K. Imaie, S. Dodo, H. Arita, and K. Tsubouchi, "A permanent-magnet synchronous generator with variable-speed input for co-generation system," in *Proc. IEEE-PES Winter Meeting 2001*, vol. 3, 26 Jan.–1 Feb. 2001, pp. 1419–1424.
[30] Kenji Amei, Yuichi Takayasu, Takahisa Ohji and Massaki Sakui, "A maximum power control of wind generator system using a permanent magnet synchronous generator and a boost chopper circuit," in *Proc. Power Conversion Conference 2002*, Osaka, 2002, vol. 3, 2-5 Apr. 2002, pp. 1447–1452.
[31] Monica Chinchilla, Santiago and Jan Carlos Burgos, "Control of permanent-magnet generators applied to variable-speed wind-energy systems connected to the grid," *IEEE Trans. Energy Convers.*, vol. 21, no. 1, pp. 130–135, Mar. 2006.

T. F. Chan (M ’95) received the B.Sc. (Eng.) and M.Phil. degrees in electrical engineering from the University of Hong Kong, Hong Kong, China, in 1974 and 1980, respectively. He received the PhD degree in electrical engineering from City University, London, UK, in 2005. Currently, Dr. Chan is an Associate Professor at the Department of Electrical Engineering, the Hong Kong Polytechnic University, Hong Kong, China, where he has been since 1978. His research interests are self-excited a.c. generators, brushless a.c. generators, and permanent-magnet machines. In June 2006, he was awarded a Prize Paper by IEEE Power Engineering Society Power Generation and Energy Development Committee.

L. L. Lai (SM’92, F’07) received the B.Sc. (First Class Honors) and the Ph.D. degrees from the University of Aston in Birmingham, UK, in 1980 and 1984, respectively. He was awarded the D.Sc. by City University London in 2005 and he is its honorary graduate.

Currently he is Head of Energy Systems Group at City University, London, UK. He is also a Visiting Professor at Southeast University, Nanjing, China and Guest Professor at Fudan University, Shanghai, China. He has authored/co-authored over 200 technical papers. In 1998, he also wrote a book entitled *Intelligent System Applications in Power Engineering - Evolutionary Programming and Neural Networks*. In 2001, he edited a book entitled *Power System Restructuring and Deregulation - Trading, Performance and Information Technology*. In 1995, he received a high-quality paper prize from the International Association of Desalination, USA. Among his professional activities are his contributions to the organization of several international conferences in power engineering and evolutionary computing, he was the Conference Chairman of the IEEE/IEE International Conference on Power Utility Deregulation, Restructuring and Power Technologies 2000. Dr. Lai is a Fellow of the IET (UK). He was awarded the IEEE Third Millennium Medal, 2000 IEEE Power Engineering Society UKRI Chapter Outstanding Engineer Award and 2003 IEEE Power Engineering Society Outstanding Large Chapter Award. In June 2006, he was awarded a Prize Paper by IEEE Power Engineering Society Power Generation and Energy Development Committee.

Received April 20 2007

7. MICRO-GRID INTEGRATION—OPPORTUNITIES AND CHALLENGES (PAPER 07GM0284)

Khaled A. Nigim (University of Waterloo, Canada),
Wei-Jen Lee (University of Texas at Arlington, TX, USA).

Abstract— Penetration of distributed generation (DG) poses significant new challenges and benefits to the existing electricity market structure. Distributed energy resources (DER) management and the successful technology advancement have paved the way for the creation of the micro grid (MG) distribution network. Having various coordinated energy conversion units under one central energy management creates new realties for efficient use of resources. This will ultimately shape the future of electricity usage and trading. There are obvious mutual benefits for all electricity generation and supply sector players. However, DG penetration and integration rules are inconsistent and will eventually weaken the improvement of the sector in terms of efficient use of resources and technology. The paper presents the opportunities and challenges facing the integration of micro grid with existing utilities and concludes with the required steps needed to minimize the challenging factors.

Index Terms—Distributed Generation, Distributed Energy Resources and Micro Grid.

I. INTRODUCTION

Demand for electricity is rapidly increasing putting pressure on many utilizes to expand their generating and distribution capacity worldwide. This is an unwelcome step in today's deregulated power industry that strives to increase productivity with minimal operational expenses. Expansion of services is an unrealistic option for investors as it burdens financial resources and challenges many communities opposing the construction of generating power plants or transmission towers in their backyard. Even if expansion is feasible by the investors, it will ultimately lead to increase in the charged rates for consumers. The apparent economical remedy is, therefore, to avoid expansion and to utilize existing dispersed generating capacity known as distributed generation (DG) that may exist in the vicinity of the power provider service area. Large capacity DG's are energized by various fuel sources whether it is fossil 'polluting and diminishing' or non-fossil 'clean and renewable'. The main criteria for selecting the type of fuel source for a DG is its local availability, conversion system technological advancement, impact on the environment and operating cost. DG's have existed in the market for many years. Large diesel or gas generating sets are used in stand-by mode to power up vital services such as hospitals, financial and commercial compounds, telecommunication centers and industrial premises. Micro turbines and fuel cells are new comers and now competing in size and efficiency with many standard generating sets and are used in many places not only as stand-by units but as prime source of power particularly when the $/KWhr rate is high [1-2].

DG's are sometimes classified according to their rated capacity or the converted prime fuel source or by ownership. Ultimately, a DG importance is basically depends on its functionality and whether it is configured to operate in a stand-by mode, isolated mode, or sharing the load through integration with existing nearby network. Utility operated DG units are integrated with the distribution network and located in strategic places. They are installed to provide strength to the distribution grid by either supporting the voltage level or amount of power to reduce the peak demand [3-4]. Independent power providers 'IPP' disbursed generating units are mainly used as stand-by power generating units which undermine the capital investment and operational support to the existing energy infrastructure.

DG's rate ($/Kwhr) is now competitive as more efficient fuel energy conversion units such as fuel cells and micro turbine are continuously improved and diversified. Through combining dispersed DG's, a distributed energy resource (DER) generating domain is developed. Various mixes of energy sources are then controlled under a central energy management controller to improve output/fuel ratio. DER operational domain is confined to supply small groups of energy absorbing loads 'motors and heaters'. DER concept includes the use of other available energy 'prime fuel' sources within the defined area of service. Heat as well as electricity are distributed under centralized resources and load management. The increasing reliability and diversity of fuel mix along the efficient conversion management of DER resources paved the way for creating a micro grid (MG) generating and distribution domain [5]. Typical MG architect supplying heat and power is illustrated in the line schematic shown in Fig. 1. Energy supplying, storage and conversion units are managed centrally by the Energy Management System (EMS) controller. EMS main function is to dispatches heat and power according to the demand and fuel availability at all times through coordination among the mix of the generating units. MG structure, therefore, is characterized by efficient fuel management, reduced vulnerability, the use of modular generating units, combining heat and power to supply both demands, friendly to the environment and has lower operational cost than central power stations. Moreover, MG can be constructed close to the demand and by doing so defer the construction of transmission lines and associated ancillary units normally needed to transfer power from centrally located power generating source.

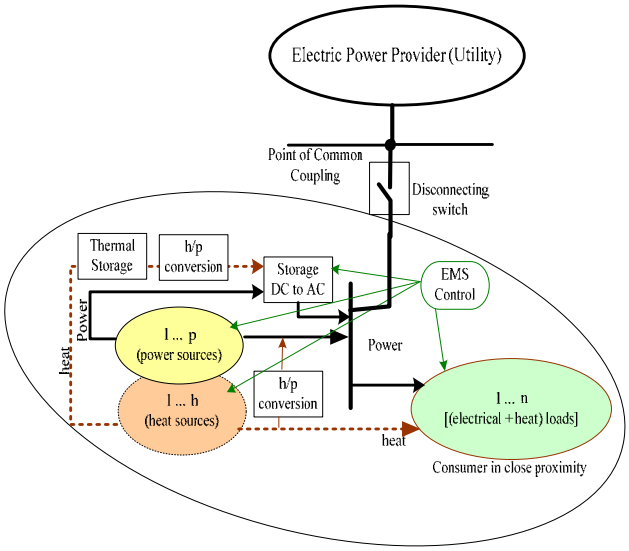

Fig. 1 Micro Grid Architecture

Despite DG existence over the past years and the acknowledgement of their impact, utilities are reluctant to install more units or to open the door for integrating Independent Power Producer (IPP) dispersed generating units. Both players in today's electricity markets acknowledge the existence of various technical and logistical challenges that need to be addressed cooperatively. It make sense that all parties agree to supporting more reliable, less vulnerable electricity infrastructure that use efficient energy management and conversion systems to target high Kwhr/fuel output. Energy consumption and conversion systems inefficiency and the slow deterioration of aging infrastructure and lack of investment in the sector will eventually result in frequent and lengthy power shortages with unpredictable and unavoidable blackout for larger served areas in many countries.

This paper presents the opportunities and challenges facing the integration of IPP structured MG with existing Utility distribution networks as a means to support the electricity infrastructure. Identifying the challenges paves the way to addressing the various blocking components slowing down the integration process and encourages researchers and legislators to start digging for reliable

solutions before disaster strikes. The work concludes with the listing of issues needed to be urgently addressed to ensure successful integration procedures that will eventually create new structures of efficient, modular and environmentally responsive electricity infrastructure that will have an impact nationally as well as globally.

II. OPPORTUNITIES

Utilization of the existing disbursed resources and their penetration into the energy market offers various merits that can be broadly presented within the following six opportunities:

1- To reduce dependency on imported fuel sources and to help in regulating prime fuel market competition. The increase interest in DG's, DER's and MG's concepts can influence the market and level of competition for prime sources of energy. Developing countries such as China and India have started to build rapidly moving production infrastructure that needs more energy. This has resulted, among other factors, in pushing the global prime fuel market to a high record. With the public support and encouragement following the rapid increase of fuel prices and environmental concern over global warming, Current DG's technologies resulted in a compatible $/KWhr rate with the Utility. Profitable DG's are fueled by available local prime fuel sources rather than imported ones. The DG market thrust is obviously driven by the economical benefits to be gained by all involved parties along the environmental positive impact of using local resources.

2- To enable the use of renewable energy sources (RES). Although RES conversion systems are characterized by their intermittent energy nature, they have minimum environment impact and offer free replenishment prime fuel source. Many countries have an abundance of natural and renewable resources that can be effectively integrated to meet a portion of the demand. An example is the distributed wind energy conversion systems success stories in Germany, Denmark and Spain where the wind penetration exceeds 5 - 10% of the total national demand [6-7]. RES generating systems can be configured to support the existing Utility network or as stand alone in either urban or rural surroundings.

3- To help rural electrification: Many developing and third world countries are in need of rural electrification resolution. African and south eastern countries in particular have the largest percentage of rural darkness. Such countries do not have the capacity or resources to build large centralized generation plants or transmission infrastructure although the sector and its services are an important driver for the country's economic development and welfare. The opportunity for MG implementation in various scales is evident when one considers how wealthy these countries are with local RES such as the sun and wind. RES are among the prime fuels that are incorporated in many residential and communities based DG applications in developing countries and are considered affordable to small rural communities [8]. It is quite possible then to incorporate dispersed MG to meet the demand of rural communities without exhausting deer financial resource.

4- To defer the constructing or extension of transmission lines: Planned installation of DG's can be used to support demand during peak periods, thus eliminating the need for installing peak generating units and enhance security benefits [9]. Moreover, DER's can be used to meet the heat and electricity demand for nearby industrial and commercial area, thus relieving the central power plant from dispatching power over long distances for heating purposes and improving the fuel/KWhr ratio.

5- To push forward the virtual power management concept that utilizes local resources nationally: Virtual power concept was introduced in late 1996 by ENCORP to help utilities in the USA to supply additional power from nearby utilities upon the first sign of deficiency in demand. Figure

2 shows an architectural layout of the virtual power concept in which nationally existing MG's are coordinated to serve existing energy infrastructure. This obviously requires a high degree of coordination and knowledge of each MG attributes and the capability of energy exchange among various domains in real time. With advances in Utility communication and the internet, such coordination is feasible using web based agents [10]. Further research and vulnerability studies are needed to check the reliability and security of supply aspects.

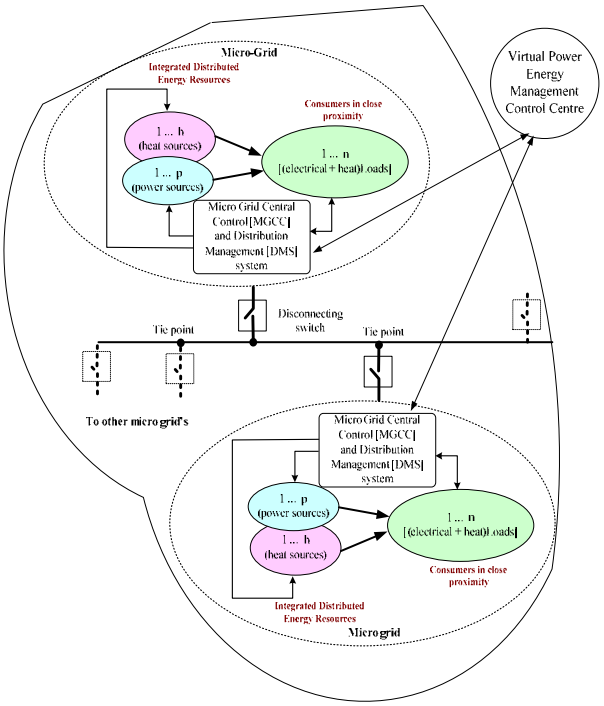

Fig. 2 Virtual Power Architecture

6- To create job opportunities in a niche area of technologies: Almost all of DG units are manufactured in developed countries. An increase in the penetration of DG and sustainable integration of MG's means more investment in complementary sustainable technologies and more employment opportunities in the manufacturing sectors.

III. CHALLENGES

Although MG existence sounds practical and provides a feasible solution to increasing energy demand, utilities are cautious in integrating dispersed generating units to their system [11]. Clear and consistent regulatory rules are needed to help both IPP's and Utilities as it is unlikely that many of the established technical performance requirements associated with centralized power generating systems will be applicable or appropriate for MG structured domain. Many IPP are indeed frustrated by the inconsistency associated with completing and administering the certification and permitting process. In many cases, new permission is required within the same state and for every new installation. Such minor logistics burden, in addition to the incurred costs that does not vary proportionally with power plant size, tends to have a high impact on MG installation than would be the case for larger, centralized power plants.

MG integration challenges can be divided broadly and collectively into two categories:

a- Technical challenges: issues such as safety, islanding, restoration from scheduled and unscheduled shut down's, protection coordination, capacity and reserve management, reliability and

power quality liability, cost development in the needed interconnection technologies are all among the urgent concerns need to be addressed [12].

b- Non-technical challenges: issues such as pricing, incentives, decision priority, risk responsibility and insurance for new technologies adaptation, interconnection standards and regulatory control and addressing barriers.

To appreciate the complexity of integrating MG into the existing market, various hurdles must be identified and individually addressed by all stakeholders collectively.

For the IPP, MG's structure can have various forms as depicted in Fig (3). Let us consider only the power supply part of the MG structure. Here MG can either by structured around generating units powered by a renewable or non renewable fuel sources as depicted in Fig. 3(a). Individually, each can generate a high quality AC power. Collectively, a local AC distribution network is created. Local demand is continuously supplied through the grid. Hypothetical power exchange with the existing Utility network is possible. Alternatively, MG could be structured around individual generating units that produce DC voltage source. Again collectively, units are networked to centralized AC interface system for the purpose of integration with the existing Utility as depicted in Fig 3(b). In scenario, different interconnection and energy management challenges need to be identified by the IPP operator and by the hosting Utility. This is evident due to the diversity of the generating units' interface, uncertainty of the power quality imposed by the individual generator, level of active and reactive power level, variations of the demand, reserve margin, overall dynamic behavior of such a mix of technologies and security and reliability of the communication commands.

Utilities, on the other hand, need to identify their own challenges such as interconnection requirements, safety, islanding, level of penetration and power exchange. The following utilities concerns are paramount [13 – 16]:

1- Maintenance worker safety. For a successful integration of load sharing between Utility and MG or even single DG's units, a safety protocol and coordination must ensure the safety of working maintenance staff. This entails the existence of maintenance disconnect accessible to the Utility engineers at the premises of the DG operator.

2- Power flow and its direction. Traditionally, electricity distribution allows a unidirectional flow of power with feeders protected with unidirectional protection gear. MG can be integrated with distribution network in two distinctive modes. The first one is the stand-by mode in which MG resources are not fully utilized and only supply its own demand once the Utility is disconnected. The second operating mode is to share power supply to its own demand with the Utility. In case of deficiency it will import from Utility and vice versa in case of a surplus. This means that the both the Utility and MG should allow bidirectional power flow between them.

3- Scheduling. In centralized power management, scheduling is an important factor for the reliability of the energy supply. DG's fueled by RES dispatcher cannot send accurate, short term prediction of the available power. For example, a wind power variation is faster than demand variations. In this way the integration of such generating systems needs a special forecasting and dispatching environment.

4- Transmission congestion. First come, first served policy. A late comer to inject power into the transmission lines will be penalized. For IPP's this is an opportunity for losing income in particular for generating units that are fueled by renewable.

5- Will islanding be permitted? The current practice for DG/Utility interconnected is to regress the grid to its original configuration (radial or meshed distribution system) with all interconnected DG units de-energized whenever an unexpected disturbance occurs in the system. Since most distribution systems comprise radial feeders, this practice leads to the discontinuation of the supply for all the downstream customers. Thus, the system reliability stays at the same level as it was before integrating the DG with the system. If interconnected DGs are permitted to supply

loads during Utility outages, the system reliability will be improved. This goal can be achieved by simply coordinating intention islanding of DG units [17].

6- What will be the DG penetration level without compromising the grid stability and reliability? Many researchers concluded that 25% penetrations are of no harm to the grid and it actually enhances the voltage stability, assuming that the DG is strategically installed, which is not always the case. Moreover, there are insufficient data on the dynamic performance of the hosting grid and the impact on the overall power quality and distribution reliability.

7- Where are the interconnection protection and communication infrastructure functionality and reliability? Relays are normally used to provide zoning protection and are independently protecting each zone without any cross-communication between the zones. Moreover, there is no real time communication in the form of wide area network nor intelligent sensing devices protocol standards available that could enhance the interconnection infrastructure.

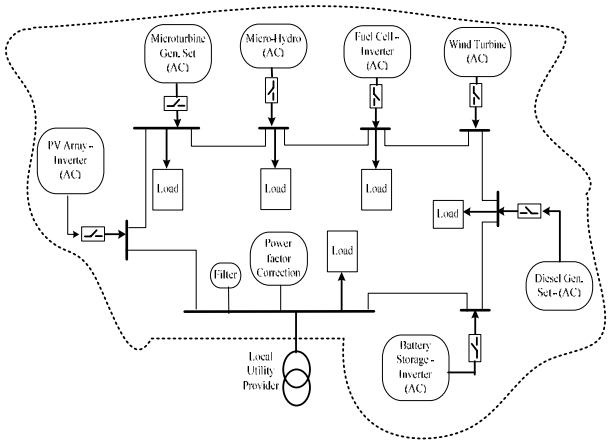

Fig. 3(a) Alternating Current Based MG Architecture

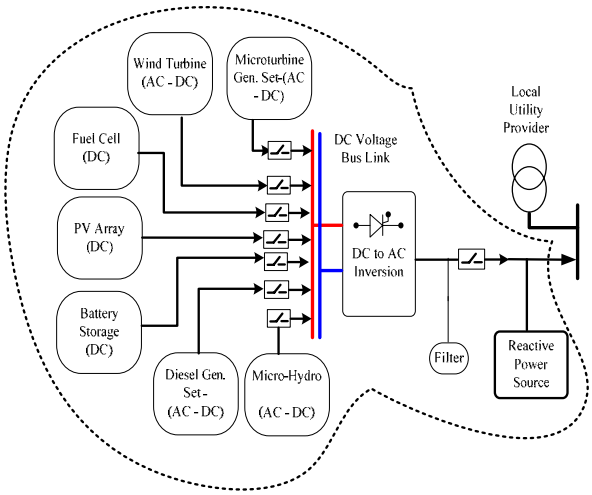

Fig. 3(b) Direct and Centralized Alternating Current Based MG Architecture

It is evident from the above argument that there are various challenges need to be addressed by all parties collectively along the regulating body to develop consentient standards and regulation to facilitate the successful penetration. P1547 compiled by the IEEE is a good model for wanted standards [18]. Other standards that address islanding, EMS protocol's and web agents are also needed.

IV. NEEDED MEASURES

The following is a short list of broadly needed measures that need to be addressed by all parties involved in the energy sector to facilitate a safe and reliable MG integration:

1. Many MG structure are still in the R&D phase. Unless field experience is conducted, many technical issues will be undiscovered and this hampers the confidence of utilities in allowing such environment to play a role in the market.
2. More technical and non-technical studies on the DG and MG penetration impact are needed to validate the expected benefits.
3. A need for clear and established interconnection and operational procedures between the supplying parties specifically during maintenance of connecting transmission lines.
4. Clear procedures of how to react and operate for cases of energy or capacity deficiency situation.
5. The need of a reliable forecasting tool for the short and long term scheduling of those generating units that considered to be intermittent such as wind and solar systems.
6. Clear and supported pricing mechanism for active and reactive power components exchange.
7. Need for adaptation of intelligent devices and remote terminal units within the existing Utility infrastructure to facility information exchange at the component level with a central control unit.
8. R&D support to develop web based EMS within a secure Supervisory Control And Data Acquisition (SCADA) system to enable real time information exchange and power dispatching among the various MG elements.

V. CONCLUSION

The article presented a short listing of merits and challenges facing MG integration. Despite the increasing reported cases of successful penetration of DG systems world wide, there are more challenges that need to be addressed collectively by all parties. MG challenges requires multidisciplinary and cross cutting technologies strategy. Despite recent advances on the component level, more in depth R&D advances are needed on the system level in related technologies such as power electronic interface, utility communication and supervisory control systems. There are also the non-technical issues such as interconnection standard, unit prices, reserve requirements and market regulatory framework are also need to be initiated and approved in a timely manner. As MG is based on fuel mix and modularity of the generating units, a complex coordination strategy is needed with clear integration and resource management rules.

MG useful integration will ultimately change how electricity is produced and traded and eventually pave the way for the possible realization of the virtual generating plant and harmonize the equation of fuel availability, the use of local natural resources effectively, minimizing the negative impact on the environment and meet the demand regardless of the geographic location.

VII. REFERENCES

[1] H. B. Puttgen, P. R. MacGregor,and F.C. Lambert, “Distributed generation: Semantic hype or the dawn of a new era?”.IEEE Power and Energy Magazine, Volume 1, Issue 1, Jan-Feb 2003, pp. 22 - 29

[2] R. C. Dugan and S. K. Price “Issues for Distributed Generation in the US”, Power Engineering Society Winter Meeting. IEEE, Volume: 1, 2002, vol.1, pp. 121- 126.

[3] P. A. Daly and J. Morrison “Understanding the potential benefits of distributed generation on power delivery systems”. Rural Electric Power Conference. 29 April-1 May 2001, pp.A2/1 - A213.

[4] H. M. Quezada, J. R. Abbad, and T. G.S. Roman, “Assessment of energy distribution losses for increasing penetration of distributed generation”. IEEE Transactions on Power Systems, Volume 21, Issue 2, May 2006, pp. 533 – 540.

[5] R. Lasseter, “Microgrids,” in Proc. Power Engineering Society Winter Meeting, IEEE, vol. 1, January 2002, pp. 27–31.
[6] G. Simons, P. Sethi, R. Davis, K. DeGroat, D. Comwell, and B. Jenkins, “The role of renewable distributed generation in California's electricity system”. IEEE Power Engineering Society Summer Meeting. Volume 1, 15-19 July 2001, pp. 546 – 547.
[7] H. G. DuPont, “Wind turbine generators gain acceptance in distributed generation applications”. IEEE Power Engineering Society General Meeting, 2003, Volume 4, pp. 13-17.
[8] P. Agalgaonkar, S. V. Kulkarni, S.A. Khaparade “Evaluation of configuration plans for DGs in developing countries using advanced planning techniques”. IEEE Transactions on Power Systems,
Volume 21, Issue 2, May 2006 , pp.73 - 981
[9] S. Grijalva, S, and A. M. Visnesky. “Assessment of distributed generation programs based on transmission security benefits”. IEEE Power Engineering Society General Meeting. 12-16 June 2005 , pp. 1441 - 1446
[10] S. A. Castelaz “Plugging Into Hidden Capacity & Networking Distributed Generation with the Virtual Power Plant™”. Standard & Poor’s Utilities & Perspectives Newsletter Special Technology Issue, January 2000, pp. 1 – 5.
[11] Kojovic and R. Willoughby “Integration of Distributed Generation in a Typical USA Distribution System”. IEE- CIRED2001 conference record, June 2001, conference publication No. 482, pp. 18 –21.
[12] N. R. Friedman “Distributed Energy Resources Interconnection Systems: Technology Review and Research Needs”. National Renewable Energy Laboratory, report SR-560-32459, September 2002.
[13] CIGRE study Committee, “Impact of increasing contribution of dispersed generation on the power system,” CIGRE study Committee no 37, Final Report, Tech. Rep., 2003.
[14] K. Kauhaniemi and L. Kumpulainen, “Impact of distributed generation on the protection of distribution networks”. Eighth IEE International Conference on Developments in Power System Protection.Volume 1, 5-8 April 2004, pp. 315 – 318.
[15] Bhowmik, A. Maitra, S. M, J. E. Schatz “Determination of allowable penetration levels of distributed generation resources based on harmonic limit considerations”. IEEE Transactions on Power Delivery, Volume 18, Issue 2, April 2003, pp. 619 - 624
[16] W. So and K. K. Li “Protection relay coordination on ring-fed distribution network with distributed generations”. Conference on Computers, Communications, Control and Power Engineering Proceedings. TENCON '02. Volume 3, 28-31 Oct. 2002, pp. 1885 – 1888.
[17] Nigim, K.A. and Y.G. Hegazy, “Intention islanding of distributed generation for reliability enhancement”, IEEE 2003 PES General Meeting, Toronto, July 2003, pp. 1- 6.
[18] “P1547 standard series for interconnecting distributed resources with electric power systems,” IEEE, 1547 Work Group, Tech. Rep., 2003.

VII. BIOGRAPHIES

Khaled Nigim (SM) has a Ph. D. in Electrical Engineering from the University of Leicester, England, UK and B. Sc. in Electrical Engineering from Zagazig University of Cairo, Egypt. He is the Coordinator of the on-line Master of Engineering degree in Electric Power at the Department of Electrical & Computer Engineering, University of Waterloo. He has more than 24 years of experience in renewable energy system design and implementation, design and assembly of industrial units that incorporate PLCs, intelligent sensors, VSD’s and decision-making, for infrastructure restoration. He is a registered professional engineer in Ontario, Canada.

Wei-Jen Lee, IEEE member(S'85-M'85-SM'97,received his B.S. and M.S. degrees in Electrical Engineering from National Taiwan University, Taipei, Taiwan, in 1978 and 1980, respectively, and a Ph.D. degree in Electrical Engineering from the University of Texas at Arlington in 1985. Since then, he joined the University of Texas at Arlington and currently is a Professor of the Electrical

Engineering Department. He has been involved in research on power flow, transient and dynamic stability, voltage stability, short circuit, relay coordination, power quality analysis, and deregulation of utility industries. He is also involved in research on the design of integrated microcomputer-based monitoring, measurement, control, and protection equipment for electric power systems. He is a senior member of IEEE and a Registered Professional Engineer in the State of Texas.

Received January 18 2007

8. A STUDY ON EFFECT OF DISPERSED GENERATOR CAPACITY ON POWER SYSTEM PROTECTION. (PAPER 07GM0503).

Yuping Lu, Lidan Hua, Ji'an Wu, Gang Wu, *and* Guangting Xu (Southeast University, Nanjing, China).

***Abstract*--**When a fault occurred in a distribution system, the load center located with Distributed Generation (DG) will have a significant impact upon protection. And the impact depends on the number, location and size of injected DG. This paper focuses on studying the effect of DG upon conventional protection. Starting with the analysis of the coordination relationship between relays to obtain the capacity requirement for single DG connected to radial distribution system, the calculation is extended to several DGs being interconnected. Examples will be used to demonstrate various issues and solutions.

***Index Terms*--** Dispersed Generation, dispatched power system, coordination, capacity

I. INTRODUCTION

Some customers of the distribution power system plan to connect Distributed Generation (DG) into the present network. In modern distribution systems, DG from both synchronous and asynchronous generators produces an additional contribution to fault level. Circuit breaker ratings and relaying coordination designed for systems, which do not have DG, may not be able to cope with the new situation[1]. The electric energy production from DGs will take an important part of the total amount, and consequently, the reliable running of DGs will be important to the reliability of power supply, with lots of DGs integrated[2,3].

The interconnection of DGs brings a great change to configuration of the utility distribution network. As a result, this leads to a big challenge for its control and management[4-6]. At present standards for interconnecting DG with the network mostly are based on the principle that DG shouldn't bring influence upon the normal operation performance for the utility protection and control system[7,8]. For example, it's demanded that DG shouldn't actively participate in the voltage regulation. And for another instance, in case of a fault in the dispatched system, it's demanded that DG should be quitted from the network to ensure the right operations of the protective devices. In this way, it guarantees the security of the system, but sacrifices the interests of the power suppliers and customers, since it brings negative effect to the area and reliability of power supply[9].

With a fault occurred in the distributed system DG could have a significant impact upon protection, depends on the number, location and size of injected DG. Based on the conventional current protection, this paper presents an analysis to the protection for the radial distribution system injected with DG and, according to both the relationship between relays and the reliability of power supply, gives an exploration to the problem of the interconnected DG size, to achieve the positive applications of DG and make the more efficient and reliable operation of the system.

This work was the Project 50577006 supported by National Natural Science Foundation of China (NSFC)

Yuping Lu, Lidan Hua, Gang Wu and Guangting Xu are with the School of Electrical Engineering of Southeast University, Nanjing 210096, China. (e-mail: luyuping@seu.edu.cn)

Ji'an Wu is with Guodian Nanjing Automation CO.LTD, Nanjing 210003, China. (e-mail: wja@sac-china.com)

II. COORDINATION DISCRIMINATION OF CONVENTIONAL PROTECTION

Figure 1(a) shows a simple radial dispatched power system, where S is the source , A, B, C, D, E are the nodes of system and their corresponding loads are load1, load2, load3, load4, load5 respectively. When a fault occurs to the line, inverse over-current protection is adopted. The setting and coordination curves of relay 1, 2, 3, 4 are showed in figure 1(b).

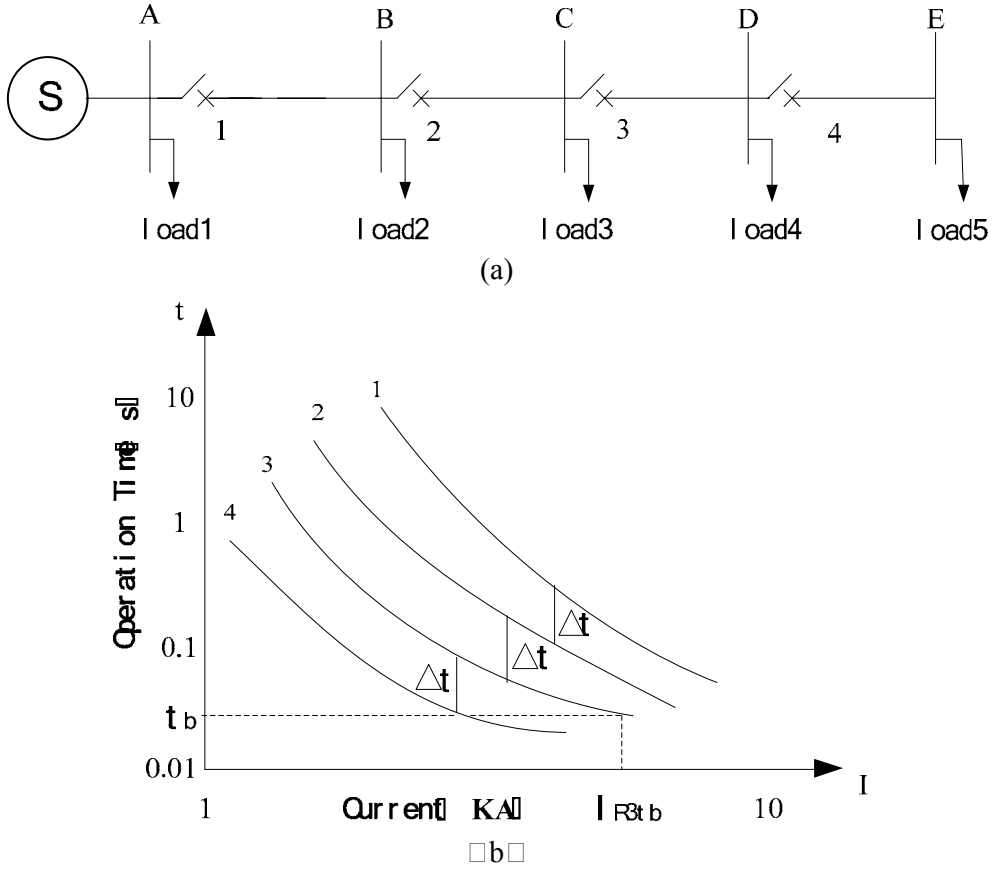

Fig.1. Coordination curves of inverse over-current relays

The general operational characteristics of relay 1,2,3,4 can be expressed by the following equation:

$$t = \frac{0.14K_i}{\left(I_{Ri}/I_{dz.i}\right)^{0.02} - 1} \tag{1}$$

$i = 1, 2, 3, 4$, where

K_i ——time constant of relay i

$I_{dz.i}$ ——pickup current of relay i

$I_{R.i}$ ——current seen by relay i

When a fault occurred at node D, the action time set of relay 4 can be instant, which is the relay inherent parameter of t_b. The philosophy here is that for a maximum current presented in section CD, i.e., with a fault occurred at node C, the time of operation of relay 2 is larger than that of relay 3 at least by a certain time interval called Δt (in figure 1(b)). Δt depends on factors such as the circuit breaker opening time, delay and return time of the measuring element, etc[10].

III. EFFECT OF DG UPON TRADITIONAL PROTECTION DG

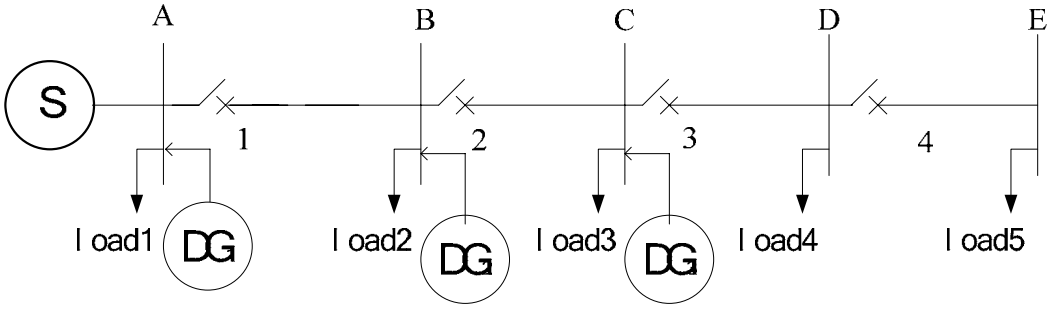

Fig.2 Distribution system with DG

Figure 2 shows a distribution network with DG. The coordination relationship between relays has changed, due to the number, location and capacity of DG interconnected[11-14]. The following cases are analyzed in this paper.

A SINGLE DG INTERCONNECTED

With DG_1 injected, for a fault downstream, e.g., a fault in section DE, relay 1, 2, 3, 4 will see the downstream fault current, which is greater than that without DG_1. Then, relay 4 will eliminate the fault and the sensitivity will be improved because of the larger fault current. The situation will be similar for a given fault in section AB, BC or CD. For a fault upstream, that is to say, with a fault occurred before node A, relay 1, 2, 3, 4 will never see the upstream fault current and won't act. Meanwhile, the over-current protective device of DG_1 will sense a fault current and then act to separate DG_1 from the utility system. Thus, the selectivity and coordination of relay 1, 2, 3, 4 will hold.

With DG_2 injected, for a fault downstream, relay 1, 2, 3, 4 will sense downstream fault currents. The fault current seen by relay 2, 3, 4 is greater than that without DG, while the current of relay 1 is less than before. For a fault in section AB, relay 2, 3, 4 will never see the upstream fault current, while relay 1 will sense a downstream fault current and operate. With a fault before node A, relay 1 will see a reversed fault current, acting when the fault current value is more than the set value. Meanwhile, DG_2 and the loads downstream will form an island. The island will run to decrease the outrage rate until it is unbalanced.

The scenarios are similar with DG interconnected at other locations.

B. Several DGs interconnected

With DG_1 and DG_2 injected, for a downstream fault of DG_2, selectivity and coordination of relay 1, 2, 3, 4 will hold; for an upstream fault of DG_1, relay 1 will operate. Then, DG_1 will be disconnected from the system, while DG_2 and the loads downstream will form an island running mode.

With DG_2 and DG_3 injected, for a downstream fault of DG_3, selectivity and coordination of relay 1, 2, 3, 4 will remain; for a fault in section AB, relay 1 will act; for a fault before node A, relay 1, 2 will see the reversed fault currents contributed by DG_2 and DG_3. In this case, the upstream currents are proportional to the capacities of DG_2 and DG_3, thus the corresponding operation time of relay 1, 2 is related to the fault injection capabilities of DG_2 and DG_3. Coordination is likely to be lost.

In the DG_1, DG_2 and DG_3 injection case, for a fault downstream, the situation is similar. Relay 2 will act for a fault in section BC and relay 1 will operate with a fault in section AB. For a fault before node A, the operation time of relay 1, 2 depends on the sizes of DG_2 and DG_3. It is obvious that the operation time of relay 1, 2, 3 will be related to the capacities of DG_1, DG_2 and DG_3 if DG_1 is connected at node D.

It comes to the conclusion that with a downstream fault of DG, selectivity and coordination remain and sensitivity is improved; for an upstream fault of DG, coordination is likely to be lost.

IV. REQUIREMENT OF DG SIZE

A. A SINGLE DG INTERCONNECTED

With DG_1 injected, for a fault at node D, relay 4 is required to operate before relay 3. In this case, as can be seen from figure 1(b), if the fault current is more than I_{R3t_b}, in theory, relay 3 and relay 4 will operate at the same time t_b explained above. Thus, coordination will be lost. In fact, the fault current reaches t_b rarely, but the operation time interval between relay 3 and relay 4 will be shorter because of the fault current contribution from DG. Relay 3 is likely to have a false action, considering that the inherent time of relays is different. In order to keep the coordination, the operation time interval between relay 3 and relay 4 should keep a margin signed as ε. If the interval is more than ε, relay 3 will never operate before relay 4.

The following equations can be obtained by linearizing (1).

$$t\left(I_{R3f}\right) = a_1 I_{R3f} + b_1 \tag{2}$$

$$t\left(I_{R4f}\right) = c_1 I_{R4f} + d_1 \tag{3}$$

Where, I_{R3f} is the fault current seen by relay 3, and I_{R4f} is the fault current sensed by relay 4.

As explained above, the following equality can be written.

$$t\left(I_{R3f}\right) - t\left(I_{R4f}\right) > \varepsilon \tag{4}$$

By substituting (2) and (3) into (4), the fault current can be achieved as (5).

$$I_{R3f} < \frac{b_1 - d_1 - \varepsilon}{c_1 - a_1} = M \tag{5}$$

The equivalent circuit is described in figure 3 for a three-phase fault current at node D.

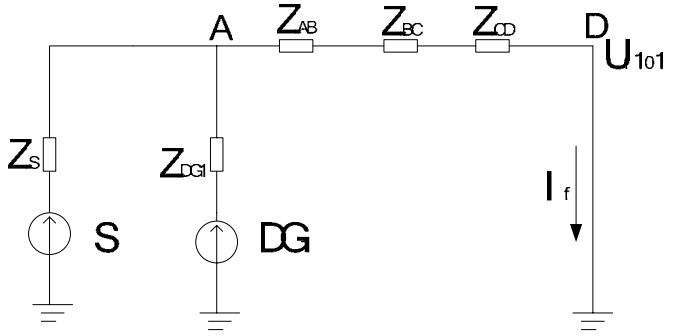

Fig.3 Equivalent circuit for a three-phase fault at node D

In figure 3, Z_S is the system impedance; Z_{DG1} is the impedance of DG_1; $U_{f|0|}$ is the normal voltage at the fault location; Z_{AB}, Z_{BC}, Z_{CD} are line impedances of section AB, BC, CD, DE respectively. They are equal to Z_L. I_f is the fault current. It is supposed that the rated voltage of the source is equal to that of DG. To begin with the following formula is assumed.

$$Z_{AB} = Z_{BC} = Z_{CD} = Z_L$$

If the basic capacity is S_B and the rated voltage of the source is equal to the reference voltage signed as U_B, then the reference current can be written as the following equation:

$$I_B = S_B / \left(\sqrt{3} U_B\right)$$

According to the per-unit calculation system, the fault current can be calculated in (6) by its substituting into and rearranging of (5).

$$I_{f*} = U_{f|0|*} / Z_* < M / I_B \tag{6}$$

The total impedance seen from the fault location is described in (7). The impedances of DG_1 and source can be written as (8) and (9) correspondingly.

$$Z_* = Z_{S*} // Z_{DG1*} + 3Z_{L*} \tag{7}$$

$$Z_{DG1*} = Z_{DG1} S_B / S_{DG1} \tag{8}$$

$$Z_{S*} = Z_S S_B / S_S \tag{9}$$

From (6), (7), (8) and (9), the following inequality can be derived.

$$S_{DG1} < \frac{MZ_{DG1} S_B}{U_{f|0|*} I_B - 3MZ_{L*}} - \frac{Z_{DG1} S_S}{Z_S}$$

Thus the maximum size of DG_1 for a three-phase fault at node D can be written as follows:

$$S'_{DG1\max} = \frac{MZ_{DG1} S_B}{U_{f|0|*} I_B - 3MZ_{L*}} - \frac{Z_{DG1} S_S}{Z_S}$$

For a phase-to-phase fault at node D, the fault current of relay 3 will be less than M and relay 3 will never operate, under the same condition when a three-phase fault occurs at node D.

Similar calculation can be carried out for relay 2 which should never operate for a three-phase fault at node C and relay 1 should never act with a three-phase fault at node B. Thus, the maximum capacity $S_{DG1\max}$ can be determined.

With DG_2 injected, the capacity of DG_2 should also be limited to ensure the correct operation for a downstream fault.

In addition, for a phase-to-phase fault before node A, the protective device of source will operate, however, the fault current will continue because of DG_2. Thus, the fault current injected by DG_2 should be enough to ensure the operation of relay 1. It is required as follow.

$$I_f > I_{dz.1}$$

The following inequation is required for a three-phase fault before node A, under the same condition.

$$I_f > 2I_{dz.1} / \sqrt{3}$$

Figure 4 shows the equivalent circuit for a three-phase fault before node A.

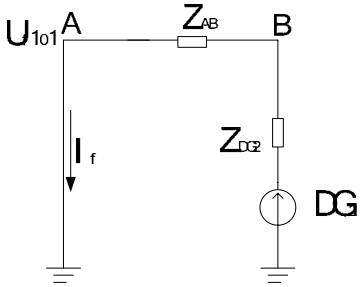

Fig.4 Equivalent circuit for a three-phase fault before node A

From figure 4, the fault current can be written as (10).

$$I_{f*} = U_{f|0|*} / \left(Z_{DG2*} + Z_{AB*} \right) > 2I_{dz.1} / \sqrt{3} I_B \tag{10}$$

where

$$Z_{DG2*} = Z_{DG2} S_B / S_{DG2} \tag{11}$$

From (10) and (11), the following inequality can be calculated.

$$S_{DG2} > \frac{2I_{dz.1} Z_{DG2} S_B}{\sqrt{3} I_B U_{f|0|*} - 2I_{dz.1} Z_{L*}}$$

Thus the minimum size of DG_2 can be written as follows:

$$S_{DG2\min} = \frac{2I_{dz.1}Z_{DG2}S_B}{\sqrt{3}I_B U_{f|0|*} - 2I_{dz.1}Z_{L*}}$$

Similarly, considering that protective devices should not have false operations for downstream faults and not have missed operations with faults upstream, the boundary value of DG capacity can be determined.

B. SEVERAL DGS INTERCONNECTED

With DG_2 connected only, the boundary size of DG_2 can be calculated from the above subsection A. For DG_3 interconnected only, the capacity calculation is similar. The following capacities can be achieved.

$$S_{DG2} \in (S_{DG2\min}, S_{DG2\max})$$

$$S_{DG3} \in (S_{DG3\min}, S_{DG3\max})$$

With DG_2 and DG_3 injected, the sizes of DG_2 and DG_3 will be subjected to new constraints according to the coordination.

For a three-phase fault at node D, the total impedance is described in (12).

$$Z_* = \left[\left(Z_{S*} + Z_{AB*}\right) // Z_{DG2*} + Z_{BC*}\right] // Z_{DG3*} + Z_{CD*} \tag{12}$$

From (6) and (12), the following inequality can be derived:

$$\left(1-N\right)\frac{Z_{DG2}S_B\left(Z_{S*}+Z_{L*}\right)S_{DG3}}{S_{DG2}\left(Z_{S*}+Z_{L*}\right)+Z_{DG2}S_B} + S_{DG3}Z_{L*} < NZ_{DG3}S_B - Z_{DG3}S_B \tag{13}$$

where

$$N = I_B U_{f|0|*} / M - Z_{L*}$$

For a three-phase fault before node A, relay 1 and relay 2 will have the reversed fault current called I_{R1f} and I_{R2f} correspondingly. The equivalent circuit is shown in figure 5. From figure 5, the following equations can be achieved.

$$Z_* = Z_{DG2*} // \left(Z_{DG3*} + Z_{BC*}\right) + Z_{AB*} \tag{14}$$

$$I_{R1f*} = I_{f*} = U_{f|0|*} / Z_* \tag{15}$$

$$I_{R2f*} = \frac{I_{f*}Z_{DG2*}}{Z_{DG2*} + Z_{DG3*} + Z_{BC*}} \tag{16}$$

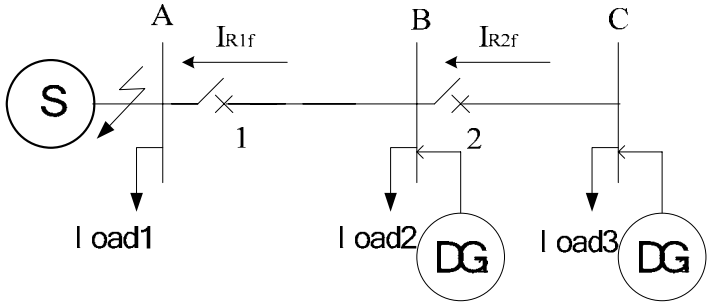

(a)

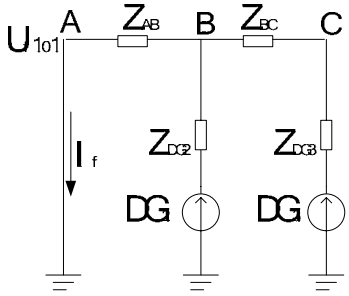

(b)

Fig.5 An upstream three-phase fault before node A

In this case, relay 1 should operate before relay 2. The following equations can be reduced by linearizing (1)(i=1, 2) to decrease the calculation task.

$t\left(I_{R1f^*}\right) = a_2 I_{R1f^*} + b_2$

$t\left(I_{R2f^*}\right) = c_2 I_{R2f^*} + d_2$

By substituting (14), (15) and (16) into (17), (18) can be derived.

$$t\left(I_{R2f^*}\right) - t\left(I_{R1f^*}\right) > \varepsilon \tag{17}$$

$$\left(\frac{c_2 AS_{DG3}}{AS_{DG3} + BS_{DG3} + Z_{L^*} S_{DG2} S_{DG3}} - a_2\right) I_{f^*} > b_2 - d_2 + \varepsilon \tag{18}$$

where

$A = Z_{DG2} S_B$, $B = Z_{DG3} S_B$,

$$I_{f^*} = \frac{U_{f|0|^*}\left(AS_{DG3} + BS_{DG2} + Z_{L^*} S_{DG2} S_{DG3}\right)}{AB + 2AZ_{L^*} S_{DG3} + BZ_{L^*} S_{DG2} + Z_{L^*}^2 S_{DG2} S_{DG3}}$$

Similarly, the following inequality will hold for a phase-to-phase fault before node A.

$$\left(\frac{c_2 CS_{DG3}}{CS_{DG3} + DS_{DG3} + Z_{L+^*} S_{DG2} S_{DG3}} - a_2\right) I_{f^*} > b_2 - d_2 + \varepsilon \tag{19}$$

where

$C = Z_{DG2+} S_B$ □ $D = Z_{DG3+} S_B$,

$$I_{f^*} = \frac{\sqrt{3} U_{f|0|^*}\left(CS_{DG3} + DS_{DG2} + Z_{L+^*} S_{DG2} S_{DG3}\right)}{2\left(CD + 2CZ_{L+^*} S_{DG3} + DZ_{L+^*} S_{DG2} + Z_{L+^*}^2 S_{DG2} S_{DG3}\right)}$$

where

Z_{DG2+}, Z_{DG3+} and Z_{L+} are the positive sequence impedances of DG_2, DG_3 and line respectively. The positive sequence impedances are assumed equal to the negative sequence impedances in this paper.

According to (13), (18) and (19), the capacities of DG_2 and DG_3 can be selected. Then, the sizes of DG_2 and DG_3 can be finally determined by making intersections with S_{DG2} and S_{DG3} expressed above.

The capacity calculation can be extended to several DGs interconnection case. The calculation steps are as follows.

Step 1: The maximum and minimum capacities can be calculated based on the requirement of fault current for single DG interconnected.

Step 2: For a fault downstream, considering that the fault current should not bring about false action, the expression consists of all the capacities can be achieved.

Step 3: For an upstream fault, other expressions contained DG capacities can be calculated by consideration of the adjacent relays' coordination.

Step 4: The appropriate capacities of DGs can be finally determined, according to all the expressions above.

V. EXAMPLES

A sampled 11kV radial distribution system with topology as shown in figure 1 is studied. All bus loads are 1MW. For each feeder segment $R = 0.25\Omega$, $X = 0.785\Omega$. The voltage descent is less than 10□. The pickup currents of relay 1, 2, 3, 4 are 650A, 500A, 300A, 180A respectively. Relay 4 is set to operate instantaneously. $t_4 = 0.03s$, $\Delta t = 0.6s$, $K_1 = 0.36$, $K_2 = 0.26$, $K_3 = 0.17$.

With DG interconnected at node B, the effect of capacity on the protection is shown in table 1 for a three-phase fault at node C, where, t_2 and t_3 are the operating time of relay 2, 3 respectively. The power factor of DG is 0.9 lagging (0.9pf). Table 2 shows the effect for a phase-to-phase fault before node A.

Table.1 Three-phase fault at node C

DG Capacity(MW)	Fault Current(A)	t_2 (s)	t_3 (s)
0.1	2505	1.120	0.533
1	3050	0.996	0.487
10	9660	0.601	0.321

Table.2 Upstream phase-to-phase fault before node A

DG Capacity MW	Fault Current A	Operation Status of Relay 1
0.01	90	Missed Operation
0.1	132	Missed Operation
1	682	Operation
5	2350	Operation

With DG_1 (0.9pf) interconnected at node B and DG_1 (0.9pf) injected at node C, the effect of capacities to the protection is described in table 3 for a three-phase fault before node A, where, I_{R1f} is the fault current of relay 1 and t_1 is the operate time. I_{R2f} is the fault current of relay 2 and t_2 is the operating time of relay 2.

Table.3 Upstream three-phase faults before node A

Capacity of DG_1 MW	Capacity of DG_2 MW	I_{R1f} (A)	I_{R2f} (A)	t_1 (s)	t_2 (s)
0.1	2	1450	1117	3.124	2.263
0.5	2	1841	1069	2.402	2.396
2	2	2210	1020	2.040	2.554
1	5	2658	2080	1.769	1.268
5	5	4065	1719	1.353	1.467
10	5	5279	1401	1.181	1.752

VI. CONCLUSION

(1) The coordination problem caused by the presence of DG can be solved by applying the inverse over-current protection.

(2) From table 1 and table 2, for a fault downstream, the more the capacity of DG is, the smaller the operating time interval is. The interval will be less than 0.3 second, thus the false operation will take place when the capacity is more than a certain value. For an upstream fault, the missed operation will occur if the capacity of DG is not enough. In addition, sizes of the adjacent DGs must be restricted as shown from the operating time equation to avoid the false action.

(3) For a downstream fault, the selectivity will be improved because of the fault current injected by DG; for an upstream fault, the selectivity is unlikely deduced as long as the minimum capacity is satisfied.

(4) Coordination problem can be settled by the directional relays. However, it is unworthy to discard the traditional protective devices because the directional relay is very costly.

(5) The study on DG capacity gives an insight into its impact to protection coordination and the exploration of DG capacity are important to the practice of DG application.

VII. REFERENCES

[1] Loi Lei Lai and Tze Fun Chan, Distributed Generation – Induction and Permanent Magnet Generators, John Wiley & Sons, UK, March 2007.

[2] Brown R E □Free L A□Analyzing the Reliability Impact of Distributed Generation[C]□Power Engineering Society Summer Meeting□Vancouver□Canada□July□2001□(2)□1013-1018□

[3] Jenkins N□Strbac G□Jenkins□Impact of Embedded Generation on Distribution System Voltage Stability[C]□IEE Colloquium on Voltage Collapse□London□1997□9□1-4□

[4] Liang Youwei□Hu Zhijian□Chen Yunping□A Survey of Distributed Generation and Its Application in Power System[J]□Power System Technology□2003□27(12)□71~76□

[5] Wang Zhiqun□Zhun Shouzhen□Zhou Shuangxi□Hunag Renle□Wang Liangui□Study on Location and Penetration of Distributed Generations[J]□Proceedings of the CSU-EPSA□2005□17(1)□53~58□

[6] Liang Caihao□Duan Xianzhong□Distributed Generator and Its Impaction on Power System[J]□Automation of Electric Power System□2001□25(6)□53~56□

[7] IEEE Std.1547□IEEE standard for interconnecting distributed resources with electric power system[S]□

[8] UK Electricity Association□Engineering recommendation G.59/1□recommendations for the connection of embedded generation plant to the regional electricity companies[S]□

[9] Yi Xin□Lu Yuping□Islanding Algorithm of Distribution Networks with Distributed Generators[J]□Power System Technology□2006□30(7)□50~54□

[10] He Jiali□Song Congju□Protective Relay Principle of Electric Power System□Third Edition□[M]□Beijing□China Electric Power Press□2003□20~28□

[11] Tales M. de Britto□Diego R. Morais□Marco A.Marin□Jacqueline G□.RoIim□Hans H.Ziirn□Raul F.Buendgens□Distributed Generation Impacts on the Coordination of Protection Systems in Distribution Networks□IEE/PES Transmission & Distribution Conference & Exposition□Latin America□2004□623~628□

[12] Adly Girgis□Sukumar Brahma□Effect of Distributed Generation on Protective Device Coordination in Distribution System□IEEE Press□2001□

[13] Michael T. Doyle□Reviewing the Impacts of Distributed Generation on Distribution System Protection□Power Engineering Society Summer Meeting□2002□IEEE□Vol.(1)□103~105□

[14] Ferry A□Viawan and Muhamad Reza□The Impact of Synchronous Distributed Generation on Voltage Dip and Overcurrent Protection Coordination□International Conference on Future Power Systems□IEEE□2005□1~6□

VIII. BIOGRAPHIES

Yuping Lu was born in Danyang, China, in Oct, 1962. He received the Ph.D. degree in electrical engineering from the City University, UK in 2003. He is working as a professor in Southeast University of China. His research interests are in power system protection, especially digital relaying of generator-transformer unit, and protection and control technique in distribution system with DGs.

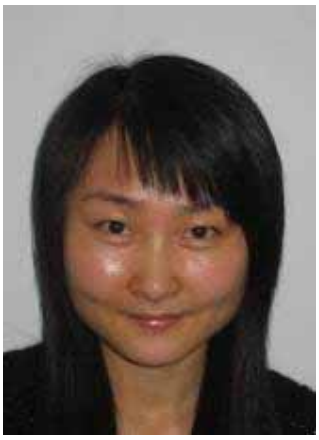

Lidan Hua was born in Changzhou, China, on Dec 10, 1980. She received the Bachelor's degree in electrical engineering from Southeast University in June 2004. Now she is pursuing her M.E. Her current research interest is in protection and control of distribution system with DGs.

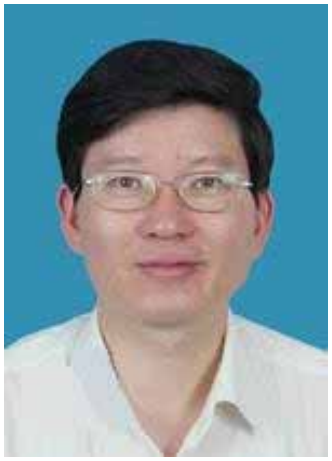

Ji'an Wu was born in Suzhou, China, on Dec 14, 1960. He graduated from Southeast University in July 1982 and April 1989, and received B.E. and M.E respectively. Now he is working as chief engineer in Guodian Nanjing Automation CO.LTD. His research interest is in Power System Protection.

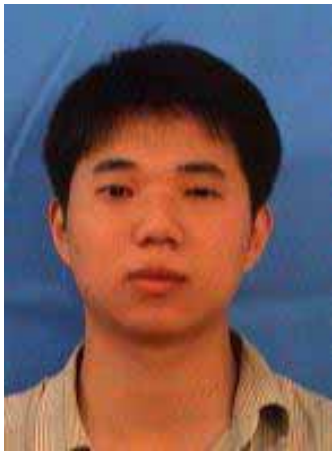

Gang Wu was born in Xuzhou, China, in 1981. He received the Bachelor's degree in electrical engineering from Hohai University in June 2004. Now he is pursuing his M.E. His current interest is in protection and control of distribution system with DGs.

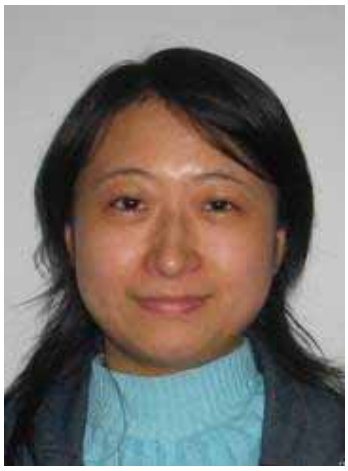

Guangting Xu was born in Xuzhou, China, in 1977. Now she is pursuing her M.E. Her current interest is in protection and control of distribution system with DGs.

9. ANALYSIS OF TRANSIENT DISTURBANCES IN DISTRIBUTION SYSTEMS: A HYBRID APPROACH (Paper 07GM1015).

U. D. Dwivedi[1], S. N. Singh[2], *Senior Member, IEEE,* S. C. Srivastava[3], *Senior Member, IEEE*

Abstract-- Built-in event diagnosis and assessment modules are the key to the power quality (PQ) monitoring systems. Discrete wavelet transform (DWT) has been used recently by many researchers for detection and analysis of the of PQ disturbances. Despite the excellent time-frequency localization property, DWT based event detectors can not adapt itself to the dynamic changes in the load configuration because of its fixed filter coefficients and, hence, generates repeated detection and processing of the same steady state disturbance. An adaptive filter on the other hand adapts its filter coefficients continuously with changing monitored signal. Therefore, an adaptive filtering and DWT based hybrid system has been proposed in this paper for the detection and analysis of transient disturbances. Adaptive filter based monitoring avoids the detection of the same study event repeatedly. Extensive tests conducted on the data obtained from a practical distribution system confirm the effectiveness of the proposed approach in automatic detection and diagnosis of transient PQ violations.

Index Terms-- Adaptive filtering, orthogonal polynomial approximation, power quality, time-frequency analysis, wavelet transform.

I. INTRODUCTION

The ongoing regulatory policy and structural changes in the electricity industry have raised the issue of power quality (PQ), a figure-of-merit amongst the competing distribution utilities. Meeting customer's expectations and maintaining customer's confidence are the strong driving factors behind maintaining the quality of power. Any electrical disturbance that damages, end users equipment or causes devices to fail or operate incorrectly, can be viewed as a power quality problem [1]. Power quality like quality in other goods and services, is difficult to quantify. Generally, when the power received can not fulfill the needs of maintaining proper sinusoidal voltage at desired magnitude and frequency, the "Quality" is said to be lacking. Some power quality problems may be caused by natural phenomena, such as lightning strikes, while others are caused by utility operations. The problem has been aggravated with the increasing use of nonlinear loads and power electronic devices. These loads and devices are a major source of waveform distortions and are themselves very sensitive to such type of voltage waveshapes.

The sources and causes of such disturbances must be known before appropriate mitigating actions to be taken, and thus their on-line detection and identification are essential. A feasible approach to achieve this goal is to incorporate detection capabilities into monitoring equipment so that events of interest can be recognized, captured, and classified automatically. Hence, good performance monitoring equipment must have capability to detect, localize, and classify transient events. Time-frequency representations of the signal, like short time Fourier transform (STFT) and wavelet transform (WT) has emerged as effective tools for more efficient characterization of the PQ waveforms for detection and automated disturbance classification [2]–[6] and for power system protection [7]. The other possible power system applications for WT analysis are detection of high-impedance faults [8] and PQ data compression [9].

A PQ monitor captures actual voltage and current waveforms, when certain threshold levels are exceeded such as magnitude of discrete wavelet transform (DWT) coefficients threshold. The main

[1] U. D. Dwivedi (e-mail: umakant@iitk.ac.in), [2] S. N. Singh (e-mail: snsingh@iitk.ac.in) and [3] S. C. Srivastava (e-mail: scs@iitk.ac.in) are with the Department of Electrical Engineering, Indian Institute of Technology Kanpur, INDIA. Telephone: +91-512-2597874, Fax: +91-512-2590063.

problem with DWT based event detection method is that, in most cases, the pre-disturbance waveforms are assumed to be sinusoidal, which may not always be possible. Practically, a large number of equipment operates on the power system, which draws or injects different nature of current and also electromagnetic interactions takes place throughout the system. Therefore, under the normal operation, the waveforms may have harmonics, noise and notches, which degrade the detection capability of a DWT, based monitoring system. To minimize the miss-alarm rate, in [10], [11] proposed two denoising algorithms, for DWT based detection and feature extraction, respectively. However, there may be dynamic changes in the systems load configurations that will change the systems steady state condition. As the filter coefficients of wavelet filter are fixed at each decomposition stage, DWT based detectors can not adapt itself to the dynamic changes in the load configuration, and may generate repeated detection and processing of the same steady disturbance.

Hence, the analysis tool, capable of adapting itself to the dynamic changes in systems' load configuration, is needed to detect new events and to avoid detection of the same steady event repeatedly. To overcome the problem associated with DWT based PQ detector, least mean squares (LMS) type adaptive filter based predictor has been proposed in this paper to accommodate changes in systems steady state condition. But, as an adaptive filter constantly changes the filter coefficients and, hence, the frequencies which are allowed to pass, it is not a good idea to use adaptive filter for feature extraction, although one can extract some information by analyzing adaptation error [12]. Despite the inability to adapt to the dynamic load changes, the DWT has been found to be a very effective means to extract frequency information of the disturbance for its classification [4]-[6].

The technique proposed in this paper, therefore, utilizes adaptive filter based event detector for detection of the transient disturbances and DWT module for feature extraction purpose. The proposed hybrid approach analysis has been tested on a large variety of PQ data, generated through simulation on the IIT Kanpur India distribution network with the help of PSCAD/EMTDC simulation software. Extensive tests using different types of transient disturbances reveal the potential capability of the proposed hybrid approach for analysis of transients in distribution systems.

In Section II, a brief review of the theory and mathematical formulation and assumptions for an LMS-type adaptation algorithm has been presented. The proposed hybrid approach has been discussed in Section III. In Section IV, simulation results to confirm the applicability of the algorithm in detection and analysis of transient disturbances has been presented and section V has highlighted main conclusions of the present work.

II. ADAPTIVE FILTERING

Adaptive filtering is a classical branch of digital signal processing (DSP). Industrial interest in adaptive filtering grows continuously with the increase in computer performance that allows increasingly more complex algorithms to be run in real-time.

A ADAPTIVE FILTER THEORY

Discrete-time (or digital) filters are ubiquitous in today's signal processing applications. Filters are used to achieve desired spectral characteristics of a signal to reject unwanted signals, like noise or interferers, to reduce the bit rate in signal transmission, etc. The notion of making filters adaptive, i.e. to alter parameters (coefficients) of a filter according to some algorithm, tackles the problems that might not be known in advance, e.g. the characteristics of the signal, or of the unwanted signal, or of a systems influence on the signal. Adaptive filters can adjust to unknown environment and even track signal or system characteristics varying over time.

In a transversal filter of length N, as depicted in fig.1, at each time n the output sample y[n] is computed by a weighted sum of the current and delayed input samples x[n], x[n - 1], . ..,x[n-k] .

$$y[n] = \sum_{k=0}^{N-1} c_k^*[n]\, x[n-k] \qquad (1)$$

where, $c_k[n]$ is the time dependent filter coefficient (here the complex conjugated coefficients $c_k^*[n]$ are used so that the derivation of the adaptation algorithm is valid for complex signals too). This equation can be re-written in vector form, using $x[n] = [\, x[n], x[n-1], ..., x[n-N+1]\,]^T$, the tap-input vector at time *n*, and $c[n] = [\, c_0[n], c_1[n], ..., c_{N-1}[n]\,]^T$, the coefficient vector at time *n*, is

$$y[n] = c^H[n]\, x[n] \qquad (2)$$

Both $x[n]$ and $c[n]$ are column vectors of length N, $c^H[n] = (c^*)^T[n]$ is the hermitian of vector $c[n]$ (each element is conjugated *, and the column vector is transposed ^{T} into a row vector). In the special case of the coefficients $c[n]$ not depending on time n: $c[n] = c$, the transversal filter structure is an FIR filter of length N. However, the present work focuses on the case that the filter coefficients are variable, and are adapted by an adaptation algorithm.

B. THE LMS ADAPTATION ALGORITHM

The LMS adaptation algorithm is used to perform the time varying prediction, because of its simplicity and fast processing, which is a practical requirement of an on-line PQ detector. The LMS algorithm is an approximation of the steepest descent algorithm, which uses an instantaneous estimate of the gradient vector of a cost function. The estimate of the gradient is based on sample values of the tap-input vector and an error signal. The algorithm iterates over each coefficient in the filter, moving it in the direction of the approximated gradient [13]. For the LMS algorithm, it is necessary to have a reference signal *d*[*n*] representing the desired filter output. The difference

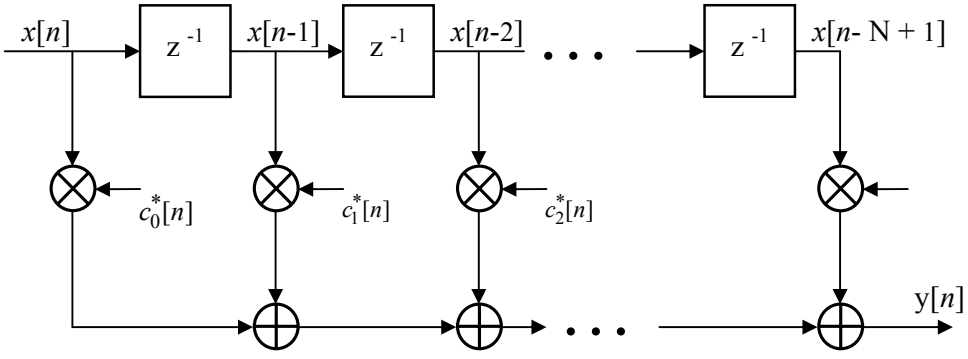

Fig. 1. Adaptive Transversal Filter

between the reference signal and the actual output of the transversal filter in (2) is the error signal.

$$e[n] \;=\; d[n] - c^{H}[n]\, x[n] \qquad (3)$$

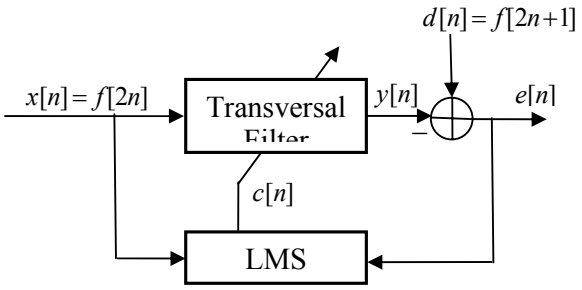

Fig. 2. LMS-type adaptive filtering based PQ event detector

A schematic of the learning set up is depicted in fig. 2. The task of the LMS algorithm is to find a set of filter coefficients c that minimizes the expected value of the quadratic error signal, i.e., to achieve the least mean squared error. The squared error e^2 and its expected value E (e^2) are (for simplicity of notation and perception the dependence of all variables on time n in (4) to (7) have been dropped) as following.

$$e^2 = \left(d - c^H x\right)^2 = d^2 - 2d\, c^H x + c^H x\, x^H c \qquad (4)$$

$$\begin{aligned} E\left(e^2\right) &= E\left(d^2\right) - E\left(2d\, c^H x\right) + E\left(c^H x\, x^H c\right) \\ &= E\left(d^2\right) - c^H 2E(d\, x) + c^H E\left(x\, x^H\right)c \end{aligned} \qquad (5)$$

The above squared error is a quadratic function of the coefficient vector c and, thus, has only one (global) minimum (and no other local minima), that theoretically could be found if the correct expected values in (5) were known. The gradient descent approach demands that the position on the error surface according to the current coefficients should be moved into the direction of the 'steepest descent', i.e., in the direction of the negative gradient of the cost function $J = E(e^2)$ with respect to the coefficient vector

$$-\nabla_c J \;=\; 2E(d\, x) - 2E\left(x\, x^H\right)c \qquad (6)$$

In (6) the expected values of $E(d\, x) = p$ and $E(x\, x^H) = R$, the cross-correlation vector between the desired output signal and the tap-input vector, and the auto-correlation matrix of the tap-input vector, respectively, would usually be estimated using a large number of samples from d and x. In the LMS algorithm, however, a very short-term estimate is used by taking into account only the current samples i.e. $E(d\, x) \approx d\, x$, and $E\left(x\, x^H\right) \approx x\, x^H$, leading to an update equation for the filter coefficients

$$\begin{aligned} c^{new} &= c^{old} + \mu/2\,(-\nabla_c J(c)) \\ &= c^{old} + \mu\, x(d - x^H c) \\ &= c^{old} + \mu\, x\, e^* \end{aligned} \qquad (7)$$

In the above equation, parameter μ, the 'step-size' has been introduced, which controls the distance moved along the error surface. In the LMS algorithm the update of the coefficients, in (7), is performed at every time instant n, using the following equation

$$c[n+1] = c[n] + \mu\, e^*[n]\, x[n] \qquad (8)$$

C. CHOICE OF STEP SIZE

The 'step-size' parameter μ introduced in (7) and (8) controls the movement along the error function surface at each update step. Parameter μ certainly has to be chosen $\mu > 0$ (otherwise it would move the coefficient vector in a direction towards larger squared error). Also, μ should not be too large, since in the LMS algorithm one uses a local approximation of p and R in the computation of the gradient of the cost function and, thus, the cost function at each time instant may differ from an accurate global cost function. Furthermore, too large a step-size causes the LMS algorithm to be unstable, i.e., the coefficients do not converge to fixed values and oscillate. Closer analysis [13] reveals that the upper bound for μ for stable behavior of the LMS algorithm depends on the largest eigenvalue $\lambda_{\max}$ of the tap-input auto-correlation matrix R and, thus, on the input signal. For stable adaptation behavior the step-size has to be

$$0 < \mu < \frac{2}{\lambda_{\max}} \qquad (9)$$

Without computing an estimate of R and its eigenvalues, $\lambda_{\max}$ is approximated using $\lambda_{\max} \approx tr(R)$ ($tr(R)$ is the trace of matrix R, i.e., the sum of the elements on its diagonal) and $-tr(R) \approx \|x[n]\|^2$, where $\|x[n]\|^2$ is the tap-input power at the current time n. Hence, the upper bound for μ for stable behavior depends on the signal power.

II. PROPOSED TECHNIQUE

The DWT has an excellent capability to characterize the transient disturbances and adaptive filtering provides an easy means to detect an event in a dynamically changing load configuration. The technique proposed in this work utilizes the best of both methods i.e. adaptive filtering for transient detection and DWT for feature extraction.

A. PROPOSED TRANSIENT DETECTOR

Change detection is a type of adaptive filtering for non-stationary signals and is also the basic tool in fault detection and diagnosis. Normally, the DWT decomposes a signal according to the frequency content of the signal with fixed wavelet filter coefficients. The adaptive prediction filter constantly changes the filter coefficients. An adaptive filter adjusts its coefficients to minimize the mean-square error between its output and that of an unknown signal. For any PQ disturbance, the transient part of the waveform produces sudden change in spectral components, and the adaptive

filter can not respond instantaneously to the abrupt waveform changes. Therefore, at the beginning of the disturbance, adaptation error signals generated are larger in magnitude than the pre-event steady-state error signals. This provides an easy means to detect the new event. The adaptive filter adjusts its coefficients to minimize the mean-square error between its output and that of an unknown signal and finally, the adaptation error settles down to a new steady state value. The adaptation time depends on the adaptation speed of the filter, which in turn depends on the adaptation method employed. Therefore, adaptive filtering of PQ waveform data avoids the detection of the same steady state event repeatedly.

The proposed transient detection algorithm is as follows. Let $f(t)$ be the PQ waveform data of finite duration and $f[n]$ be its discrete equivalent. Then, the proposed transient detector based on the LMS-type adaptation algorithm, described in the previous section, can be summarized as:

1. **Filter operation:** $y[n] = c^H[n]\, x[n]$, $x[n] = f[2n]$
2. **Error calculation:** $e[n] = d[n] - y[n]$, $d[n] = f[2n+1]$, where $d[n]$ is the desired filter output or reference signal
3. **Coefficient adaptation:** $c[n+1] = c[n] + \mu\, e^*[n]\, x[n]$

where, $f[2n]$ and $f[2n+1]$ are the alternate sampling points of $f[n]$. In the above algorithm, as shown in the fig.2, alternate sampling points of $f[n]$ are used for input to the filter and desired filter output to exploit the correlations of the adjacent samples. This also helps in faster convergence of adaptation error.

To monitor disturbances, PQ waveform data are processed through the proposed detector and, whenever there is a change in the PQ waveform, the adaptation error *e* goes high and finally settles around some new steady state value, depending upon the nature of the disturbance. Therefore, by observing adaptation error *e,* new PQ event can be detected.

B. FEATURE EXTRACTION

Once a new event is detected using the proposed transient detector, the next important task is to extract the relevant features for its classification. The frequency content or spectral decompositions are irrelevant using adaptive filter due to the fact that adaptive prediction filter constantly change the filter coefficients. Therefore, it is not a good idea to use adaptive filter for feature extraction.

The Multi-Resolution Analysis (MRA) is one of the most active branches of the DWT theory. Introduced by Mallet [14] in 1989, the MRA provides an effective way to examine the features of a signal at different frequency bands. These features may be essential for pattern recognition. Hence, it is well suited for the analysis and classification of the PQ events. The windowing of wavelet transform is adjusted automatically for low and high frequencies, i.e. it uses short time intervals for high frequency components and long time intervals for low frequency components and, thereby, each frequency component gets treated in the same manner without requiring any reinterpretation of the results. This gives the wavelet transform much greater 'compact support' for the analysis of the signals with localized transient components. The time frequency localization means that more energetic wavelet coefficients are localized. These are useful for feature extraction.

Because of its low dimensionality and shift invariant nature, energy distribution of the distorted signal at different frequency bands has been found to be more suitable and robust discriminatory feature generator for classification of PQ disturbances. The energy of distorted signal at the frequency resolution level *m* for *J* levels of DWT decomposition can be obtained as [11],

$$P_f(m) = \sum_{i=1}^{N_m} (w_m(i))^2 \qquad (10)$$
$$m \in [1, 2, \ldots . J],$$

where, vector w_m is the wavelet coefficient vector and N_m is the number of available wavelet coefficient at resolution level *m*. The feature vector, thus obtained, can be used as the input to the classifier for classifying the disturbance type.

IV. SIMULATION RESULTS AND DISCUSSION

The effectiveness of the proposed method has been tested and compared with DWT using a large number of PQ data, in general, and transient disturbance data, in particular, obtained from PSCAD/EMTDC simulation of distribution system of Indian Institute of Technology Kanpur (IITK), India. The single line diagram of the existing IITK distribution system is shown in the fig.3. Apart from normal residential loads, IITK distribution network has a wind tunnel in the Aerospace Department, which is having a dc motor rated at 1 MW, 660 V and is connected from substation-1. The armature control of the motor is achieved with three phase full wave converter. The input supply of the dc motor depends on the load which is connected at the shaft of the motor and can be varied by changing the firing angle of the thyristors used in the converter. Thus, the variation in firing angle produces harmonics and notches in the supply voltage, which varies as the firing angle changes.

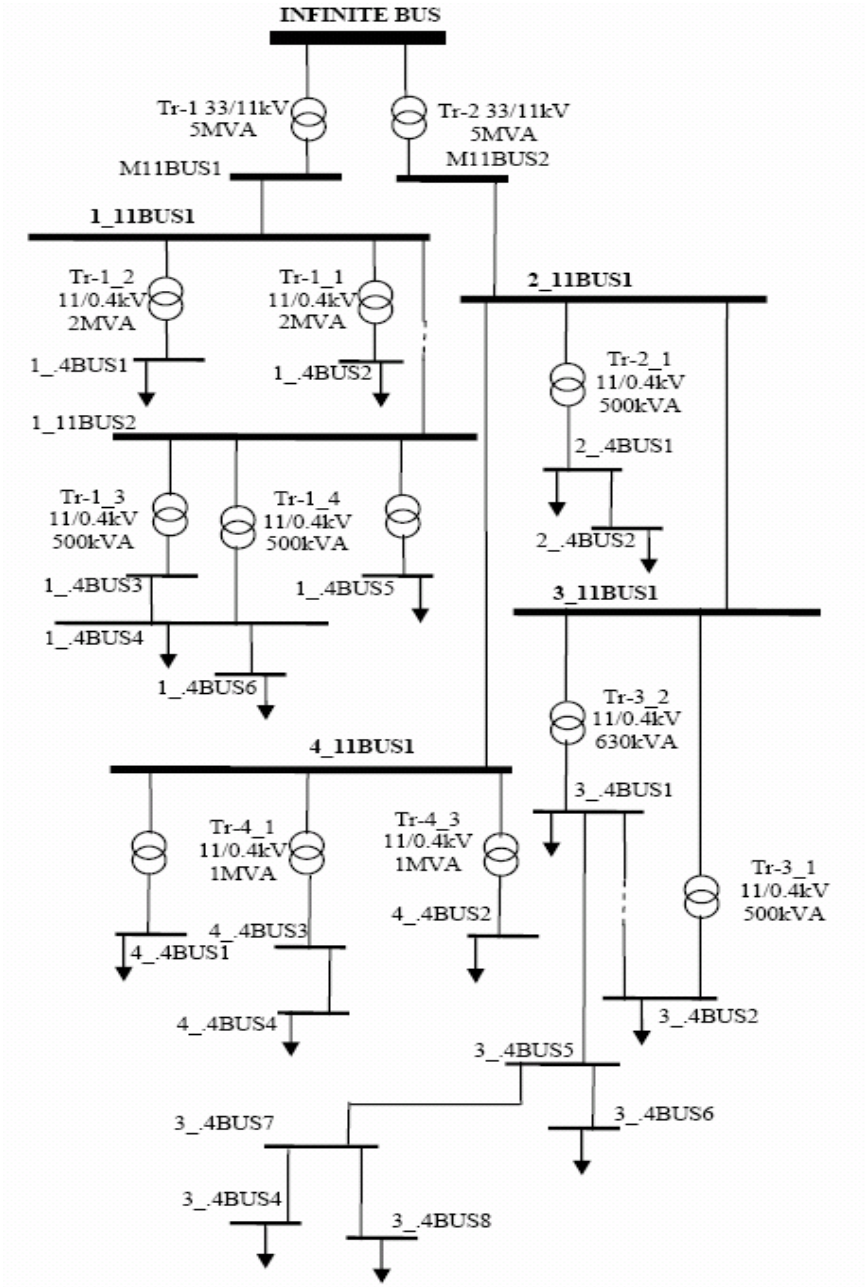

Fig. 3. Single line diagram of IITK distribution system

UPS systems connected to the various buses of the network are another major source for the harmonic injection. IITK network also has three 96.162 kVAr delta connected capacitor banks for power factor improvement. Relevant line and load data are given in the Appendix of the paper. Through the simulation on this practical system, various types of disturbances were generated by triggering different types of abnormalities in the system at different locations and through the dynamic load changes. Thus, most of the PQ disturbances (the transient and steady state disturbances), which can occur in a distribution system, have been obtained. These are mixed with random noise to test the effectiveness of the proposed scheme.

All the simulated waveforms were obtained for a power frequency of 50Hz, and for a sampling frequency of 6.2 kHz. The PQ data were normalized before these were given to the hybrid algorithm for detection and feature extraction. When analyzing signal with hybrid algorithm, the

step size μ has been set to 0.1 which is well within the upper bound as given in (9). Daubechies "db4" wavelet [15] has been used because of its compactness and localization properties in time-frequency plane and 8-level DWT decomposition of each PQ waveform data (under investigation) has been performed to extract the energy features. In this work, the adaptation error signal, generated by processing PQ waveform data, through LMS adaptation algorithm, has been referred as adaptation error (AE) coefficients due to its analogy with .

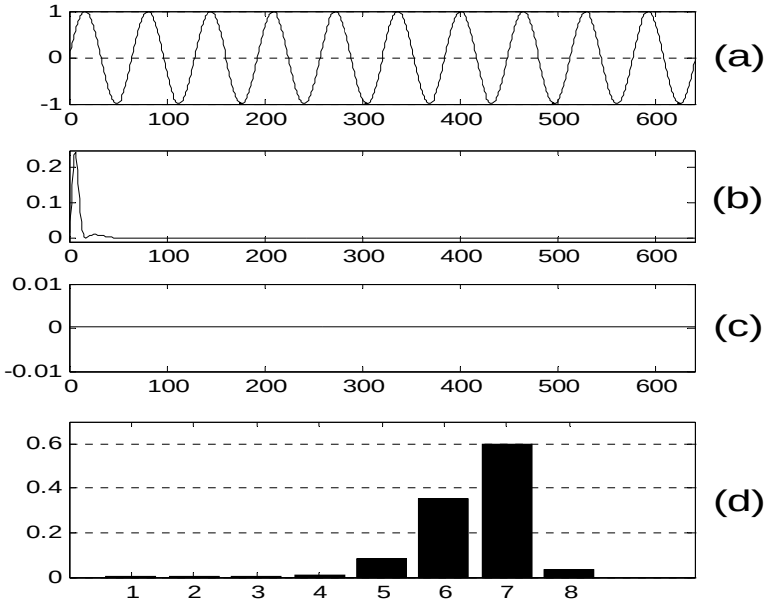

Fig. 4. (a) The pure power frequency voltage signal. (b) The adaptation error signal of the adaptive filter. (c) First scale wavelet coefficients. (d) The energy distribution pattern in DWT domain.

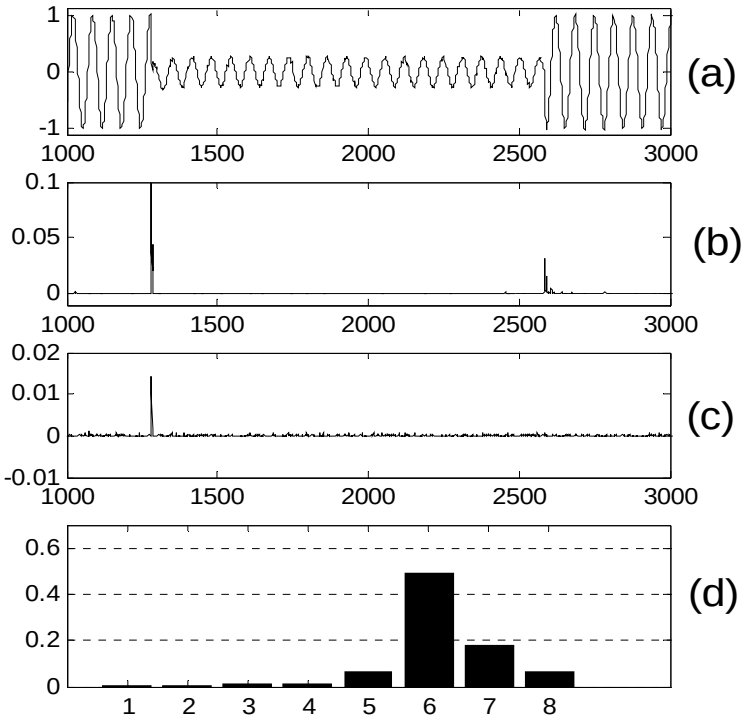

Fig. 5. (a) The normalized PQ disturbance (sag). (b) The adaptation error signal of the adaptive filter. (c) First scale wavelet coefficients. (d) The energy distribution pattern in DWT domain.

DWT coefficients.

Though, perfect sinusoidal voltage and current waveforms are rare in any practical system, its analysis is necessary to obtain a reference for the analysis of PQ disturbances. Fig. 4(a) shows a pure power frequency sinusoidal signal. When this pure waveform was processed through the proposed event detector and DWT based disturbance detector, signals as shown in fig. 4(b) and fig. 4(c), were respectively, obtained. It can be seen that no disturbance was detected by the two detectors as both AE and DWT coefficients were zero. Initially some AE coefficients were nonzero because of absence of signal at the starting of the LMS adaptation algorithm. Fig. 4(d) shows the energy pattern of the same pure PQ waveform in DWT domain. Fig. 5(a) shows a voltage-sag signal mixed with 45dB random white Gaussian noise (AWGN), caused by single line to ground fault and fig. 5(b) and fig. 5(c) show the squared AE and DWT coefficients of fig. 5(a), respectively. From the observation of AE coefficients, both start and end of the sag event can be detected. While DWT based detector fails to find the end of the sag event as shown in fig. 5(c), it is clear from the energy pattern of the sag waveform in fig. 5(d) that energy pattern has altered from that of the pure signal as shown in fig. 4(d). The variation occurred at the energies of the sixth and seventh scales as these represent the low frequency band (around power frequency) of the DWT decomposition.

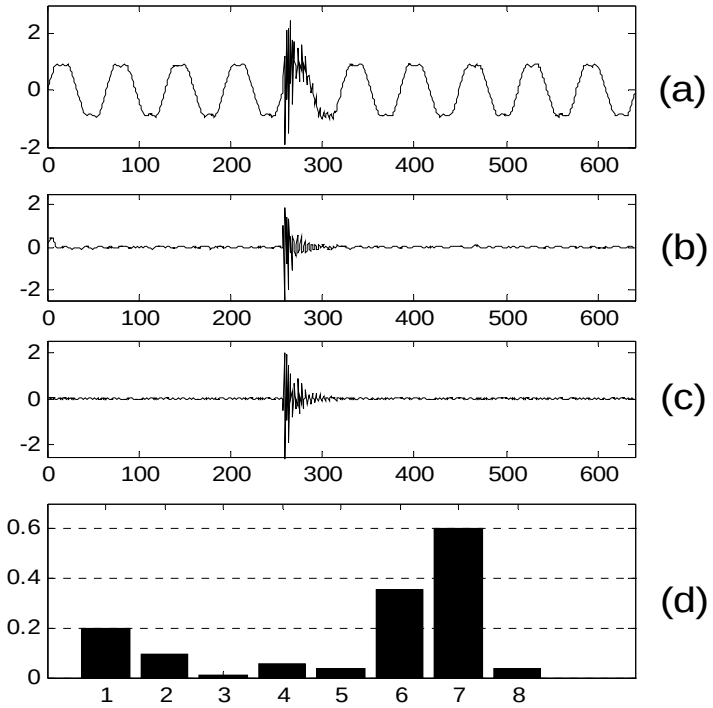

Fig. 6. (a) A mixed PQ disturbance. (b) The adaptation error signal of the adaptive filter. (c) First scale wavelet coefficients. (d) The energy distribution pattern in DWT domain

To test the effectiveness of the proposed scheme of the PQ monitoring system under practical pre-event waveform (enriched with harmonics and noise), a case of high frequency transient was studied. The PQ waveform, shown in fig. 6(a), contains a high frequency oscillatory transient and figs. 6(b), 6(c), and 6(d) show its AE coefficients, DWT coefficients and energy distribution pattern, respectively. For the signal under investigation, both adaptive filtering and DWT were found effective in detecting the disturbance. The energy feature extracted using DWT clearly

exhibits the increase in the energies of first two higher frequency bands, as expected, and shown in fig. 6(d).

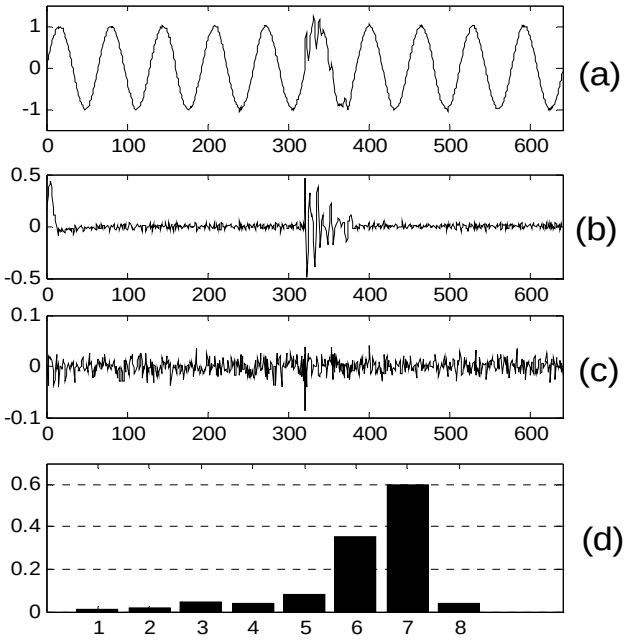

Fig. 7. (a) The normalized PQ disturbance (low frequency transient). (b) The adaptation error signal of the adaptive filter. (c) First scale wavelet coefficients. (d) The energy distribution pattern in DWT domain.

Similarly, fig. 7(a) depicts a waveform of capacitor switching transient and figs. 7(b), 7(c), and 7(d) show its AE coefficients, DWT coefficients and energy distribution pattern, respectively. The proposed detector easily detects the disturbance as shown in fig. 7(b). From fig. 7(c), it can be observed that the DWT based detector fails to detect the disturbance if the detector's threshold is set at a low value, and it will generate repeated alarm if it is tuned for detecting this disturbance under ideal waveform conditions. However, there is increase in the energy of the third scale DWT decomposition, proving it as an excellent feature generator for classification of the disturbance..

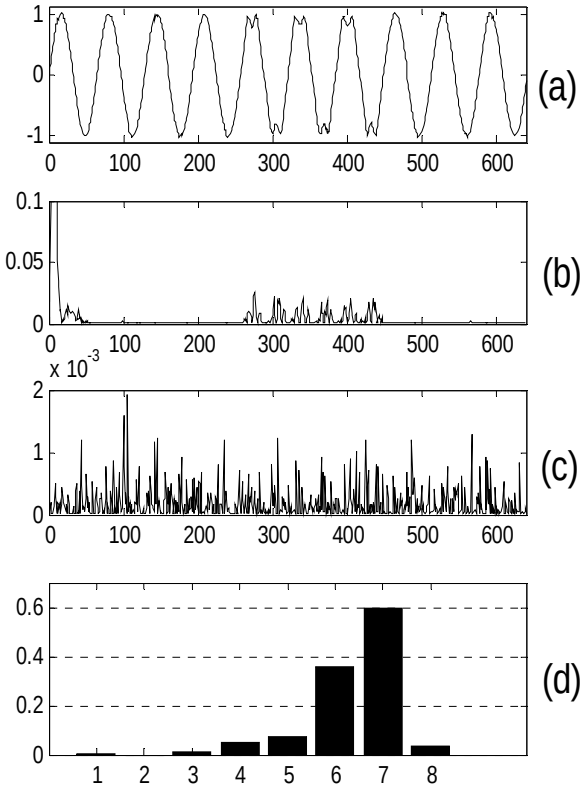

Fig. 8. (a) The PQ disturbance (high frequency transient). (b) The adaptation error signal of the adaptive filter. (c) First scale wavelet coefficients. (d) The energy distribution pattern in DWT domain

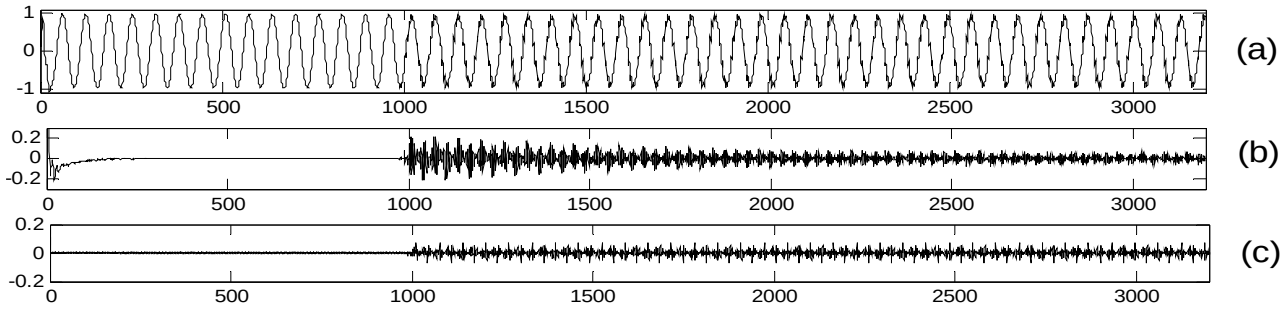

Fig. 9. (a) The PQ waveform data (changing load condition). (b) The adaptation error signal of the adaptive filter. (c) First scale wavelet coefficients.

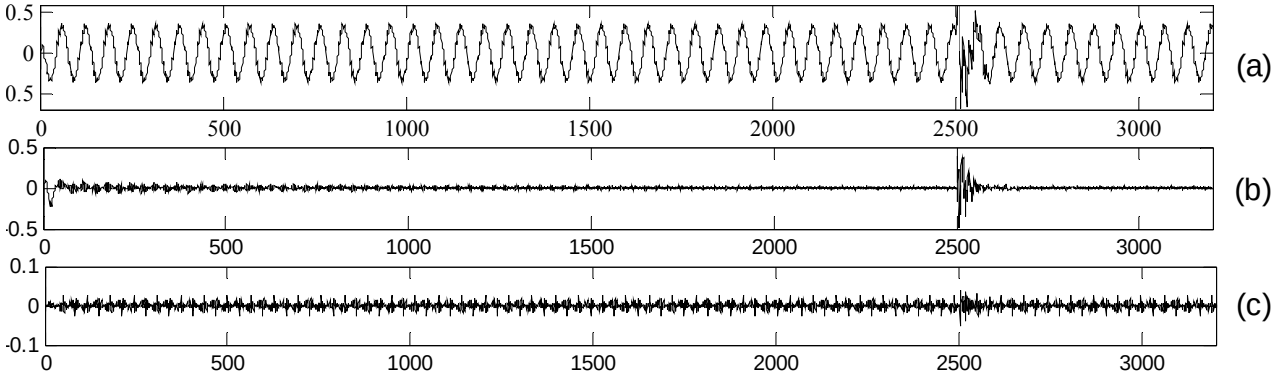

Fig. 10. (a) A PQ disturbance (transient). (b) The adaptation error signal of the adaptive filter. (c) First scale wavelet coefficients.

A voltage waveform data under dynamically changing load condition, simulated by switching on a large nonlinear load for three cycles, is depicted in fig. 8 (a). In this case also, the DWT based detector either misses it or generates repeated alarm depending on the DWT coefficients threshold setting.

To further validate the performance of the adaptation scheme and to demonstrate how it adapts itself to the changes in the system load configuration, The PQ waveform shown in fig. 9(a) and fig. 10(a) were selected. After 15 cycles of normal system, operation its load configuration was changed by switching on the wind tunnel load and some other nonlinear loads simultaneously at different locations in the system. As depicted in fig. 9(a), the AE coefficients increases suddenly at the instant of the change in the voltage waveform, and finally settle around some new steady state value owing to its adaptive nature. But DWT coefficients, because of its fixed subband filter coefficients, attain a constant value after the event as shown in fig. 9(b). Hence, the DWT based detector sometimes fails to recognize the new event as shown in fig. 10(c), where it has missed a transient disturbance. In such conditions, the pre-event waveform dictates its detection capability, while, due to its adaptation property, the proposed detector has recognized the transient event as shown in fig 10(b).

V. CONCLUSION

In this paper, a new PQ detection and analysis method, that uses combination of adaptive filtering for event detection and wavelet transform as feature extractor has been suggested. For PQ event detection, the proposed method utilizes the adaptation error of the LMS-type adaptive predictor which increases considerably with a sudden change in the steady state value of the signals' frequency and magnitude. The proposed approach outperforms the wavelet based event detector under changing load configurations and when the normal operation waveforms contain harmonics and noise. DWT alone, in such conditions would result in repeated alarm and processing of the data or in some cases may fails to detect the disturbance. It has been used as a feature extractor, because of its excellent signal representation property in time-frequency plane. The results show a high success rate of the proposed approach in detecting transient PQ events in dynamically changing load conditions.

VI. APPENDIX

IIT Kanpur distribution system receives power at 33 kV which is stepped down to 11kV by two transformers of 6.25MVA rating each, power from these transformers is transmitted to different,

substation, where the 11kV voltage is stepped down to 415V to supply L.T. loads. The load data and line data of this system is given in Table I and Table II, respectively.

VII. ACKNOWLEDGEMENT

Financial support obtained by the Department of Science and Technology, India vide project no. DST/EE/20040252 is gratefully acknowledged.

TABLE I
LOAD DATA OF IITK DISTRIBUTION NETWORK

Node Number	Real and Reactive power loads in each phase at respective node					
	Phase A		Phase B		Phase C	
	kW	kVAr	kW	kVAr	kW	kVAr
1_.4BUS1	150.0	15.0	120.0	12.0	108.0	18.0
1_.4BUS2	200.0	20.0	160.0	16.0	144.0	24.0
1_.4BUS3	300.0	30.0	240.0	24.0	216.0	36.0
1_.4BUS4	300.0	30.0	240.0	24.0	216.0	36.0
1_.4BUS5	100.0	10.0	80.0	8.0	72.0	12.0
1_.4BUS6	150.0	15.0	120.0	12.0	108.0	18.0
2_.4BUS1	550.0	55.0	440.0	44.0	396.0	66.0
2_.4BUS2	100.0	10.0	80.0	8.0	72.0	12.0
3_.4BUS1	100.0	10.0	80.0	8.0	72.0	12.0
3_.4BUS2	550.0	55.0	440.0	44.0	396.0	66.0
3_.4BUS4	50.0	5.0	40.0	4.0	36.0	6.0
3_.4BUS8	50.0	5.0	40.0	4.0	36.0	6.0
4_.4BUS1	800.0	80.0	640.0	64.0	576.0	96.0
4_.4BUS2	500.0	50.0	400.0	40.0	360.0	60.0
4_.4BUS4	200.0	20.0	160.0	16.0	144.0	24.0

TABLE II
LINE DATA OF IITK DISTRIBUTION NETWORK

Line Number	From Line	To Line	Length in kms	Impedence of Lines (Ω/km)
1	M11BUS1	1_11BUS1	1.5788	0.167+j0.092
2	2_11BUS1	1_11BUS2	1.0628	0.167+j0.092
3	2_11BUS1	4_11BUS1	0.7215	0.167+j0.092
4	2_.4BUS1	2_.4BUS2	0.0010	0.103+j0.072
5	4_11BUS1	3_11BUS1	0.5160	0.442+j0.106
6	M11BUS2	2_11BUS1	0.5642	0.167+0.092
7	1_11BUS1	4_11BUS1	1.0739	0.167+0.092
8	4_.4BUS2	4_.4BUS1	0.0010	0.103+j0.072
9	4_.4BUS3	4_.4BUS4	0.0010	0.103+j0.072
10	1_.4BUS4	1_.4BUS6	0.0010	0.103+j0.072
11	1_.4BUS3	1_.4BUS4	0.0700	0.077+j0.072
12	2_11BUS1	3_11BUS1	1.1355	0.325+j0.100
13	3_.4BUS1	3_.4BUS5	0.0500	0.103+j0.072
14	1_.4BUS4	1_.4BUS7	0.010	0.103+j0.072
15	3_.4BUS5	3_.4BUS7	0.010	0.103+j0.072
16	3_.4BUS4	3_.4BUS7	0.010	0.103+j0.072
17	3_.4BUS7	3_.4BUS8	0.010	0.103+j0.072
18	3_.4BUS8	3_.4BUS3	0.010	0.103+j0.072
19	3_.4BUS4	3_.4BUS3	0.010	0.103+j0.072
20	3_.4BUS5	3_.4BUS6	0.010	0.103+j0.072

VIII. REFERENCES

[1] Roger C. Dugan, M. F. McGranaghan, S. Santoso and H. W. Beaty "*Electrical Power Systems Quality",* Second Edition, McGraw Hill Book Company, New York, 2003.

[2] Gu YuHua, Math H. J. Bollen, "Time-Frequency and Time-Scale Domain Analysis of Voltage Disturbances survey", *IEEE Trans. on Power Delivery,* vol. 15, pp.1279-1284, Oct. 2000.

[3] Santoso, S., Powers, E. and Hofmann, P., "Power quality assessment via wavelet transform analysis", IEEE Trans. on Power Delivery, vol. 11, pp. 924-930, April 1996.

[4] Anis Ibrahim, W. R., Morcos, M. M., "Artificial intelligence and advanced mathematical tools for power quality applications: a survey", IEEE Trans. on Power Delivery, vol. 17, pp. 668-673, April 2002.

[5] Abdel-Galil, T.K.; Kamel, M.; Youssef, A.M.; El-Saadany, E.F.; Salama, M.M.A.; "Power quality disturbance classification using the inductive inference approach" *IEEE Trans .on Power Delivery*, vol. 19, pp. 1812 - 1818, Oct. 2004.

[6] Zhu, T.X.; Tso, S.K.; Lo, K.L.; "Wavelet-based fuzzy reasoning approach to power-quality disturbance recognition" *IEEE Trans. on Power Delivery*, vol. 19, pp. 1928 – 1935, Oct. 2004.

[7] O. Chaari, M. Meunier, and F. Brouaye, "Wavelets: A new tool for the resonant grounded power distribution system relaying," *IEEE Trans. on Power Delivery*, vol. 11, pp. 1301–1308, 1996.

[8] M. Michalik, W. Rebizant, M. Lukowicz, Lee Seung-Jae, Kang Sang-Hee, "High-impedance fault detection in distribution networks with use of wavelet-based algorithm", *IEEE Trans. on Power Delivery,* vol. 21, pp. 1793 - 1802, Oct. 2006.

[9] S. Santano, E. J. Powers, and W. M. Grady, "Power quality disturbance data compression using wavelet transform methods," *IEEE Trans. on Power Delivery*, vol. 12, pp. 1250–1257, 1997.
[10] U. D. Dwivedi and S. N. Singh, "An Adaptive Window-Based Denoising Scheme to Enhance Power Quality Monitoring Systems", *IEE International Conference on Advances in Power System Control, Operation and Management (APSCOM 2006),* Hong Kong, China, 30 Oct. - 2 Nov, 2006.
[11] U. D. Dwivedi and S. N. Singh, "A Robust Energy Features Estimation for Detection and Classification of Power Quality Disturbances," *in Proc. 2006 IEEE Power Engineering Society power India Conf*., pp. 384–390.
[12] Ömer Nezih Gerek and Dogan Gökhan Ece, "An Adaptive Statistical Method for Power Quality Analysis", *IEEE Trans. on* Instrumentation and Measurement, vol. 54, no. 1, pp. 184-191, Feb., 2005.
[13] Simon Haykin, "*Adaptive Filter Theory*"', Third Edition, Prentice-Hall, Inc., NJ, 1996.
[14] S. Mallat, "A theory for multi-resolution signal decomposition the wavelet representation", *1EEE Trans. on Pattern Analysis and Machine Intelligence,* vol. 11, no. 7, pp. 674-693, 1989.
[15] I. Daubechies, "Ten Lectures on Wavelets*", SIAM, Philadelphia, PA,* 1992.

IX. BIOGRAPHIES

U. D. Dwivedi received his B. Tech degree in Electrical & Electronics engineering from National Institute of Technology (NIT) Calicut, India, in 1997 and M. Tech degree in electrical engineering from the Indian Institute of Technology (IIT) Kanpur, in 2003. Presently he is a Ph. D. Student in the Department of Electrical Engineering at IIT Kanpur, India. His research interests include power quality, signal processing applications to power systems, FACTS, and adjustable speed drives.

S. N. Singh (SM'02) received the Ph.D. degree in Electrical Engineering from the Indian Institute of Technology Kanpur, India, in 1995. Currently, he is an Associate Professor in the Department of Electrical Engineering at the Indian Institute of Technology Kanpur. He was with the Department of Electrical Engineering at the Hong Kong Polytechnic University, Hong Kong, China, and was Assistant Professor with the Energy Program at Asian Institute of Technology (AIT) Bangkok, Thailand. His research interests include power system restructuring, flexible ac transmission systems (FACTS), power system optimization and control, security analysis, and power system planning. Dr. Singh is a Fellow of the Institution of Engineers (India) and IETE (India). He has received several awards including Young Engineer Award 2000 of Indian National Academy of Engineering, Khosala Research Award, and Young Engineer Award of CBIP New Delhi (India).

S. C. Srivastava (SM'91) was born in 1955. He received the B.Tech degree in Electrical Engineering from Banaras Hindu University, Varanasi, India, in 1976 and the Ph.D. degree from the Indian Institute of Technology Delhi, India, in 1987. Presently, he is a Professor with the Electrical Engineering Department, Indian Institute of Technology, Kanpur, India. His research interests include energy management system, power system optimization, security analysis, voltage stability analysis, and power system restructuring. Dr. Srivastava is a Fellow of the Institution of Engineers (India), IETE (India), and the Indian National Academy of Engineers (INAE).

Received January 29 2007-01-29

10. A PRACTICAL APPROACH TO WIRELESS GPRS ON-LINE POWER QUALITY MONITORING SYSTEM (PAPER 07GM1010).

Ringo Lee[#], Director, "Your Network System Integrator", Powerpeg NSI Limited, Hong Kong, China
L. L. Lai (City University London, UK

Abstract: In this paper, the authors discuss the way to adopt the cost effective GPRS applications. Although there have been lots of theories and concepts on the GPRS applications but the real applications applying to a large network, distributed power generation or building energy/power distribution monitoring are limited. The authors focus the application of the GPRS to this on-line system application and the techniques. A practical scheme is proposed and its use to real-life system will be introduced. A practical implementation for a wireless GPRS on-line Power Quality Monitoring System will be illustrated. Results and benefit to the end users in some practical applications will be discussed.
Keywords: PQ meter, network architecture, wireless communication

I. INTRODUCTION

GPRS (General Packet Radio Service) is the world's most common wireless data service, based on the GSM network, GPRS solution based on Internet Protocols that supports a wide range of enterprise and consumer applications. The data rates can go up to 40 kbit/s from GPRS in which users have a similar access speed to a dial-up modem, but with the convenience of being able to connect from anywhere and GPRS consumers can enjoy advanced, feature-rich data services such as color Internet browsing, e-mail on the move, powerful visual communications, etc. Owing to the popular usage of GPRS applications, the price is more cost effective which is acceptable to on-line applications in some cases.

For power or energy monitoring applications, the adoption of GPRS may be one of the quick and cost-effective strategy such as revenue meter data collection, fault indicators or power quality monitoring which may have a lot of raw data as well [1-3].

GPRS not only supports the real first wave of mobile Internet services, but also represents a big step towards 3GSM (or wideband-CDMA) networks and services. During the implementation of the GPRS application, some experience can be learnt for 3G applications when the price being more competitive in future.

The on-line power quality monitoring system in a large network is mainly to monitor the power quality of the supplied power from the power utility. With the on-line monitoring implementation, the suppliers can understand the instant power quality issue such as voltage dips happened from high voltage (HV) down to low voltage (LV) at that moment quickly. The pattern from the fault such as lightning or local fault caused by customers and their impact can be traced back quickly from the power utility control center and provide a quick response to serve better.

The authors focus on a practical approach which was implemented from experience.

II. THE SYSTEM

[#] P.K. Lee is with Powerpeg NSI Limited, Hong Kong,, E-mail: r_lee@hk.supernet
L.L. Lai is with Energy Systems Group, City University, London, UK Email: l.l.lai@city.ac.uk

i) System configuration and design consideration

The scale of the system and the database storage will affect the overall design a lot. For example, the server hardware and software for monitoring 10 remote substations with 1 year storage is totally different from that of 200 sites.

For example, approx 50MB per site per month approx. with transient, sag/swell voltage waveform and EN50160 data logging, the database will be 0.5GB per month. For 12 months, it is 6GB.

However, 200 sites will be 120GB database for 1 year storage. If mirror image is needed, the configuration will need 2 mirror HD with 146GB which is typical in size.

For 10 remote sites, the server requires single CPU at P4 2GHz with 512MB and window 2000 professional/server could be acceptable. However, running 200 sites will need dual Xeon or dual core CPU at 2.8GHz or above and memory up to 2GB to 4GB depending on the usage required.

Other factors including database management strategy, fault reporting requirement, system hardware and software diagnostic, etc. and this paper focuses on the implementation of wireless GPRS communication.

ii) Power quality (PQ) meter characteristic

The PQ meter should have enough data buffer that meets the requirement of the users such as 1 week memory storage in case of the failure of network or server. The meter may need to tolerate longer timeout when uploading data to the central server between each poll. The timeout from the communication port should be adjustable from min 1 second up to 10 seconds or even more. The point is that the GPRS network delay may vary from about 1 second to few seconds depending on the network traffic.

iii). Central polling software

The software should be able to upload data log from all the PQ meters in sequence or simultaneously and it should be able to tolerate longer and adjustable timeout when communicate with the PQ meters owing to the GPRS network delay as mentioned above. Also, the network communication and data upload diagnostic log should be available for checking.

iv) Network architecture

The PQ monitoring system should be designed to support many remote substations via direct or virtual com ports, Ethernet connection via intranet, telecommunication channel, wireless radio frequency, dial-up modems, hybrid combination of the above media and GPRS or 3G in future.

Figure 1 below illustrates the network architecture for communicating with different remote sites.

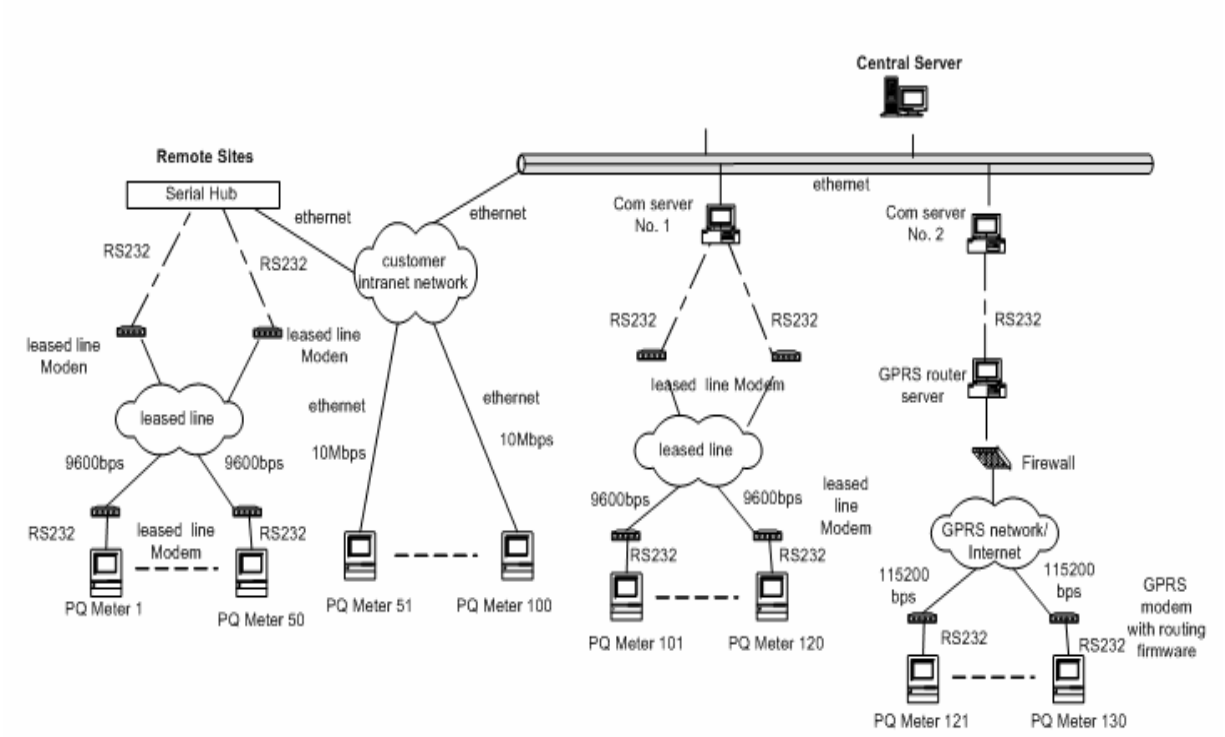

Fig. 1. Network architecture

For a large network, it will connect many different remote sites via fixed line, pilot, radio frequency, dial-up, Ethernet, DSL modems, etc.

However, there may have some remote sites in which no fixed line communications is available and the wireless GPRS communication may be introduced to resolve the issue.

The authors have implemented the on-line power quality monitoring system and will introduce the concept for GPRS implementation especially for those high density and busy GPRS network.

v) Communication

Communication is one of the most critical factors to make it successful. With wired communication provided, and even they are hybrid combinations, it is straight forward. Wireless RF communication is good if they are available in line of sight without blocking from high rise buildings. For those remote sites, the above conditions are not available or the routing change without replacement in short time or they are ad-hoc purpose such as fault investigation, GPRS wireless solution may be adopted to on-line monitoring once the service plan drops to affordable price in some countries. Regarding this implementation, the following points are recommended for consideration.

1) Tariff charge for GPRS plan

Typically, they are charged based on the data volume. More data transfer will cost more money. In some countries, unlimited plan are offered in good price. It is affordable to select the plan. Naturally, more people will join the cheaper plan and less people will join the more expensive plan. By experience, the following situation will happen practically.

The latter one may have better communication performance on network delay and the frequency of drop line since lessen people use the network. The service providers appreciate the users to consume more data volume to increase the revenue and it may keep the GPRS on-line in longer duration. However, the former one has many users to keep the communication network busy and thus to cause longer network traffic delay or frequent drop line in peak hour when the GPRS network is not able to handle them simultaneously.

For example, a GPRS modem used in Australia's local service providers is kept running well. However, the same modem with the router firmware/program used in Hong Kong has frequent drop line and may not be able to transfer the data smoothly depending on the network situation.

The GPRS modems and routers should have some intelligent firmware/program to cater different cases practically in order to resume the connection.

2) Test on the network delay and the frequency of drop line

After the selection of the cost effective GPRS plan, it is recommended to test the following points before the adoption.

a) Turn around time – setup a connection and test it. You may setup 2 hyper-terminals from windows with 2 PCs for both end and test it. It is better to test it for both weekday and weekend. Also, test it during the peak hour such as

- 8:00AM to 10:00AM
- 12:00PM to 2:00PM
- 5:00PM to 7:00PM

Record the pattern and understand the worst turn around time. Make sure that your system can cater this response time which includes the network delay. It is a common mistake that people will consider the com speed such as 19200, 57600, 115200 bps as the real communication speed only. With the network delay included, the result may behave as slower speed depending on the applications.

b) Frequency of drop line – setup a test to measure this behavior and adjust your firmware/program in GPRS modem and/or GPRS router to cater for this pattern.

With the above known data and pattern, your may adopt the GPRS connection via the adjustment of the GPRS router, GPRS modem with routing firmware, Central Server and the PQ Meter to the on-line application such as power quality monitoring system which involve lots of raw data transfer.

Figure 2 below is a schematic diagram for the wireless GPRS connection applied to practical applications.

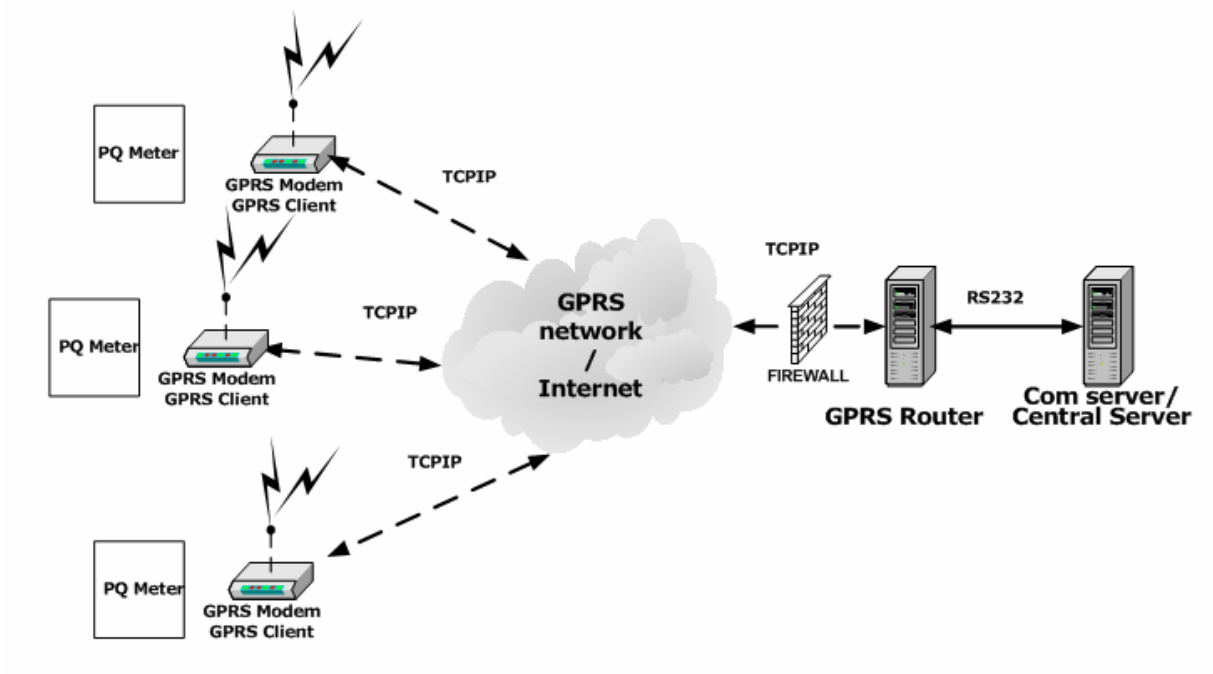

Fig. 2 A schematic diagram for a wireless GPRS connection

3) Setup the GPRS connection

The following information is needed for the test and implementation on the GPRS setup for the remote sites:

a) Access Point Node (APN): check the names for the mobile service providers
b) Server IP: server fixed IP is needed or fixed host name with dynamic IP is used.
c) Port number assigned: manage the opened port number for the data routing.
d) Reboot interval: 1 hour or 1 day, etc.
e) Acknowledge message between server and remote GPRS modems to design the way or communication between server and remote GPRS modem in order to keep them on-line since it may be forced to drop line by service providers once the network is busy.
f) Setup the modem speed to match the remote site devices such as 115200, 57600, 19200, etc.
g) Data Encryption and firewall.
h) Multi-site router configuration design.
i) Traffic monitoring.
j) Statistics summary for the accumulative data volume and check up.

Figure 3 below shows the GPRS router program setup page to monitor the communication traffic during the GPRS routing for multiple remote sites. Figure 4 is an example of messages. The red color is the request message from central server while the blue color is the reply message from the PQ Meter at remote sites.

4) Result and applications

With the captioned application, data can be uploaded to the central server continuously even there are drop line and network delay issues from different service providers. The GPRS connection can

be resumed automatically via the GPRS router server and modem program/firmware. The authors have implemented 15 GPRS sites for this configuration but this method can be scaled up to 100 or even more as shown figure 5 below:

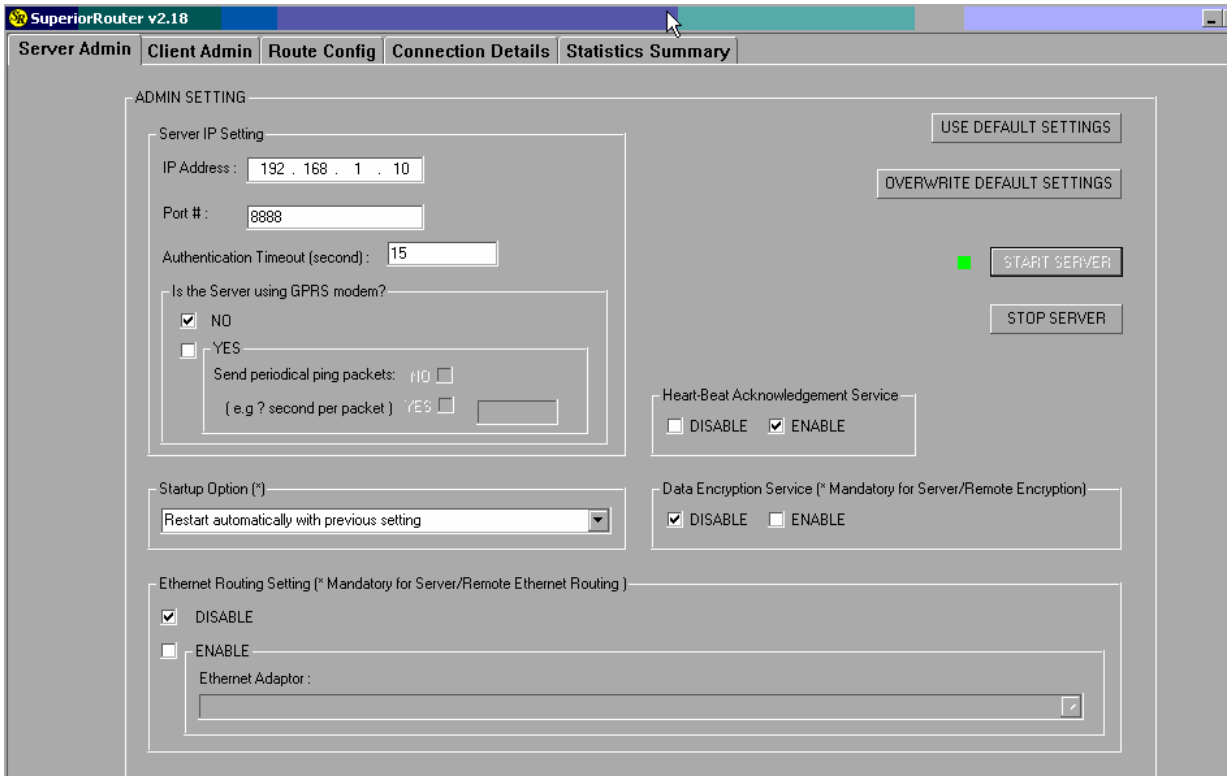

Fig. 3. An example of GPRS router program setup page

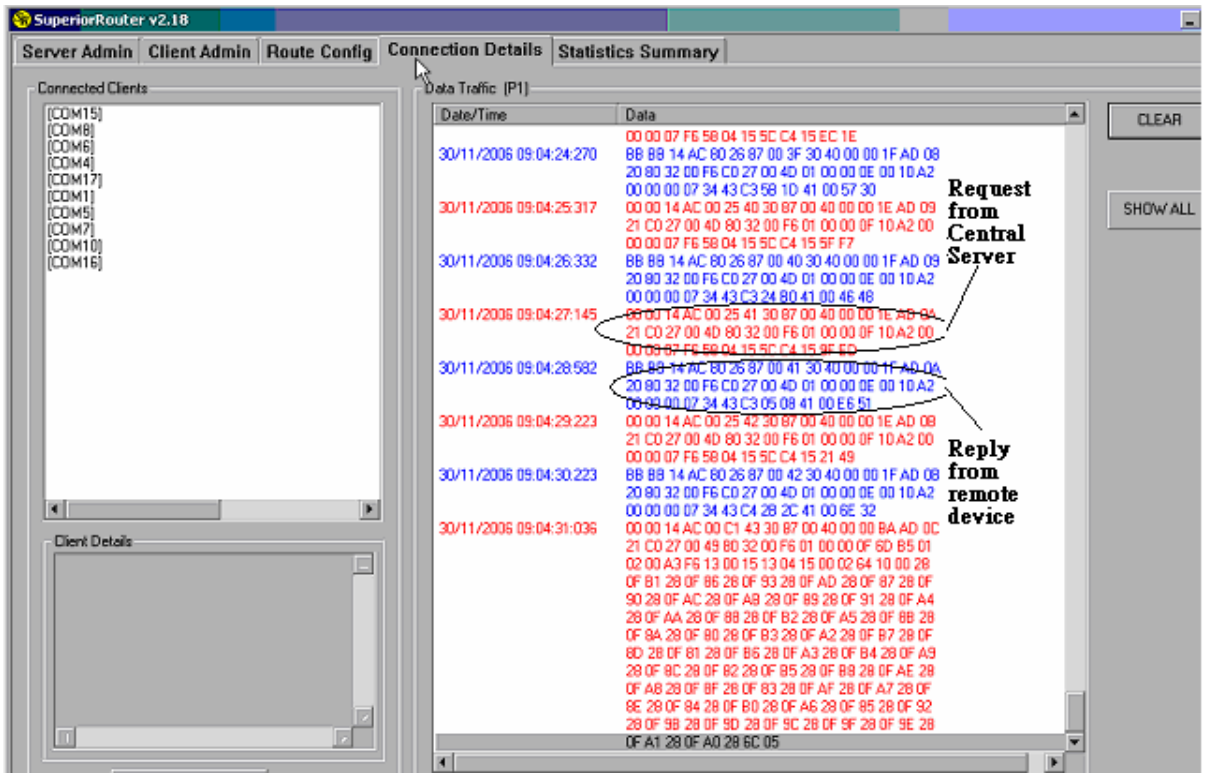

Fig. 4. An example to illustrate request and reply messages

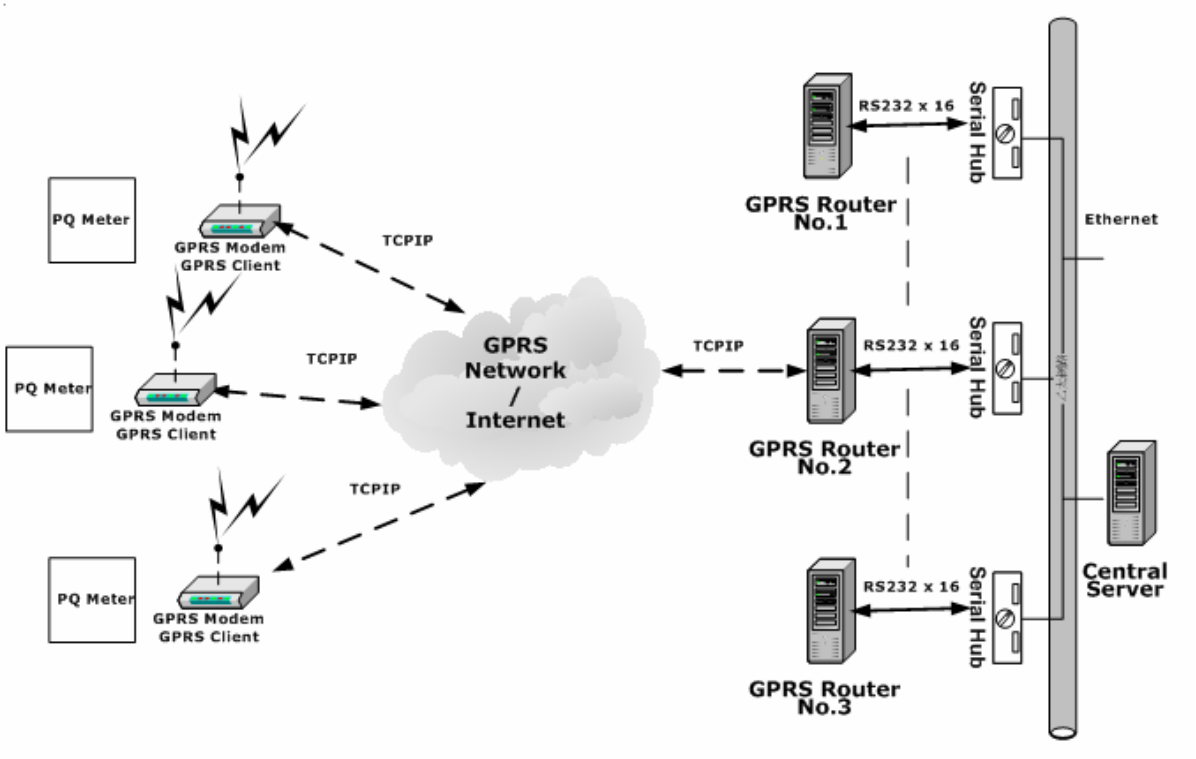

Fig. 5. GPRS configuration

The important points to be considered are the bandwidth of the broadband, the nos. of com ports available, the cost of the unlimited/limited plan from GPRS data communication, allowable time delay, frequent of the drop line and criteria to trigger the reconnection between server and the remote devices.

If cost effective GPRS plan is available, the following applications can be implemented to benefit the distribution generation and energy conservation.

1) **Building energy/power system** – Energy audit and power quality monitoring may be a temporary survey in some organizations such as properties management. They need to manage many properties at different locations. Fixed communication link may not be available for the temporary measurement, portable Power Analyzer with GPRS wireless connection can help for the energy profile logging and power quality monitoring periodically without going to the sites for data upload. After the audit has been done, the facilities/energy engineer can relocate them to other area more conveniently.

   For multiple sites applications, consultants or facilities engineers may compare different buildings at the same time and benchmark the most efficient usage of energy/power from properties.

2) Distribution power generation – When deregulation has been implemented in some countries, power quality issue may be an impact and need to be monitored [4]. For example, a property owner has installed a new Generating Set connected to the grid for peak use. The transient may be fed into the supply network during the operation or switching and it needs to be monitored to make sure that it operates properly. Power utility may need to monitor this supply grid for a period of time to make sure it operates properly. The portable Power Analyzer with GPRS wireless connection can be applied in this application in real life. The same way can be applied to multiple sites monitoring.

III. CONCLUSIONS

Based on practical experience of the authors, the paper has elaborated the basic considerations for the system design of GPRS on-line application to power quality monitoring for network of various sizes. The practical approach was introduced and some critical points had been mentioned for consideration during the implementation. However, the same techniques can be adopted widely such as areas in Building energy/power system and Distribution power generation. The latest communication technology will be applied for multiple sites monitoring or control in future. The GPRS communication link is just one of the selections. Thanks to the rapid development of telecommunication technology. A more and more completed and comprehensive design from latest technology such as 3G may be implemented and contributed to the multiple sites distributed energy/power monitoring when the price being cost effective in the near future.

IV. REFERENCES

[1] Design_Handbook Nov 2005 Power Measurement Ltd. P.17 – 26.

[2] Mark McGranaghan, “Trends in Power Quality Monitoring”, IEEE Power Engineering Review, Oct. 2001, pp. 3-9.

[3] Rong-Ceng Leou, Ya-Chin Chang, Jen-Hao Teng, “A Web-based Power Quality Monitoring System”, Power Engineering Society Summer Meeting, 2001, Vol. 3 , 2001, pp. 1504 – 1508.

[4] Loi Lei Lai (Editor), *Power System Restructuring and Deregulation: Trading, Performance and Information Technology*, John Wiley & Sons, UK, Aug. 2001.

V. BIOGRAPHIES

Lee. P.K. Ringo received the B.Eng (First Class Honors) from University of Sunderland (ie. former Sunderland Polytechnic), UK, in 1991. Currently he is Director of Powerpeg NSI Limited in Hong Kong which has been a network system integrator for Intelligent Power Management/Monitoring System for both supply and demand sides in HK.

L. L. Lai (SM'92, F'07) received the B.Sc. (First Class Honors) and the Ph.D. degrees from the University of Aston in Birmingham, UK, in 1980 and 1984, respectively. He was awarded the D.Sc. by City University London in 2005 and he is its honorary graduate.

Currently he is Head of Energy Systems Group at City University, London, UK. He is also a Visiting Professor at Southeast University, Nanjing, China and Guest Professor at Fudan University, Shanghai, China. He has authored/co-authored over 200 technical papers. In 1998, he also wrote a book entitled *Intelligent System Applications in Power Engineering - Evolutionary Programming and Neural Networks*. In 2001, he edited a book entitled *Power System Restructuring and Deregulation - Trading, Performance and Information Technology*. In 1995, he received a high-quality paper prize from the International Association of Desalination, USA. Among his professional activities are his contributions to the organization of several international conferences in power engineering and evolutionary computing, he was the Conference Chairman of the IEEE/IEE International Conference on Power Utility Deregulation, Restructuring and Power Technologies 2000. Dr. Lai is a Fellow of the IET (UK). He was awarded the IEEE Third Millennium Medal, 2000 IEEE Power Engineering Society UKRI Chapter Outstanding Engineer Award and 2003 IEEE Power Engineering Society Outstanding Large Chapter Award. In June 2006, he was awarded a Prize Paper by IEEE Power Engineering Society Energy Development and Power Generation Committee.

PANELISTS

1. Tom Hammons
   Chair International Practices for Energy Development and Power Generation
   Glasgow University
   11C Winton Drive
   Glasgow G12 0PZ
   UK
   E-mail: T.Hammons@ieee.org
   Tel: +44 141 339 7770

   Loi Lei Lai
   Energy Systems Group
   School of Engineering and Mathematical Sciences
   City University
   London, EC1V 0HB
   UK
   E-mail: l.l.lai@city.ac.uk
   Tel: +44 20 7040 3889
   Fax: +44 20 7040 8568

2. Professor Kwang Y. Lee
   Department of Electrical Engineering
   Pennsylvania State University
   University Park
   Pennsylvania, PA 16802
   USA
   E-mail: kwanglee@psu.edu
   Tel: 814-865-2621
   Fax: 814-865-7065

   Prof. Se-Ho Kim
   Department of Electrical Engineering
   Cheju National University
   66 Jejudaehakno, Jeju-Si
   Jeju Province 690-756
   Korea
   E-mail: hosk@cheju.ac.kr
   Tel: 82-64-754-3675
   Fax: 82-64-756-5281

3. Norman Tse
   Senior Lecturer
   AScBSE Programme Leader
   City University of Hong Kong
   Hong Kong
   Email: bsnorman@cityu.edu.hk
   Tel: + 852 2788 9836
   Fax: + 852 2788 9716

4. Dip. -Ing. V. Swaroop Pappala

University of Duisburg-Essen
Bismarckstr. 81 BA 072
47057 Duisburg
Germany
E-mail**:** venkata.pappala@uni-due.de
Tel: +49-0203-379-1015
Fax: +49-0203-379-2749

Prof. Dr.-Ing. Istvan Erlich
University of Duisburg-Essen
Bismarckstr. 81 BA 072
47057 Duisburg
Germany
E-mail: erlich@uni-duisburg.de
Tel: +49-0203-379-1032
Fax: +49-0203-379-2749

5. Professor Nikos Hatziargyriou
Zoe Vrontisi
Antonius G. Tsikalakis
National Technical University Athens
9 Heroon Polytechniou Str
157 73 Zografou
Athens
Greece
Nh@power.ece.ntua.gr
www.ntua.gr
Tel: +30 210 772 3661
Fax: +30 210 772 3968

6. Professor Tze-Fun Chan
Department of Electrical Engineering
Hong Kong Polytechnic University
Hong Kong
E-mail: eetfchan@inet.polyu.edu.hk
Tel: (852) 27666183
Fax: (852) 23301544

Loi Lei Lai
Energy Systems Group
School of Engineering and Mathematical Sciences
City University
London, EC1V 0HB
UK
E-mail: l.l.lai@city.ac.uk
Tel: +44 20 7040 3889
Fax: +44 20 7040 8568

7 Khaled Nigim, SMIEEE
ECE Dept. University of Waterloo
Waterloo, Ontario, Canada, N2L 3G1

E-mail knigim@ece.uwaterloo.ca
Tel: +1 519 888 4567 Ext 35018

Wei-Jen Lee, Ph.D, SMIEEE
Electrical Engineering Dept
University of Texas at Arlington
416 Yates Street
Nedderman Hall, Rm 517-518
Arlington, TX
USA
E-mail: lee@exchange.uta.edu
Tel: +1 817-272-5046

8. Prof Yuping Lu PhD, MIEEE
Dept of Electrical Eng
Southeast University
Nanjing, Jiangsu
P.R.China (210096)
E-mail: luyuping@seu.edu.cn
Tel: +8613809002279
Fax: +862583791817

Miss Lidan Hua
Dept of Electrical Eng
Southeast University
Nanjing,Jiangsu,P.R.China (210096)
E-mail: linda_hualidan@163.com
Tel: +862583794792
Fax: +862583791817

Mr. Ji'an Wu MIEEE
General Manager
Guodian Nanjing Automation CO.LTD
Nanjing,Jiangsu,P.R.China (210096)
E-mail: wja@sac-china.com
Tel: +862583418700
Fax: +862583422174

Mr. Gang Wu
Dept of Electrical Eng
Southeast University
Nanjing,Jiangsu,P.R.China (210096)
E-mail: wu1gang23@163.com
Tel: +862583794915
Fax: +862583791817

Miss Guangting Xu
Dept of Electrical Eng
Southeast University
Nanjing,Jiangsu,P.R.China (210096)
E-mail: chri119@163.com

Tel: +862583794792
Fax: +862583791817

9 Mr Umakant Dhar Dwrivedi,
Department of Electrical Engineering
Indian Institute of Technology Kanpur
Kanpur-208016, INDIA
E-mail: umakant@iitk.ac.in
Tel: +91-512-259 7874
Fax: +91-512-259 0063

Dr SN Singh,
Department of Electrical Engineering
Indian Institute of Technology Kanpur
Kanpur-208016, INDIA
E-mail: snsingh@iitk.ac.in
URL: http://home.iitk.ac.in/~snsingh/
Tel: +91-512-259 7009
Fax: +91-512-259 0063

Professor SC Srivastava,
Department of Electrical Engineering
Indian Institute of Technology Kanpur
Kanpur-208016, INDIA
E-mail: scs@iitk.ac.in
Tel: +91-512-259 7625
Fax: +91-512-259 0063

10. Ringo Lee
Director
"Your Network System Integrator"
Powerpeg NSI Limited
Unit D, 35/F., Morrison Plaza,
9 Morrison Hill Road, Wanchai, Hong Kong
E-mail: r_lee@hk.super.net
Tel : +1 (852) 2627-1347
Fax : +1 852) 2323-4983

PANEL SESSION CHAIRS

Tom Hammons
Chair International Practices for Energy Development and Power Generation
Glasgow University
11C Winton Drive
Glasgow G12 0PZ
UK
E-mail: T.Hammons@ieee.org
Tel: +44 141 339 7770

Loi Lei Lai
Energy Systems Group
School of Engineering and Mathematical Sciences

City University
London, EC1V 0HB
UK
E-mail: l.l.lai@city.ac.uk
Tel: +44 20 7040 3889
Fax: +44 20 7040 8568

E N D